**Schweizerische Meteorologische Anstalt**
**Institut suisse de météorologie**
**Istituto svizzero di meteorologia**
**Swiss Meteorological Institute**

No. 189

# SMI CONTRIBUTION TO ETEX PROJECT IN 1994

Daniel Schneiter

July 1996

Arbeitsberichte der SMA
Rapports de travail de l'ISM
Rapporti di lavoro dell'ISM
Working Reports of the SMI



**Schweizerische Meteorologische Anstalt**
**Krähbühlstrasse 58, Postfach**
**CH-8044 Zürich**

Tel. (01) 256 91 11, Fax (01) 256 92 78, Telex 81 73 73 met ch

No. 189

# SMI contribution to ETEX project

**D. Schneiter**

**July 1996**

## Summary

The Swiss Meteorological Institute (SMI) participated in the ETEX project by undertaking special meteorological measurements and by sampling air for tracer concentration observations in Switzerland. Calculation of the tracer dispersion forecasts and analyses over Europe have been realized with the LORAN model.

Aerological soundings, performed every six hours at Payerne during the tracer experiments, give a detailed description of atmospheric flow stratification evolution during these periods. SMI technical staff went to the release site (near Rennes in Brittany, France) to measure vertical wind profiles with a SODAR, and CVB (Constant Volume Balloon) trajectories. Air samplings at Payerne, Zürich-Kloten, Arosa and Jungfraujoch were taken every three hours for detecting eventual arrival of tracer over Switzerland.

Concentration forecast and analysis calculations with the LORAN dispersion model, made available to the SMI by the JRC (Joint Research Centre, Ispra), have been done for the three preliminary dry runs and in real time during the two experiments with tracer releases.

Principal characteristics of the LORAN model are explained in order to supply users with information necessary to run the model and to interpret the results. Preprocessing of meteorological data provided by ECMWF allows an optimal use of the model on real time for forecast purposes or on delayed time for subsequent analyses.

Post-processing codes are used to adapt LORAN results into the standardized format required for easy comparison with results of other models involved in the ETEX project. They also deliver plots for a quick visual interpretation.

Ground concentration evolution calculated for the three dry runs and for the two tracer experiments show great diversity of results according to the meteorological situations.

## Résumé

L'Institut Suisse de Météorologie (ISM) a participé au projet ETEX en effectuant des mesures météorologiques spéciales et des prises d'échantillon d'air pour observer les concentrations du traceur en Suisse. Les calculs de prévision et d'analyse de la dispersion du traceur en Europe ont été réalisés avec le modèle LORAN.

Les sondages aérologiques, effectués toutes les six heures à Payerne durant les expériences avec traceur, donnent une description détaillée de l'évolution de la stratification des courants atmosphériques pendant ces périodes. Une équipe technique de l'ISM s'est rendue sur le site d'émission du traceur (près de Rennes, en Bretagne, France) pour y effectuer des mesures de profil du vent par SODAR, et des mesures de trajectoires par BVC (Ballon à Volume Constant).

Les prélévements d'échantillons d'air à Payerne, Zürich-Kloten, Arosa et au Jungfraujoch ont été effectués toutes les trois heures, en vue de détecter l'arrivée éventuelle du traceur en Suisse.

Les calculs de prévision et d'analyse des concentrations au moyen du modèle de dispersion LORAN, mis à disposition par le JRC (Joint Research Centre, Ispra), ont été effectués en temps différé pour les trois essais à blanc et en temps réel pour les deux essais avec traceur.

Les caractéristiques principales du modèle LORAN sont décrites, afin de donner aux utilisateurs les renseignements indispensables pour son utilisation et pour l'interprétation correcte des résultats. Les procédures de preprocessing, en conjonction avec les analyses et les prévisions numériques calculées à l'ECMWF de Reading (UK) permettent une utilisation optimale du modèle en temps réel et en temps différé.

Les programmes de post-processing préparent les résultats numériques du modèle sous la forme standardisée requise pour les comparaisons avec les résultats des autres modèles engagés dans le projet ETEX. Ils livrent aussi des représentations graphiques pour une interprétation rapide des résultats.

L'analyse de l'évolution des concentrations au sol obtenues pour les trois périodes d'essai à blanc et pour les deux expériences réelles avec traceur montrent bien la diversité des résultats en fonction des situations météorologiques.

## Zusammenfassung

Die Schweizerische Meteorologische Anstalt (SMA) hat am ETEX Projekt teilgenommen, und zwar sowohl bei der Durchführung von meteorologischen Spezialmessungen als auch bei der Sammlung von Luftproben, um die Tracer-Konzentrationen in der Schweiz zu ermitteln. Zusätzlich wurden Tracer-Ausbreitungsprognosen mit Hilfe des Modells LORAN realisiert.

Die aerologischen Sondierungen, die in Payerne während des Tracer-Experiments alle sechs Stunden durchgeführt wurden, geben eine detaillierte Beschreibung der atmosphärischen Strömung und deren Schichtung während dieser Periode. Ein technisches Team der SMA hat sich an den Tracer-Emissionsort begeben, (nahe Rennes, in Bretagne, West Frankreich), um Messungen von Windprofilen mittels SODAR sowie Trajektorien mittels Verfolgung von BKV (Ballonen mit Konstantem Volumen) durchzuführen. In der Schweiz wurden an vier Standorten (Payerne, Zürich-Kloten, Arosa und Jungfraujoch) Luftproben gesammelt, um die Tracer-Konzentrationen zu messen.

Prognosen und Analysen der Konzentrationsverteilung wurden mit dem Ausbreitungsmodell LORAN, vom JRC Ispra zur Verfügung gestellt, für die drei Vorversuche zeitverschoben und für die zwei Tracer-Experimente in Echtzeit erstellt.

Die Hauptcharakteristiken dieses Modells werden beschrieben, um den Benützern die nötigen Informationen für die Handhabung des Programms und die richtige Interpretation der Resultate zu vermitteln. "Preprocessing"-Verfahren für die Vorbereitung der meteorologischen Daten, die auf ECMWF-Analysen und -Prognosen basieren, erlauben eine optimale Benützung des Modells, sei es zeitverschoben oder in Echtzeit.

Die "Post-processing"-Programme dienen dazu, die numerischen Resultate dem standardisierten Format anzupassen, die es erlauben, die Resultate mit anderen in ETEX eingesetzten Modellen zu vergleichen. Diese Programme liefern zusätzlich graphische Darstellungen, die eine rasche Visualisierung und Überprüfung der Ergebnisse ermöglichen.

Die Analyse der Entwicklung der Bodenkonzentrationen während der drei Probeläufe und der zwei Tracer-Experimente zeigen klar die Verschiedenheit der Ergebnisse in Abhängigkeit der meteorologischen Bedingungen auf.

## Riassunto

L'Istituto Svizzero di Meteorologia (ISM) ha partecipato al progetto ETEX effettuando delle misure meteorologiche speciali e dei prelevamenti di campioni d'aria per osservare le concentrazioni del tracciante in Svizzera. I calcoli delle previsioni e delle analisi della dispersione del tracciante in Europa sono stati realizzati col modello LORAN.

I sondaggi aereologici, effettuati ogni 6 ore a Payerne durante le esperienze col tracciante, danno una descrizione dettagliata dell'evoluzione della stratificazione delle correnti atmosferiche durante questi sondaggi aereologici, effettuati ogni 6 ore a Payerne durante le esperienze col tracciante, danno una descrizione dettagliata dell'evoluzione della stratificazione delle correnti atmosferiche durante questi periodi. Una squadra tecnica dell'ISM é andata sul luogo dell'emissione del tracciante in Francia (vicino a Rennes, in Bretagna) per effettuare delle misure di profili di vento col SODAR e delle misure di traiettoria col BVC (Pallone a volume costante). In Svizzera, i rilevamenti dei campioni necessari alla misura delle concentrazioni del tracciante sono stati realizzati in quattro località: Payerne, Zurigo-Kloten, Arosa e Jungfraujoch.

I calcoli di previsione e di analisi delle concentrazioni per mezzo del modello di dispersione LORAN, messo a disposizione dal JRC d'Ispra, sono stati effettuati in differita per le tre prove a vuoto e in tempo reale per le due prove col tracciante.

Le caratteristiche principali di questo modello sono state descritte, per fornire agli utenti le informazioni indispensabili per l'interpretazione dei risultati. Le procedure di "preprocessing" unite alle analisi e alle previsioni numeriche calcolate all'ECMWF di Reading (GB), permettono un'utilizzazione ottimale del modello in tempo reale e in differita.

I programmi di "post-processing" preparano i risultati numerici del modello nella forma standardizzata richiesta, per essere paragonati con i risultati degli altri modelli utilizzati nel progetto ETEX. Questi programmi forniscono pure delle rappresentazioni grafiche per un'interpretazione rapida dei risultati.

L'analisi dell'evoluzione delle concentrazioni al suolo ottenute per i tre periodi di prova a vuoto e per le due esperienze reali col tracciante mostrano bene la diversità dei risultati in funzione delle situazioni meteorologiche.

## Table of Contents

# List of figures

# List of tables

# 1. INTRODUCTION

## 1.1 Historical context

Industrial accidents of major dimension with releases into the atmosphere of harmful radioactive or chemical materials can have detrimental consequences on regions extending to hundreds even thousands of kilometres. Because of their effects on human and animal health, at short and long term, they may be considered as ecological disasters and have, to say the least, large negative economic impacts. Let us remember, for instance, the nuclear accident of Chernobyl (1986), or the chemical accidents of Seveso (1976), Bhopal(1984), or in less extent the fire at Schweizerhalle (1986).

The Chernobyl accident showed that West Europe was not shielded from radioactive fallout coming from Eastern Countries, where security constraints on nuclear installations are far away from the very tight regulations applied in the Western Countries.

The renewal of such an accident is thus not highly improbable. If measures can be undertaken for an optimum protection against radioactive fallouts, they will be most effective the sooner they are activated. Therefore trajectories and dispersion forecasts of pollutants must be rapidly obtainable.

Many countries have implemented atmospheric transport models for emergency purposes. They need to be promptly activated and they must deliver credible results.

Dispersion data measured in Europe after the Chernobyl accident have been used retrospectively in the international project ATMES (Atmospheric Transport Model Evaluation Study) sponsored by the EC (European Commission), IAEA (International Atomic Energy Agency) and WMO (World Meteorological Organization) (ref. /10/). Despite the fact that ATMES was highly successful, some uncertainties remained, mainly connected to the actual value of the source term. Moreover, this study gives no indication on the ability of the different models to produce real-time response in emergency situations. Therefore a follow--up international programme has been organized under the name of ETEX (European Tracer Experiment).

## 1.2 Overall objectives of ETEX

The general objectives of ETEX were the following:

1. To realize a long-range atmospheric tracer experiment, with concentration measurements at a distance up to some 2000 km from the release point.
2. To test the capability of the participating institutions to provide, in real time, rapid forecasts of atmospheric dispersion over long distances, after notification of the coordinates of the release site and the time of emission onset, duration and intensity.
3. To evaluate the quality of forecasts retrospectively, by comparing them with the evolution of tracer concentrations measured over more than one hundred stations spread over central and northern Europe, including some Eastern Countries.
4. To establish a well documented database of source terms, meteorological and concentration data, to allow the validation of present and future long-range atmospheric dispersion models.

## 1.3 ETEX project activities

The three main ETEX activities have been:

1. Tracer experiments.
2. Real time modelling.
3. Atmospheric model evaluation.

### 1.3.1 Tracer experiments

Two controlled tracer releases have been conducted by the Joint Research Centre (JRC) at Ispra from the site of Monterfil, near Rennes (Brittany, West of France), on the 23rd of October and the 14th of November, 1994. The non-toxic gases used are detectable at very low concentration (1 part per $10^{15}$) by gaschromatography. These analytical techniques were developed by the Brookhaven National Laboratory and have been adopted by the Environment Institute of the JRC. They have been applied with success to long-range experiments in the United States for the Cross Appalachean Tracer Experiment (CAPTEX) and for the Across North America Tracer Experiment (ANATEX), and also in Europe in mesoscale experiments like the Transalpine Atmospheric Transport project (TRANSALP) or the Transport over Complex Terrain project (TRACT).

#### 1.3.1.1 Experiments organization

Two tracer experiments were realized in autumn 1994. The first (ref. /11/) started on the 23rd of October at 16 h UT, with the emission of perfluormethylcyclohexane and the second on 14th November at 15 h UT with the emission of perfluormethylcyclopentane. Both releases were undertaken on the site of Monterfil.

The weather situations were chosen by their ability to disperse tracers over the region equipped with chemical sampling devices. **Figure 1** shows the position of the 167 sampling stations located in countries of the Centre, North and East of Europe.

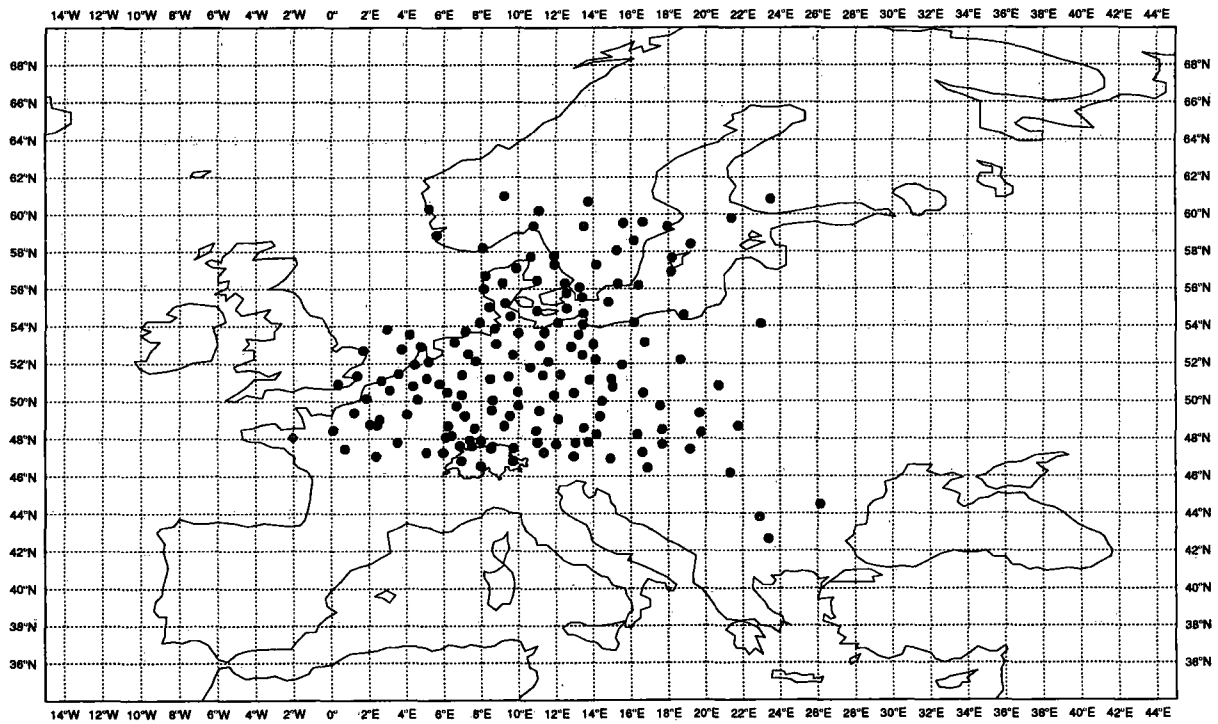


**Figure 1.** Location of tracer sampling stations

#### 1.3.1.2 Tracer sampling and analysis

For practical reasons, all sampling devices were installed by the JRC at existing synoptic weather stations. On 72-hours' sampling time, successive air samples of 3 hours were collected at all stations. About 10'000 absorbing tubes had to be carefully analysed in laboratory in order to measure their tracer content. In Switzerland, the four stations chosen were Payerne,

Zürich-Kloten, Arosa and the Jungfraujoch. Three aircraft (the Hercules of the British Met Office, the Stemme Motorglider of the Swiss MetAir and the DO228 of the German Weather Service) were involved to collect information on the horizontal and vertical structure of tracer cloud (ref. /12/). They intersected the plume one day after the release at a distance of 400 km to 700 km downwind from the source and at altitudes ranging from 300 m to 1200 m AMSL.

#### 1.3.1.3 Meteorological observations

Besides the routine weather observations provided by Météo France, special meteorological measurements have been carried out on the release site at Monterfil, in order to provide more information about the behaviour of the tracer plume during its first phase of dispersion. Vertical wind profiles were continuously performed by the SMI (Swiss Meteorological Institute). Trajectories of air parcels at two different levels were tracked with both the CRA (Centre de Recherches Atmosphériques, Université Paul Sabatier, Lannemezan, France) and the SMI, using CVB's (Constant Volume Balloons) (ref. /9/).

At Payerne, the routine wind soundings of 6 h UT and 18 h UT were replaced during the two experiments by full PTU (Pressure, Temperature, hUmidity) aerological soundings for the five days following the beginning of releases.

### 1.3.2 Real-time modelling

As in a real accident, participants have been informed shortly after the release start of the precise location and characteristics of the emission (intensity, height above ground, duration). Each modeller was requested to predict, as soon as possible, the evolution of the tracer cloud. They had to determine the arrival time and the residence time of the tracer at locations of the measuring station given on **Figure 1**, and also on all grid points of $1^{o}$ covering the whole of Europe. In order to demonstrate that computing was completed in real time, each participant was requested to send by fax, within a defined time frame, forecast plots for +24 h, +36 h and +48 h to the JRC at Ispra.

The plume predictions were updated each 12 hours with new available meteorological analyses and updated forecasts. Thus each participant finely computed 6 successive sets of concentration fields, extending from the first guess (set 1), only based on forecasts, to the most precise description, based on analysed wind fields (set 6), giving also intermediate results (set 2 to set 5) relying on both analyses and forecasts. The complete data were transmitted on informatic support to the JRC at Ispra for a detailed statistical study (ref. /12/) on the ability of the models to predict the measured tracer concentration fields.

For the relative evaluation of the quality of the different models, it was also necessary to consider the response time of the model which is an important parameter in emergency conditions.

Three dry run exercises were realized to test communications between ETEX organizers and modellers and to give to the participants the opportunity to be confronted with real time difficulties. These first attempts gave also the possibility to compare the trajectories and concentration evaluations delivered by the participating models, based on several meteorological forecast systems and using more or less sophisticated dispersion schemes. The rather complicated weather situations chosen gave large differences between modelling results. These preliminary exercises stimulated the improvement of the communication system. The SMI only participated in real time in the third dry run, nevertheless the dispersion for the first two dry runs were computed afterwards and the results are presented further in this report in sections 3.1 to 3.3.

### 1.3.3 Models evaluation

In order to realize this part of the project, all the participating modellers sent their numerical results to the JRC at Ispra. They had to follow very precise informatic format specifications to

allow the establishment of a coherent database suitable for extended statistical analysis by computer and to yield the quality of each model, by comparison with terrain measurements of concentration and with results of all the other models. This study will not be finished before the end of 1996.

### 1.3.4 Project planning

The organization of a European experiment on such a large scale involving more than five hundred people working for the management, the tracer release, concentration sampling and analyses, meteorological measurements, modelling and statistical studies, needs a thorough planning to guaranty the success of the exercise. Such an experiment cannot be repeated too often because the remaining atmospheric tracer concentration has to be kept as low as possible for the sake of future large scale studies. This is why only dry exercises have been done to test communications and model availability in real time.

The difficulties encountered during and after the Chernobyl accident (April 1986) to predict with accuracy the diffusion of the radioactive species at large scale stimulated the improvement of existing models and for developing new codes based on better meteorological models. The calibration and the validation of a large scale model need intense international collaboration. The coordination of such a large experiment can only be done by well established international institutions. This is why the three international organizations which sponsored the first ATMES projects (ref. /10/) were again solicited in 1991 to patronise the ETEX project. Principal phases and milestones of the project are presented in **Table 1**.

**Table 1.** Management and realization plan of ETEX

| | |
|---|---|
| 1991 | ETEX project is proposed as a following-ATMES project |
| 3-4 June 1992 | Consultation of experts to plan the ETEX project, WMO, Geneva |
| 21 Oct. 1992 | First test of LORAN model at SMI (Locarno) |
| 4-5 Nov. 1992 | Consultation of experts to plan the ETEX project, WMO, Geneva |
| 21 Oct. 1993 | ETEX Real Time Modellers Meeting, WMO, Geneva |
| 19 Apr. 1994 12h UT | First dry run, Munich, Germany |
| 7 Dec. 1993 15h UT | Second dry run, Nancy, France |
| 27 Jul. 1994 10h UT | Third dry run, Frankfurt, Germany |
| 23.Oct. 1994 16h UT | Run 1 with tracer, Monterfil near Rennes, France |
| 14.Nov. 1994 15h UT | Run 2 with tracer, Monterfil near Rennes, France |
| 23-26 Oct. 1995 | ETEX Real-time Modellers' Meeting, Prague, Czech Rep. |
| 1996 - 1997 | ETEX final report, JRC, Ispra, Italy |

# 2. LORAN Model

The purpose of this brief description of the LORAN model is to supply to the users detailed information needed to run the programme and to interpret its results.

## 2.1 General characteristics and functionality

The LORAN (Long Range Atmospheric Advection of Nuclides) model was developed at Ispra by C. Tassone and S. Galmarini in 1992 (ref. /6/). The code is written in FORTRAN language. It simulates the long range behaviour of a radioactive pollutant emitted into the atmosphere and forecasts the evolution of ground concentrations. The cumulative deposition is calculated on the continental scale and over a time-space of a few days. The simplified version of LORAN, used for ETEX, considers only a single windfield chosen at 850 hPa and only one source point. As the tracer used was a non-radioactive inert gas, the possibilities of computing the dry and wet depositions and the radioactivity decay were not activated.

In its concept, the LORAN model needs only a short computing time (about 1 minute for a 72-hour trajectory forecast on a SUN Sparc2 workstation), when the suitable meteorological data are available. Due to the sequential structure of the model, the memory needed is less than one Mbyte.

## 2.2 Structure of the LORAN model

The LORAN model runs in two well distinct phases. In the first one the plume horizontal extent is computed and in the second one the pollutant ground concentration is determined according to the horizontal extent of the plume, the boundary layer depth, wet and dry depositions. The mixing layer height is computed on the base of available meteorological fields, following a method given in Appendix A.

### 2.2.1 Input data

Four types of input data are requested by LORAN:

1. *Control data*, that is data controlling timing and internal parameters needed by the model to synchronize meteorological data and time of release and to define proper physical parameters for deposition and radioactive decay.

2. *Fixed input data* are external physical data fixed for the whole experiment (albedo and roughness).

3. *Release data.*

4. *Meteorological data* for a period of 96 hours.

A more detailed description of input data is given in the following paragraphs.

#### 2.2.1.1 Control data

Data needed to control the LORAN model is given by an ASCII file named "*startdat.dat*". This file can be edited by any text editor before starting a new simulation. The principal information requested is the following:

**Table 2.** Control data for LORAN

| |
|---|
| Date (year, month, day, hour) of the simulation beginning. |
| Date (year, month, day, hour) of the simulation end. |
| Time interval for the mean concentration and the mean deposition in hours (for instance 3 h). |
| Average time for a given pollutant (or tracer) release mass (usually 1 h). |
| Simulation time step (usually 1 hour). |
| Time interval between sets of meteorological analyses or forecasts (for ECMWF 6 h). |
| Pollutant chemical symbol (not interpreted, but used for tables or plots labels). |
| Dry deposition velocity in m/hour (set to 0. for ETEX). |
| Washout coefficient (set to 0. for ETEX). |
| Exponent for precipitation on wet deposition (set to 0. for ETEX). |
| Half Life (only for radioactive species) in hours, days or years (set to 30 years for ETEX). |
| Geographical coordinates of the source point. |
| Date (year, month, day, hour) of the first and the last meteorological fields supplied. |

### 2.2.1.2 Fixed input data

For the determination of the mixing layer height, the model needs to know the ground roughness and the ground albedo, given by clear sky (without clouds). The albedo is changing from one season to another, particularly in winter when the ground is covered by snow. The same albedo file was used throughout the whole ETEX project. Albedo and roughness are delivered for each grid point in an ASCII file named "*mixfix.dat*" as given in **Table 3.**

**Table 3.** Fixed input data

| |
|---|
| Albedo of the ground given with a one-degree geographical resolution. |
| Roughness of the ground given with a one-degree geographical resolution. |

### 2.2.1.3 Release data

The emission characteristics are given in another file named "*ril.dat*" containing the mean mass emitted for each hour following the start of the release. The input mass unit corresponds to the unit in which the resulting concentrations are given. For example, an emission given in ng $h^{-1}$ (1 ng = $10^{-12}$ kg) will provide concentration results in ng $m^{-3}$. Hourly released mass can be replaced by an hourly mean of radioactivity given in Bq (1 Becquerel = 1 radioactive desintegration per second) and results are then delivered in Bq.

### 2.2.1.4 Meteorological data

Meteorological data supplied to the model (**Table 4**) are given for all grid points extending from latitude 32.625° N to 72.00° N and from longitude 15.75° W to 45.00° E, in a grid mesh of

1.125°. These limits are defined in the LORAN code and cannot be easily changed by the user, because this would require also an adaptation of the preprocessing system located at ECMWF and of the LORAN code itself.

Meteorological fields are given every six hours. For real time computing, all these fields are forecasted. Subsequently, forecasted fields are to be replaced by analyses, that is by fields better linked to real observations which have become available in the meantime. One of the ETEX objectives is to compare concentration results obtained firstly with forecasts and secondly with weather analyses.

**Table 4.** Meteorological data

| |
|---|
| Horizontal wind vectors fields at 850 hPa. |
| Horizontal wind vectors fields at 10 m above ground. |
| Temperature fields at 2 m above ground. |
| Total cloud cover. |
| Precipitation. |

### 2.2.2 Trajectory computation

LORAN is a gaussian model which disperses the pollutant through a segmented plume.

In the first phase of computing, the central trajectory is determined by adding hourly wind vectors transporting the pollutant horizontally from the release point. These successive wind vectors are obtained by linear interpolation in space and time of synoptic fields provided every six hours by the ECMWF meteorological model.

To obtain the wind vector at the point P (**Figure 2**) for a given time T, the model uses the two winds fields available at synoptic times $T_1$ and $T_2$, repetitively, just before and just after time T.

The transportation vector V of an air parcel staying at time T at the position P is obtained by linear time interpolation between vectors $V_1$ and $V_2$. The vector $V_1$ is computed by linear space interpolation between the four vectors $V_{A1}$, $V_{B1}$, $V_{C1}$ and $V_{D1}$, given by the ECMWF model for the time T1, at the four nearest corners A, B, C and D from the extremity P of the trajectory. Similarly vector $V_2$ is the interpolated wind vector at time $T_2$.

All wind vectors are given at the same pressure level, chosen for ETEX at 850 hPa. When the interpolated wind speed lies below 1 $ms^{-1}$, it is replaced by an arbitrary south-western wind of 1 $ms^{-1}$, to avoid the transported parcels being trapped into a zone without wind, from where they could not escape any more.

### 2.2.3 Plume lateral extension calculation

The lateral atmospheric dispersion of the plume is determined by the formula suggested by Gifford in 1984 (ref. /7/) and tested by Carras and Williams (1988 ref. /5/):

$$\sigma = 0,5t \qquad \textit{Eq. 1}$$

| | | |
|---|---|---|
| $\sigma$ | [m] | Half width of the plume |
| t | [s] | Elapsed time after release |

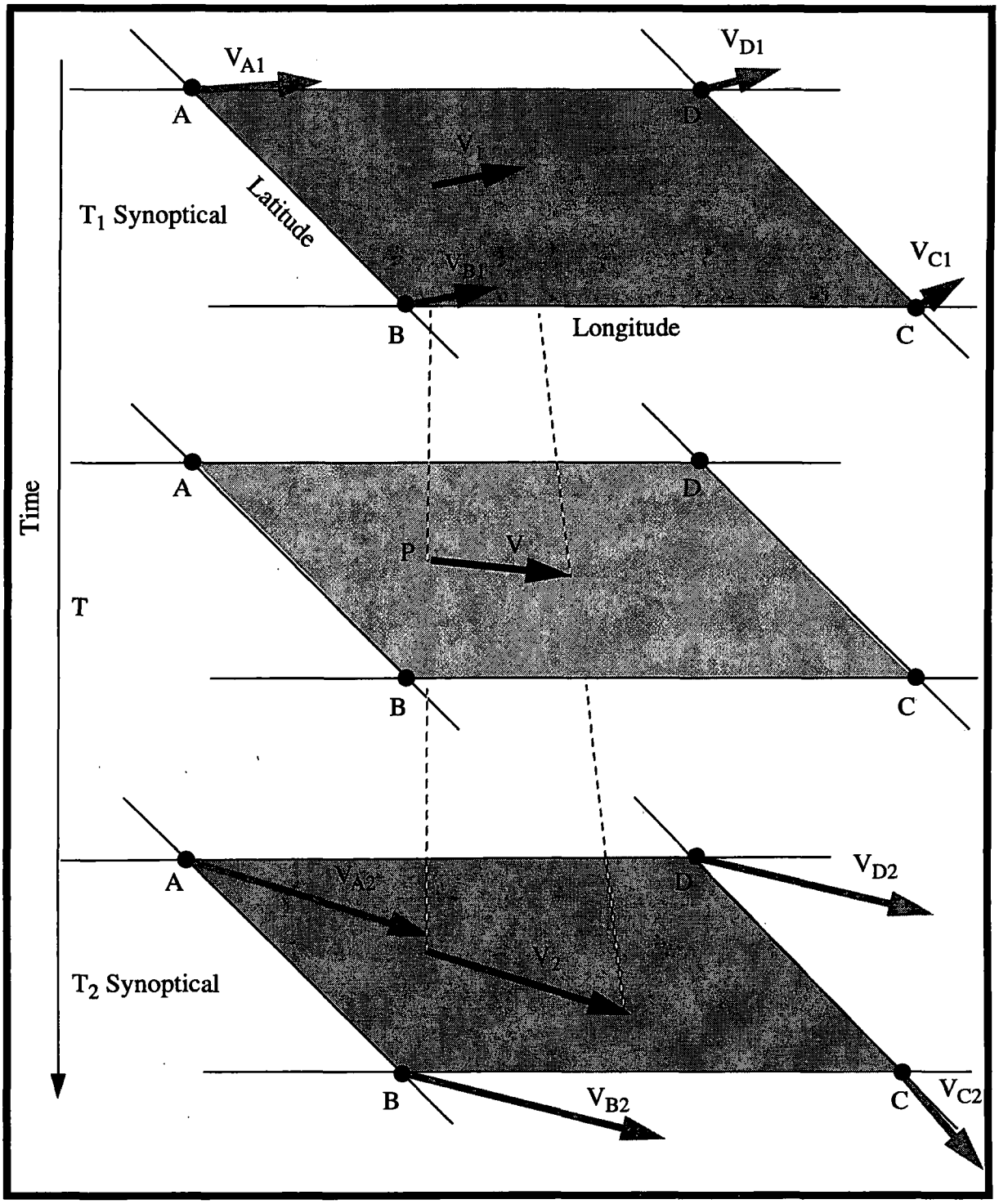


**Figure 2.** Wind interpolation scheme

The LORAN model uses another coefficient better adapted to long range dispersion:

$$\sigma = 0,825t \qquad \textit{Eq. 2}$$

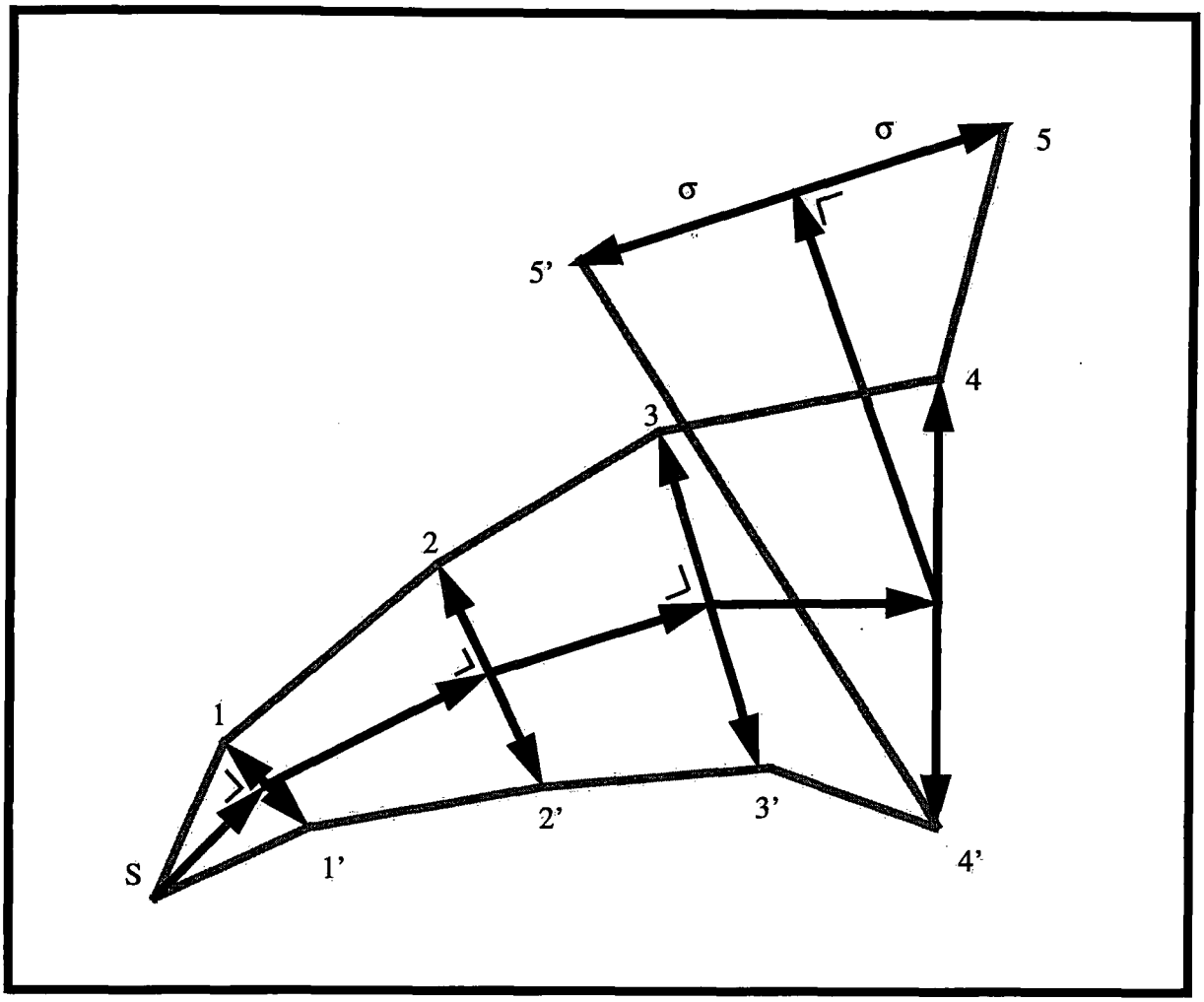


**Figure 3.** Horizontal trajectory with lateral dispersion

At each step of trajectory computation, the width σ is placed perpendicularly on both sides of the plume (**Figure 3**). When the wind direction turns rapidly (let us say more than 90°) The point 5, following the point 4, is not placed on the left side of the plume, but goes on the right side to avoid a crossing of the plume borders. The realism of this simple gaussian dispersion decreases with time and distance, but remains certainly valuable on the first few days of simulation. During the first hour, plume widens from 0 km to 5.9 km. In 24 hours it becomes 142 km wide, and after 60 hours the transversal segment has already a length of $2\sigma = 356$ km. At this stage, a moderate wind direction variation displaces the extremities of the dispersion segment on so large distances, that the process becomes less realistic. The advantage of this method lays in the computing speed and in the good simulation of reality during the first two days after the release time. Then, the most distant part of the plume only gives approximate, though useful information on regions which could be touched by the pollutant.

During this first phase of calculation, the LORAN model simulates the trajectories and the lateral expansion of successive hourly emissions at the source point S. For example, one hour after the beginning of the release, the particles emitted during the first hour are located within the triangle S-1-1' (**Figure 3**). Two hours after the beginning of the release they are to be found in the quadrilateral 1-1'-2'-2, and after 5 hours they have reached the quadrilateral 4-4'-5'-5. This geometry is considered to be independent of the strength of the emission, it only depends on time and on the wind fields' evolution at 850 hPa. The trajectory and dispersion of particles emitted during the second hour are calculated separately. The shape of the plume at a time T is given by the position of all the transversal segments situated at the end of each of the successive trajectories (see for instance **Figure 4**).

### 2.2.4 Concentration calculation

In a second phase, the model computes concentration fields at ground level. Hourly emission intensity and altitude of release are given in the input file named "*ril.dat*". One of the principal characteristics of the LORAN model is the rather accurate determination of the mixing layer height h along all the trajectories. This height is a function of stability parameters L (Obukhov length), $u_*$ (friction velocity) and $\theta_*$ (temperature scale) which are determined with a method proposed by Van Ulden and Holtslag (ref. /15/) based on the similarity theory. The formulae used rely on common meteorological data like temperature, cloud cover and horizontal windspeed. They depend also on albedo, roughness of the ground, latitude, season and the time of day.

#### 2.2.4.1 Mixing layer height

The LORAN model computes the mixing layer height for each time step (one hour) as a function of its geographical location (roughness of the soil and albedo), of the time (day or night) and principally of the atmospheric stability. According to the similarity theory, three main parameters are firstly determined:

| | |
|---|---|
| $u_*$ | Friction velocity |
| $\theta_*$ | Temperature scale |
| L | Obukhov length |

These three parameters are computed by solving a set of three equations given in Appendix A. Relations defining $u_*$ and $\theta_*$ differ from day to night. The solution is obtained by iterative process. A first rough guess of the Obukhov length L allows the calculation of $u_*$ and $\theta_*$, which are used to recalculate L, taken again as a new guess. This iterative process is stopped when the difference between guessed L and recalculated L becomes lower than an assigned value or after a maximal number of steps fixed to 20.

The Obukhov length L defines four stability classes: stable, neutral, quasi neutral and instable. For each stability class, a particular set of relations is used to obtain the mixing layer height h. They are described in Appendix A.

#### 2.2.4.2 Mass balance (deposition, washout)

The pollutant mass emitted at the source point is distributed within two layers. The first is lying between ground and the top of the mixing layer. The second extends above the mixing layer and is limited by a reference height fixed at $H_R = 2000$ m above ground. The total emitted mass decreases because of washout and dry and wet deposition. These three processes are not activated for gaseous tracer like those emitted for ETEX experiments.

When the height of emission is below the height of the mixing layer, the total amount of the mass remains within the first layer near the ground. When the height of both the emission and the mixing layer are equal, the mass is split in two equal amounts spread below and above the mixing height. If the mixing layer height is below the source, the whole mass begins its dispersion in the upper layer, at least during the first trajectory step. Within the mentioned layers, the pollutant concentration is supposedly homogeneous. At each computing step of one hour, the mass distribution between the two layers is modified according to the mixing layer depth evolution. Heights $Z_1$ and $Z_2$ of the mixing layers calculated respectively at the beginning and at the end of the computing step are compared to each other and also to the reference height $H_R$. The five possible cases are described in **Table 5**.

**Table 5.** Mixing layer height evolution

| Case | | | |
|---|---|---|---|
| a | $Z_2 > Z_1$ | $Z_1 < H_R$ | $Z_2 < H_R$ |
| b | $Z_2 < Z_1$ | $Z_1 < H_R$ | and thus $Z_2 < H_R$ |
| c | $Z_2 < H_R$ | $Z_1 > H_R$ | and thus $Z_2 < Z_1$ |
| d | $Z_2 > H_R$ | $Z_1 < H_R$ | and thus $Z_2 > Z_1$ |
| e | $Z_2 > H_R$ | $Z_1 > H_R$ | $Z_1 < Z_2$ or $Z_1 > Z_2$ |

For each case, the new distribution into $M_{u2}$ (bottom layer, under the mixing layer) and $M_{o2}$ (above the mixing layer) of the total initial Mass $M_2$ is recalculated with simple algorithms, as a function of the preceding distribution into $M_{u1}$ and $M_{o1}$ of the total mass $M_1$. If we do not take into account washout and dry and wet deposition, and if the gas is non radioactive, we have the simplified relations given in equations 3 to 5, respectively for cases a to c.

Case a)

$$M_{u2} = M_{u1} + M_{o1}\left(\frac{Z_2 - Z_1}{H_R - Z_1}\right)$$

$$M_{o2} = M_{o1} - M_{o1}\left(\frac{Z_2 - Z_1}{H_R - Z_1}\right)$$

*Eq. 3*

Case b)

$$M_{u2} = M_{u1} - M_{o1}\left(\frac{Z_1 - Z_2}{Z_1}\right)$$

$$M_{o2} = M_{o1} + M_{o1}\left(\frac{Z_1 - Z_2}{Z_1}\right)$$

*Eq. 4*

Case c)

$$M_{u2} = (M_{u1} + M_{o1})\frac{Z_1 Z_2}{H_R^2}$$

$$M_{o2} = (M_{u1} + M_{o1})\frac{(H_R - Z_2)\,Z_1}{H_R^2}$$

*Eq. 5*

For the last two cases d) and e), the whole mass is back into the bottom layer. For each new step of the trajectory, the mixing layer height is only calculated in the centre of the plume and is used along the whole dispersion segment perpendicularly to trajectory. As already mentioned (§2.2.3), after 60 hours, this segment has an extension of $2\sigma = 356$ km, and thus extends over several grids elements.

### 2.2.4.3 Dilution volume

After each new step of one hour trajectory progression, the dilution within the plume is obtained by the assumption that the pollutant is homogeneously distributed within the new part of the plume. The volume of dispersion is estimated by searching and counting (k) all the grid cells having their centre within the new part of the plume. The total surface $A_T$ of the new part of the plume is estimated by adding the individual surface A(k) of all these grid cells. The total mass per height unit $M_c$ is distributed into each cell indexed (i,j) by the relation:

$$M_t(i,j) = \frac{M_c A(k)}{A_T} \qquad \textit{Eq. 6}$$

The mean concentration over 3 hours and per surface unit is finally obtained by time averaging:

$$C(i,j) = \frac{\sum_{t=1}^{3} M_t(i,j)}{3A(i,j)} \qquad \textit{Eq. 7}$$

## 2.3 Preprocessing

The preprocessing has to collect and prepare the data needed to run the LORAN model. Three times a day an automatic procedure gets analyses and forecasts from ECMWF as soon as they are available. They are stored on a disk at Payerne and used to update meteorological data from previous days, analyses replacing forecasts and new forecasts replacing older ones. In case of emergency, this procedure ensures that the last available meteorological data are already at disposition. This allows the user to start without delay transport and concentration calculations with real or fictitious emission data in order to obtain a first description of the region possibly touched by pollutant and of the distribution of dilution factors in the lee of the release site.

## 2.4 Post-processing

The post-processing allows concentrations to be calculated at given locations (for instance at the tracer sampling stations) and at grid points. Graphical representations are used to display the results (trajectories or plumes and concentration fields) for an easy visual verification. Wind fields involved in the plume calculation are also represented, see for instance **Figure 4**.

## 2.5 Real time procedure

After the notification of a major accident, deciding authorities need, as soon as possible, a first guess of trajectories and concentration fields, based on meteorological fields immediately available and issued from a previous run (older than 12 h) of the ECMWF forecast model. These first results will be improved by ordering at ECMWF the last available forecasts, but this will take a certain time (1 hour to 2 hours), depending on the load of the computer and communication systems.

These first trajectories and concentration estimates for the next 96 hours following the accident are based only on forecasts. As the time goes on, new meteorological observations are used every 12 hours to build analyses of the weather situation and to initialize new forecasts. At the end, that is after at least 96 hours, all forecast fields can be replaced by analyses which are in principle better representations of the observed weather. The chronogram given in **Table 6** explains in more details the successive sets of data available for the particular case of the first ETEX tracer experiment, on the 23rd of October at 15 h UT.

For a real time application, it is strongly recommended to have meteorological fields (analyses and forecasts) available at any time in the local computer, even if these data are not the very latest computed at the ECMWF. In case of emergency, this procedure allows one to yield a first guess rapidly, even if it is not the most suitable one. This method is more independent of any communication problems due to overflow of data exchange with the ECMWF after the notification of a major accident.

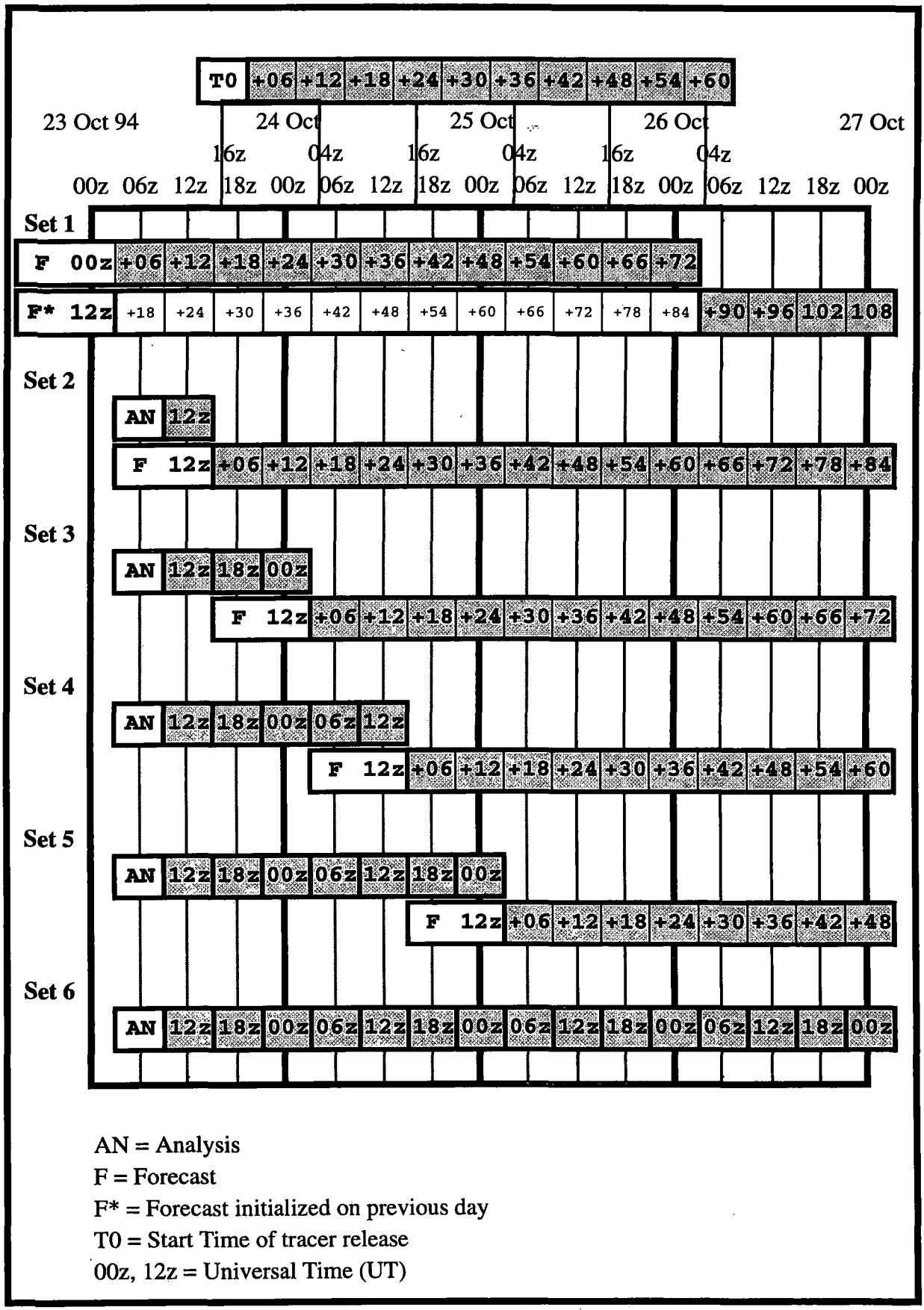


**Table 6.** Chronogram of the first tracer experiment

## 2.6 Limitations of the LORAN model

All users of the LORAN model should be well informed of the main characteristics of the model and particularly aware of its limitations. Mainly due to its simplicity, the model runs very fast. However this characteristic limits its ability to forecast precise plume behaviour. One of the main objectives of this report is to describe the principal features of the model and to deduce how the user can benefit from its ability to simulate the plume dispersion at great distance and by the same occasion, to warn him against wrong interpretations of the given results. The main points to be mentioned are the following:

1. The trajectory of all parts of the plume are obtained by only one wind field, chosen for ETEX at the pressure level of 850 hPa. This means that the model is not able to consider any wind shear. These features were well demonstrated by comparison of LORAN results with the results of other more sophisticated models and with observations. This was particularly true during the first real run of ETEX. We will see (section 3.4) that the LORAN programme cannot forecast the whole lateral extent of the plume, when the dispersion is strongly influenced by wind stratification disturbing the normal symmetrical turbulent diffusion.

2. The mixing layer height is computed in a rather sophisticated way based on the well accepted similarity theory of the atmospheric boundary layer. This is an important characteristic of the model which parameterizes local, though very efficient, vertical dispersion processes strongly dependent on the stability of the low troposphere. The mixing layer height is computed at the last determined point of the trajectory and this value is used for all the grid cells having their centre inside the last plume section. This feature of the model procedure is completely justified at the beginning of the trajectory where the plume is narrow. The enlarging of the plume as the time goes on and also the elongation of the trajectory by strong winds may produce situations where the computed mixing height is finally applied to regions situated far away where it should actually be recalculated with local parameters.

3. The plume enlarges with time. After 60 hours, it has a width of 356 km. When the wind direction is turning, the two lateral extremities of the plume always placed on a perpendicular to the direction of the trajectory may sweep over large surfaces. The corresponding dilution is probably overestimated in these cases.

4. When the plume leaves the geographical zone covered by the model, the results are no longer reliable even if the trajectory comes back into the investigated region. The user is informed by a warning (*'acos: DOMAIN error'*).

5. In some particular cases the determination of grid cells having their centre inside the plume boundary fails because of the alignment of three points of the boundary quadrilateral, which is determined by two successive lateral segments of dispersion. In this case, the programme produces a warning message (*'pericolo incrocio'*) and stops. In this situation, a small change of the release coordinates usually solves the situation.

6. It must be mentioned that the 850 hPa pressure surface lays around 1500 m AMSL. In the alpine region, this layer is below the mountain top, but as the field is continuously defined the plume can cross the Alps without discontinuity. The result has to be considered with caution.

7. As the albedo by clear sky is given as a fixed value for each grid cell, there is no seasonal variation. The mixing layer height is probably too high in winter when the ground is covered by snow. This limitation is not due to the model but to the way it is used. Updated albedo fields are available at the ECMWF and should be added to the daily meteorological data supply.

# 3. LORAN simulation results

## 3.1 First dry run on the 19th of April 1993

This first exercise, without real emission of tracer, was defined as in **Table 7**:

**Table 7.** 1st dry run, release specifications

| | |
|---|---|
| Release location | Munich, Germany |
| Latitude $\phi$ | 48.15 deg. North |
| Longitude $\lambda$ | 11.6 deg. East |
| Release height | At ground level |
| Release time | 19 April 1993, 12h00 UT |
| Release period | 6 hours |
| Source strength | 1 $gs^{-1}$ |
| Material | Inert gas, non-depositing |

The definitions of the six sets calculated for the 1st dry run are presented in **Table 8**. The first available meteorological field (column 2) necessary to compute dispersion must precede release time. When the time of forecasts initialization (column 3) precedes the time of first available meteorological field all fields are forecasted (set 1). If this initialization matches or succeeds the first available meteorological field time, only the fields for times after initialization are forecasted, the others being analysed (sets 2 to 6). Meteorological fields are given for every 6 hours. The sum of the number of forecasts with the number of analyses gives the 16 input fields needed for the 96-hour period covered by the model (16 x 6 hours = 96 hours).

**Table 8.** 1st dry run, sets definition

| Set number | First available meteo field time | Forecasts initialization time | Number of 6-hour forecasts | Number of 6-hour analyses |
|---|---|---|---|---|
| Set 1 | 19 Apr. 93, 12z | 18 Apr. 93, 12z | 16 | 0 |
| Set 2 | 19 Apr. 93, 12z | 19 Apr. 93, 12z | 15 | 1 |
| Set 3 | 19 Apr. 93, 12z | 20 Apr. 93, 12z | 11 | 5 |
| Set 4 | 19 Apr. 93, 12z | 21 Apr. 93, 00z | 9 | 7 |
| Set 5 | 19 Apr. 93, 12z | 21 Apr. 93, 12z | 7 | 9 |
| Set 6 | 19 Apr. 93, 12z | - | 0 | 16 |

In **Figure 4** concentrations are calculated with LORAN for 12 hours. after the beginning of the fictitious tracer release by means of forecasts initialized on the 18th of April 1993, 12 h UT (set 1). Wind vectors at 850 hPa are given every 1.125 degrees. The position of the maximum concentration indicated at the lower right corner of the plot is marked by a square.

**Figure 5** shows the same situation, but calculated by means of analyses only (set 6). After 24 hours. (**Figures 6 and 7**) the plume is quickly transported by the strong north-westerly wind. Very few differences are perceptible between forecasts and analyses of the wind field.

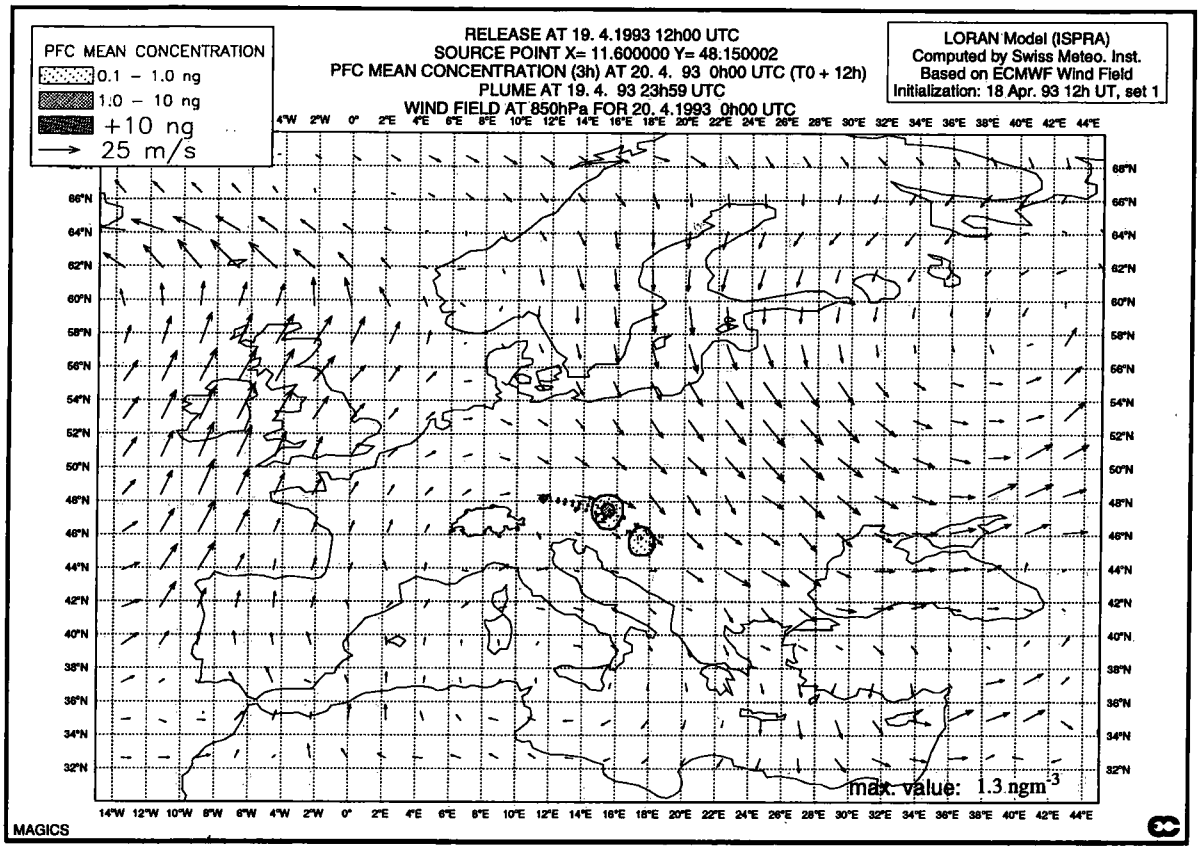


**Figure 4.** 1st dry run, concentrations at $T_o$ + 12 h, based on forecasts (set 1)

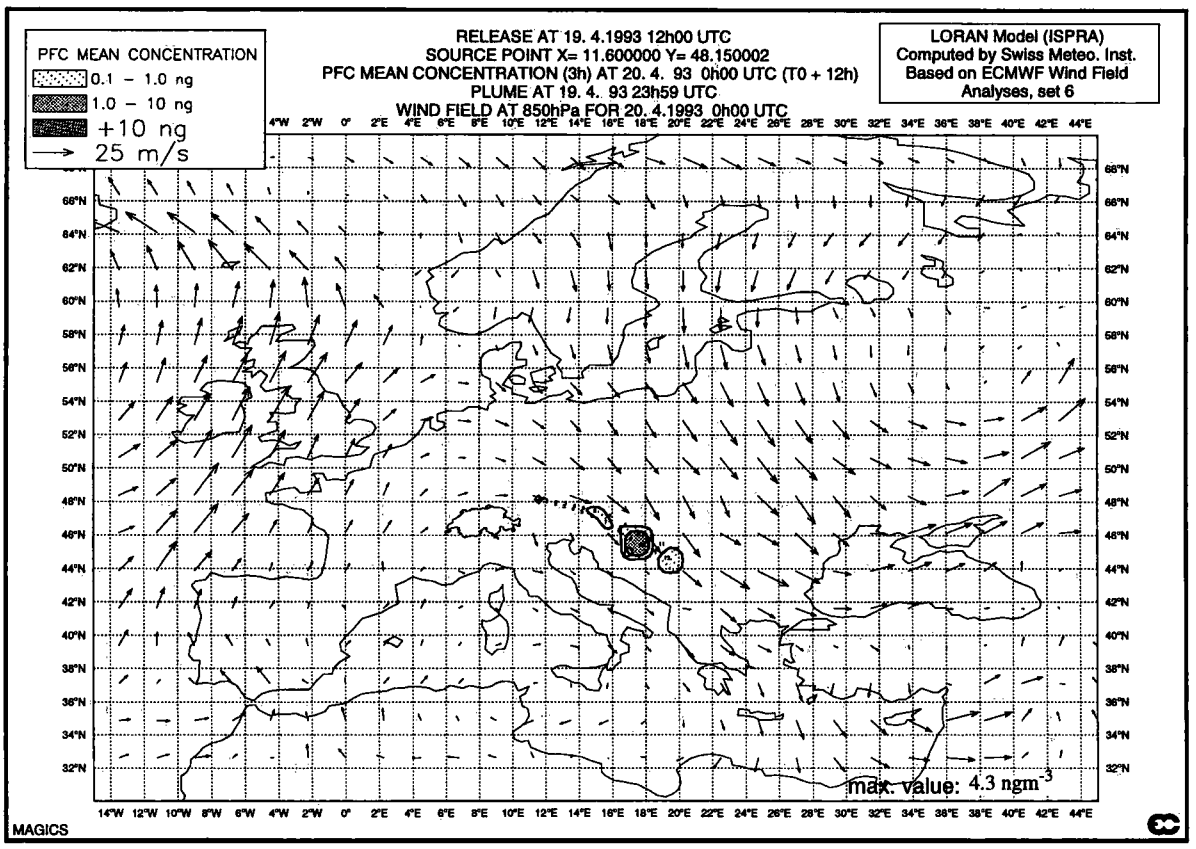


**Figure 5.** 1st dry run, concentrations at $T_o$ + 12 h, based on analyses (set 6)

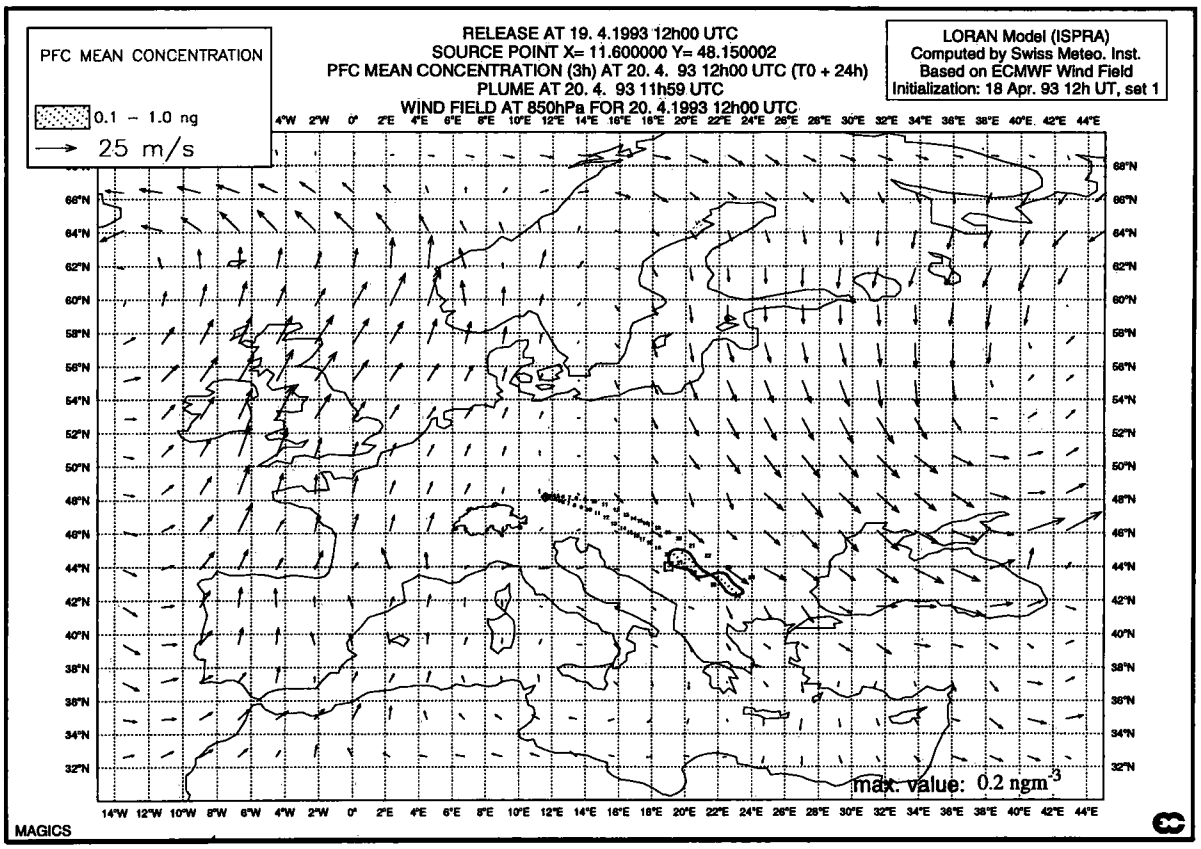


**Figure 6.** 1st dry run, concentrations at $T_0$ + 24 h, based on forecasts (set 1)

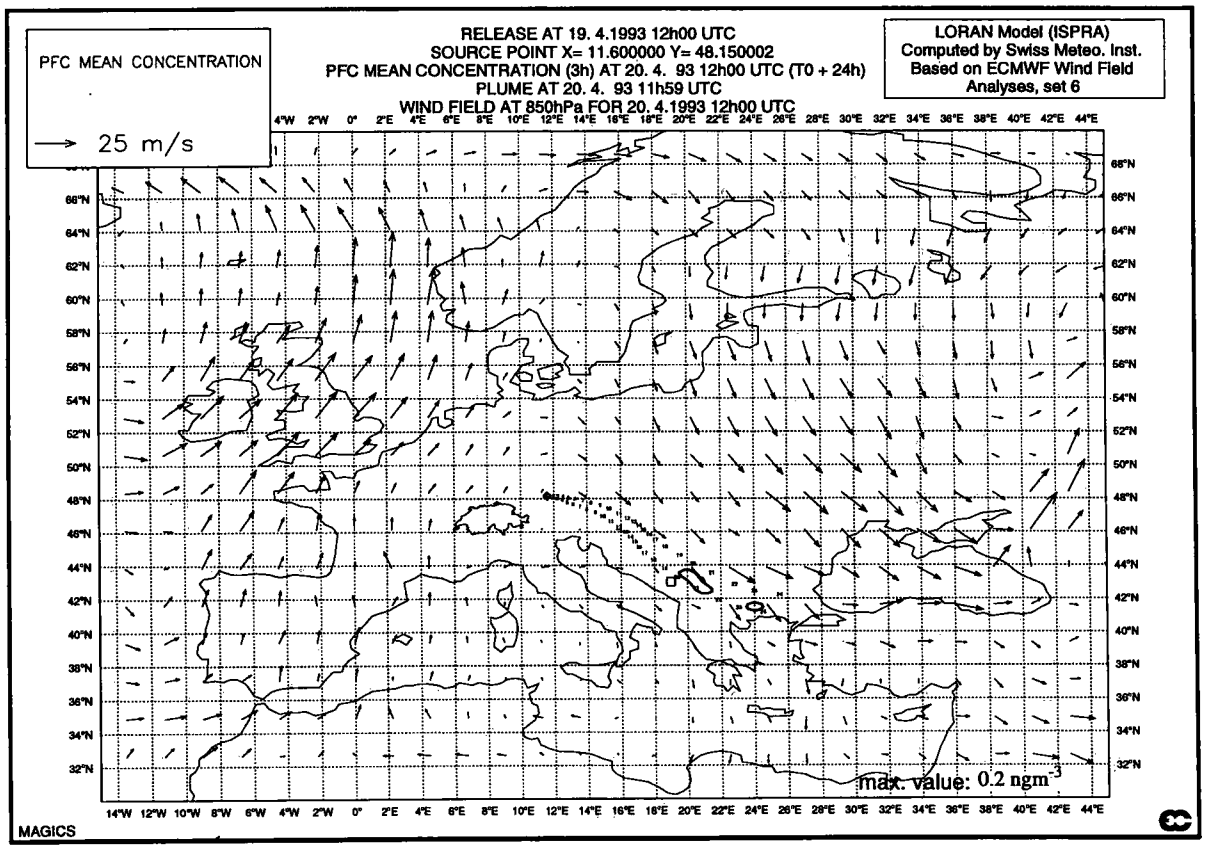


**Figure 7.** 1st dry run, concentrations at $T_0$ + 24 h, based on analyses (set 6)

## 3.2 Second dry run on the 7th of December 1993

Time and location of the second dry run are given in **Table 9**.

**Table 9.** 2nd dry run, release specifications

| | |
|---|---|
| Release location | Nancy, France |
| Latitude $\phi$ | 48.7 deg. north |
| Longitude $\lambda$ | 5.8 deg. east |
| Release height | Surface |
| Release time | 7 December 1993, 15h00 UT |
| Release period | 6 hours. |
| Source strength | 10 $gs^{-1}$ |
| Material | Inert gas, non-depositing |

The definitions of the six sets calculated for the 2nd dry run are listed in **Table 10**. Set 1 is completely based on forecasts. The first field of set 2 represents the analysis of the 7th of December, 12 h UT, used as the initialization for the next 15 forecasted meteorological fields. Set 6, completely based on analyses, was only available 5 days after the beginning of the release.

**Table 10.** 2nd dry run, sets definition

| Set number | 1st available meteo field time | Forecasts initialization time | Number of 6-hour forecasts | Number of 6-hour analyses |
|---|---|---|---|---|
| Set 1 | 7 Dec. 93, 12z | 6 Dec. 93, 12z | 16 | 0 |
| Set 2 | 7 Dec. 93, 12z | 7 Dec. 93, 12z | 15 | 1 |
| Set 3 | 7 Dec. 93, 12z | 8 Dec. 93, 12z | 11 | 5 |
| Set 4 | 7 Dec. 93, 12z | 9 Dec. 93, 00z | 9 | 7 |
| Set 5 | 7 Dec. 93, 12z | 9 Dec. 93, 12z | 7 | 9 |
| Set 6 | 7 Dec. 93, 12z | - | 0 | 16 |

As shown in **Figure 8**, the plume forecasted 24 h after the beginning of the fictitious release has already travelled over Western Countries of Europe, transported by a strong westerly wind. The same situation recalculated with analyses (**Figure 9**) shows a more spread out plume. We see that minor variations in wind field can have great influences on the dispersion of the plume. These differences are even more significant after 48 hours (**Figures 10 and 11**).

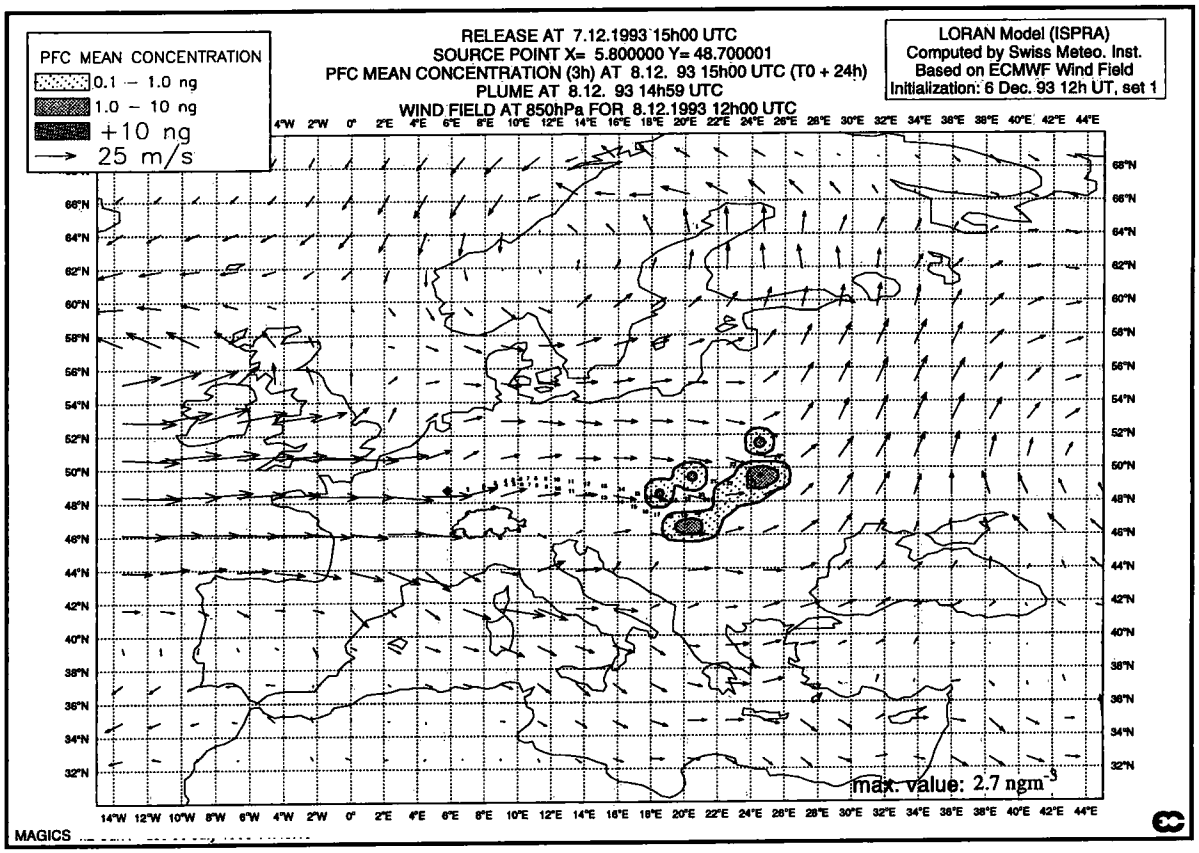


**Figure 8.** 2nd dry run, concentrations at $T_o$ + 24 h, based on forecasts (set1)

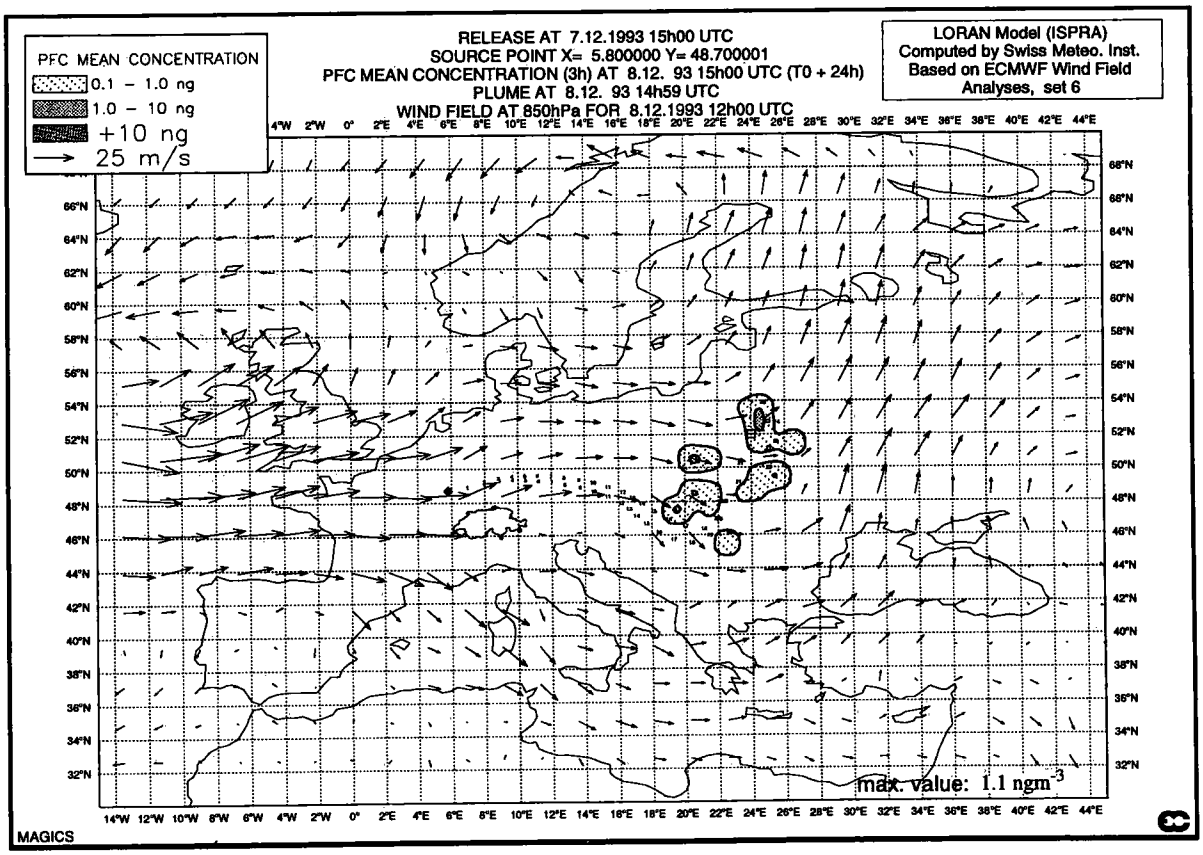


**Figure 9.** 2nd dry run, concentrations at $T_o$ + 24 h, based on analyses (set 6)

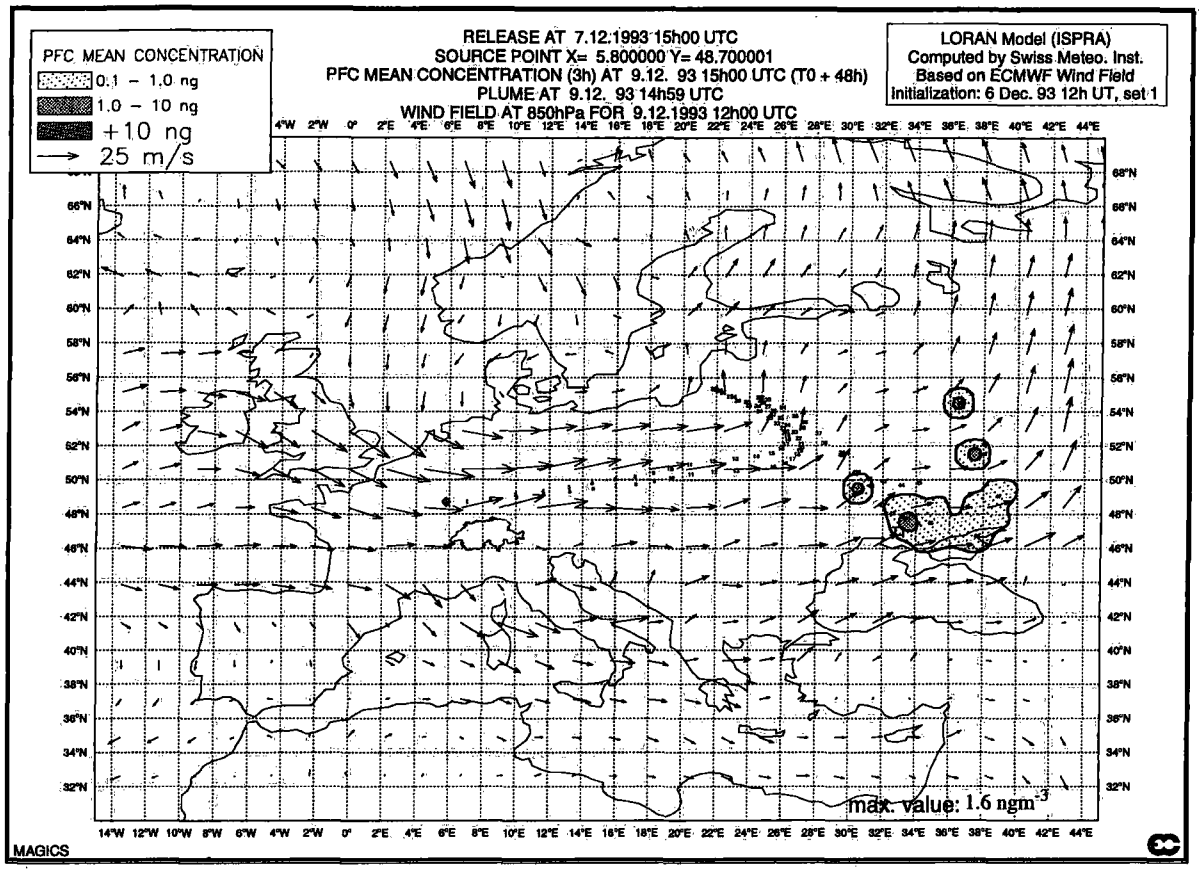


**Figure 10.** 2nd dry run, concentrations at $T_0 + 48$ h, based on forecasts (set 1)

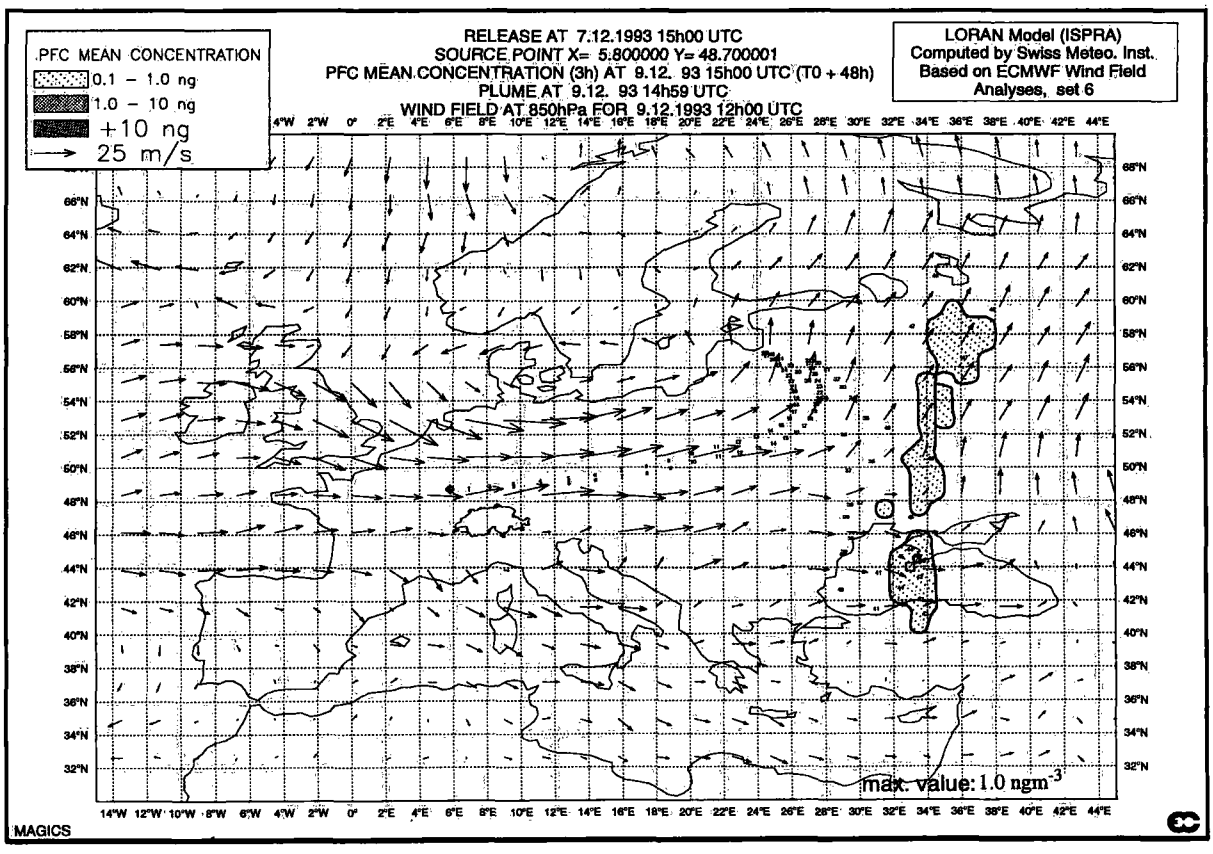


**Figure 11.** 2nd dry run, concentrations at $T_0 + 48$ h, based on analyses (set 6)

## 3.3 Third dry run on the 27th of July 1994

This third and last exercise was announced with specifications given in **Table 11**

**Table 11.** 3rd dry run, release specifications

| | |
|---|---|
| Release location | Frankfurt, Germany |
| Latitude $\phi$ | 50,1 deg. north |
| Longitude $\lambda$ | 8,7 deg. east |
| Release height | Surface |
| Release time | 27th July 1994, 10h00 UT |
| Release period | 6 hours |
| Source strength | 10 $gs^{-1}$ |
| Material | Inert gas, non-depositing |

For this third dry run, the different calculated sets have been defined as shown in **Table 12.**

**Table 12.** 3rd dry run, sets definition

| Set number | First available meteo field time | Forecasts initialization time | Number of 6-hour forecasts | Number of 6-hour analyses |
|---|---|---|---|---|
| Set 1 | 27 July 94, 00z | 26 July 94, 12z | 16 | 0 |
| Set 2 | 27 July 94, 00z | 27 July 94, 12z | 15 | 1 |
| Set 3 | 27 July 94, 00z | 28 July 94, 00z | 13 | 3 |
| Set 4 | 27 July 94, 00z | 28 July 94, 12z | 11 | 5 |
| Set 5 | 27 July 94, 00z | 29 July 94, 00z | 9 | 7 |
| Set 6 | 27 July 94, 00z | - | 0 | 16 |

In rather low wind conditions, the plume calculated 24 h after the beginning of release is moving slowly towards the North Sea (**Figure 12**). The same situation described by analyses (**Figure 13**) yields quite the same resulting plume. After 48 hours (**Figures 14 and 15**) the plume reaches Denmark and keeps a rather high concentration with either calculation based on forecasts or on analyses.

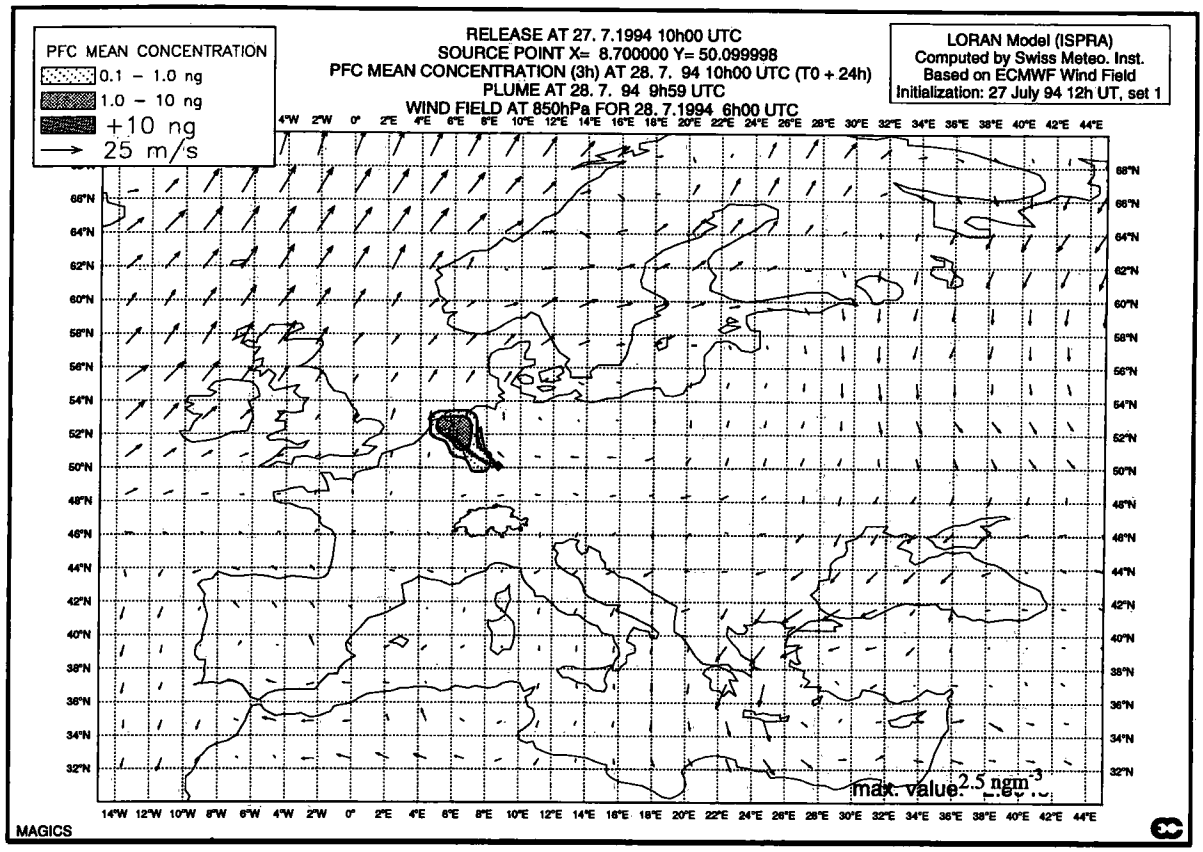


**Figure 12.** 3rd dry run, concentrations at $T_0$ + 24 h, based on forecasts (set 1)

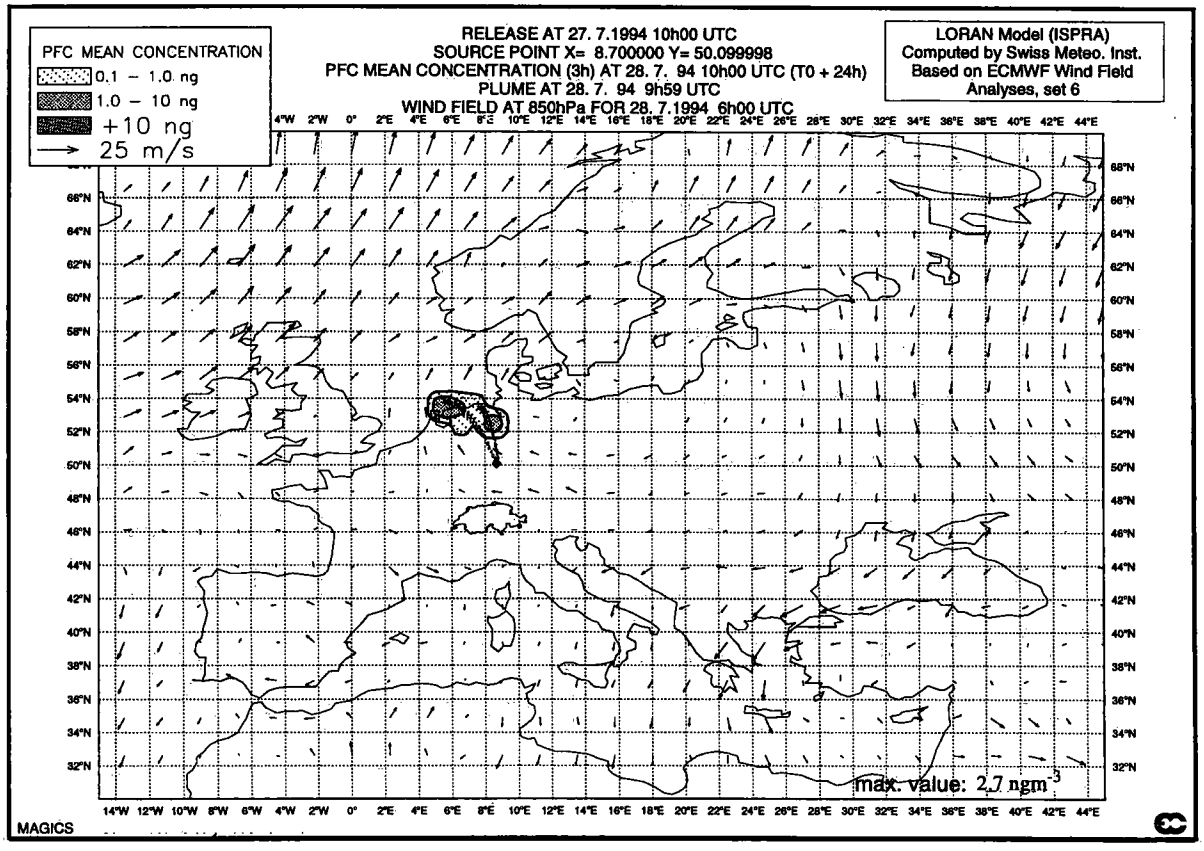


**Figure 13.** 3rd dry run, concentrations at $T_0$ + 24 h, based on analyses (set 6)

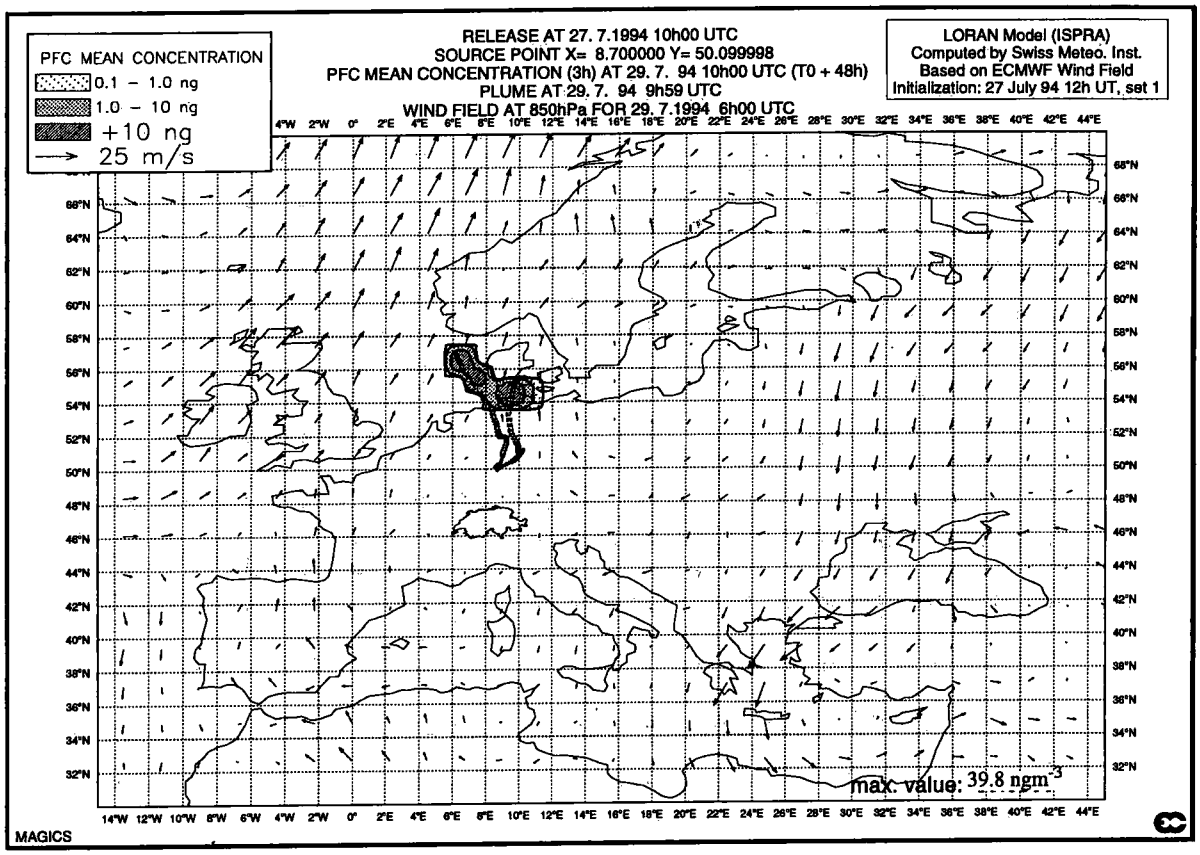


**Figure 14.** 3rd dry run, concentrations at $T_o$ + 48 h, based on forecasts (set 1)

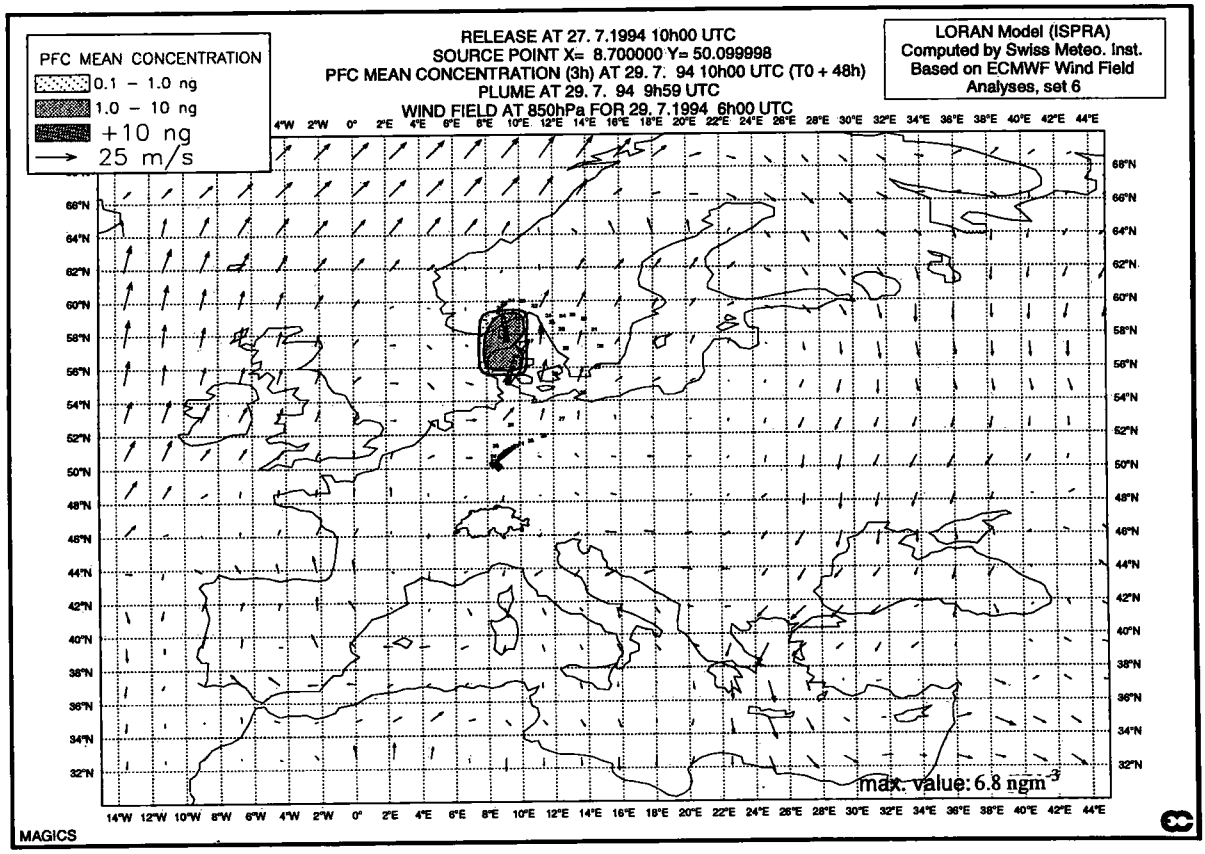


**Figure 15.** 3rd dry run, concentrations at $T_o$ + 48 h, based on analyses (set 6)

## 3.4 First tracer experiment on the 23rd of October 1994

After two years of intensive preparation needed by the JRC to install about 170 tracer sampling stations and complete administrative work and negotiations with all participating countries, it announced that it was ready to undertake the first experiment between the 15th of October and the 15th of December 1994. The first occurrence of a suitable weather situation providing the best chance for the tracer to cross the region equipped with measurement stations appeared in the second part of October 1994. The release was decided for the 23rd of October, at 16 h UT and was announced to participants only one hour before. The specifications are detailed in **Table 13.**

**Table 13.** Release specifications for the 1st tracer experiment

| | |
|---|---|
| Release location | Monterfil near Rennes, France |
| Latitude $\phi$ | 48,04 deg. north |
| Longitude $\lambda$ | 2,01 deg. west |
| Release height | Surface |
| Release time | 23 October 94, 16h00 UT |
| Release period | 12 hours |
| Source strength | 7,9 $gs^{-1}$ |
| Material | Perfluormethylcyclohexane |

The different sets calculated after the alert and during the following days are described in **Table 14**. The first set was calculated immediately after the official announcement of the experiment. At that time (23th of October 15h UT) the last forecast available was based on the initialization of 23 October 0 h UT. Set 2 was only computed in late afternoon, when forecasts based on the initialization of 23 October 12 h UT became available from the MARS (Meteorological Archive and Retrieval System) database at the ECMWF.

**Table 14.** Sets definition for the 1st tracer experiment

| Set number | 1st available meteo field time | Forecasts initialisation time | Number of 6-hour forecasts | Number of 6-hour analyses |
|---|---|---|---|---|
| Set 1 | 23 Oct. 94 12z | 23 Oct. 94 00z | 16 | 0 |
| Set 2 | 23 Oct. 94 12z | 23Oct. 94 12z | 15 | 1 |
| Set 3 | 23 Oct. 94 12z | 24 Oct. 94 12z | 11 | 5 |
| Set 4 | 23 Oct. 94 12z | 25 Oct. 94 00z | 9 | 7 |
| Set 5 | 23 Oct. 94 12z | 25 Oct. 94 12z | 7 | 9 |
| Set 6 | 23 Oct. 94 12z | - | 0 | 16 |

The forecast of tracer motion after 24 hours by rapid west wind prevailing over Central Europe is shown in **Figure 16**. The same situation calculated with analyses (**Figure 17**) displays a plume spreading a little more southward. In reality, the air sampling collected at that time in

Switzerland revealed no tracer at all. The provisional tracer measurements data set (version of the 5th of May 1996) of the first experiment made available to the ETEX participants by the JRC Ispra shows that the plume was detected at ground level more to the north than calculated by LORAN.

After 48 hours, the plume already reached countries east of the 15° longitude (Czeck and Slovak Federal Republic, Hungary), pushed by a strong westerly wind (**Figure 18).** Analyses tend to move the plume more southerly (**Figure19**) than it was forecasted.

Wind profiles observed over Payerne by aerological soundings on the 24th of October 94 at 12 h UT and 18 h UT (respectively 20 hours and 26 hours after release) show a general west-south-westerly circulation, turning to south-west near the ground (**Figure 20**). This is due to the influence of the Jura Mountains and the Alps, channelling the flow over the Swiss Plateau. The cause of the absence of tracer detection in Switzerland is to be found in the southern rotation of the wind near ground, pushing the plume to the north relative to the 850 hPa general westerly wind given by the ECMWF. This effect also appears slightly on results of the Swiss Model (SM) showed on **Figure 21** (p.37) for the level 850 hPa (at about 1500 m AMSL) and in more details on **Figure 22,** displaying the wind computed at 10 m above the topography of the model. The flow deviation to north-west at the left of the Jura Mountains appears very well and produces a good argument to explain why Switzerland was protected from tracer inflow. The virtual trajectories computed from plain stations (**Figure 23**) and mountain stations (**Figure 24**) are obtained by adding six successive hourly wind measurements at 10 m above ground. The general south-west wind direction prevails on most of the Plateau stations. Plain stations in the Alps indicate very different wind directions, because of the canalization into narrow valleys. Such types of plots are useful to compare wind fields predicted or analysed by numerical models and wind measurements really observed on complex terrain which are influenced by small scale topography, not included in the model. They agree more or less with the computed ground wind field given by the SM model. This is an encouragement to involve this mesoscale model for future work on regional dispersion study.

On the release site, at Monterfil, the vertical profile of the horizontal wind observed by Sodar (**Figure 25**) indicates, on the 23rd of October, between 16 h and 18 UT, a slight wind rotation from west-south-west near the ground to west at 300 m above ground. At the beginning of the release, the plume was already transported further north in comparison with the computed model. From 16 h to 20 h the vertical component of the wind (**Figure 26**) denotes ascending flow due to instabilities well observed by the corresponding BVC trajectory described in section 4.2.

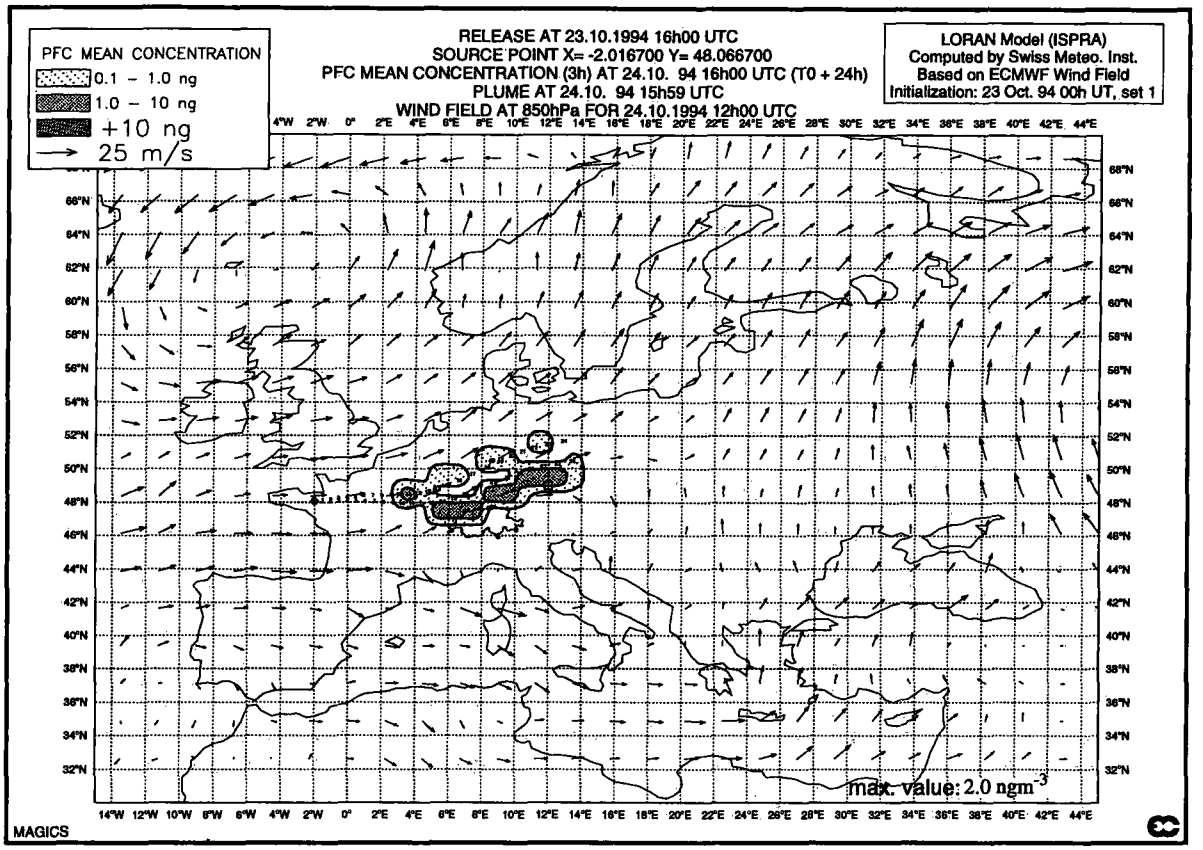


**Figure 16.** 1st experiment, concentrations at $T_o$ + 24 h, based on forecasts (set 1)

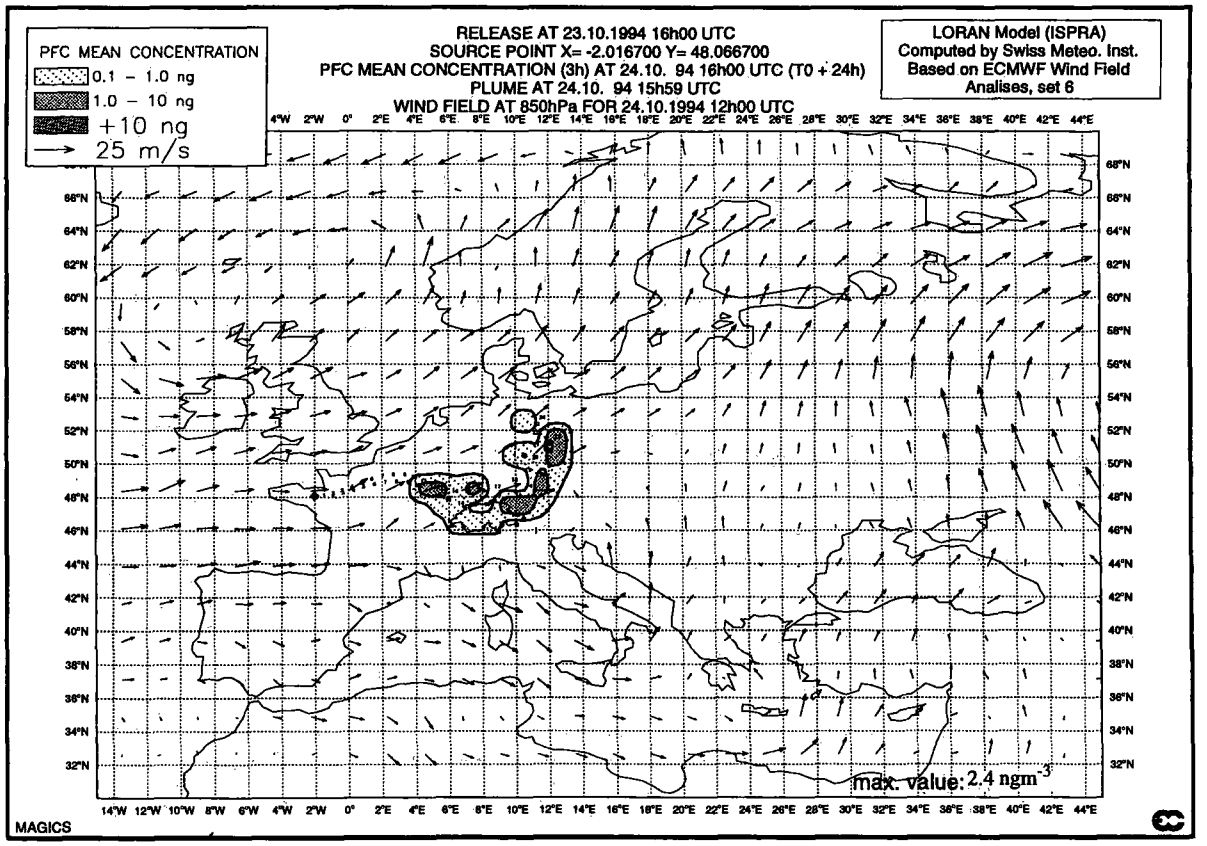


**Figure 17.** 1st experiment, concentrations at $T_o$ + 24 h, based on analyses (set 6)

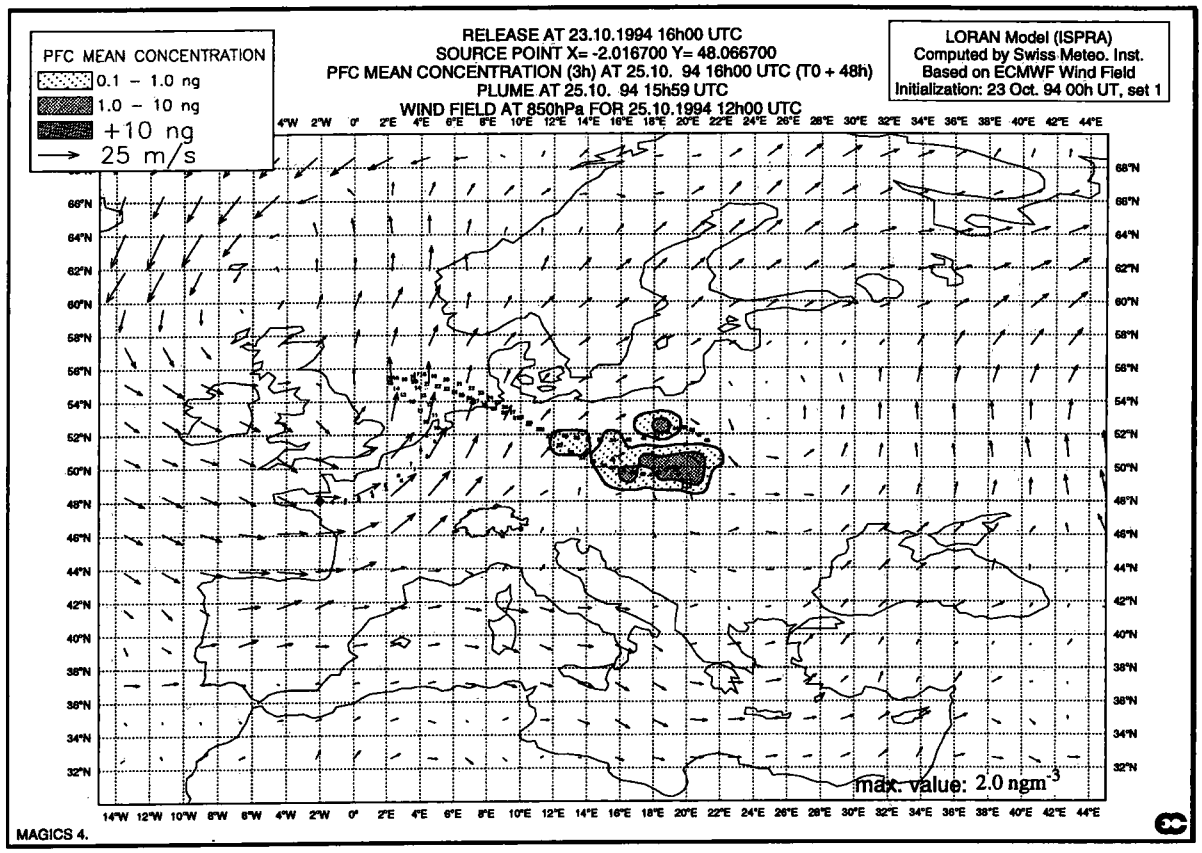


**Figure 18.** 1st experiment, concentrations at $T_o$ + 48 h, based on forecasts (set 1)

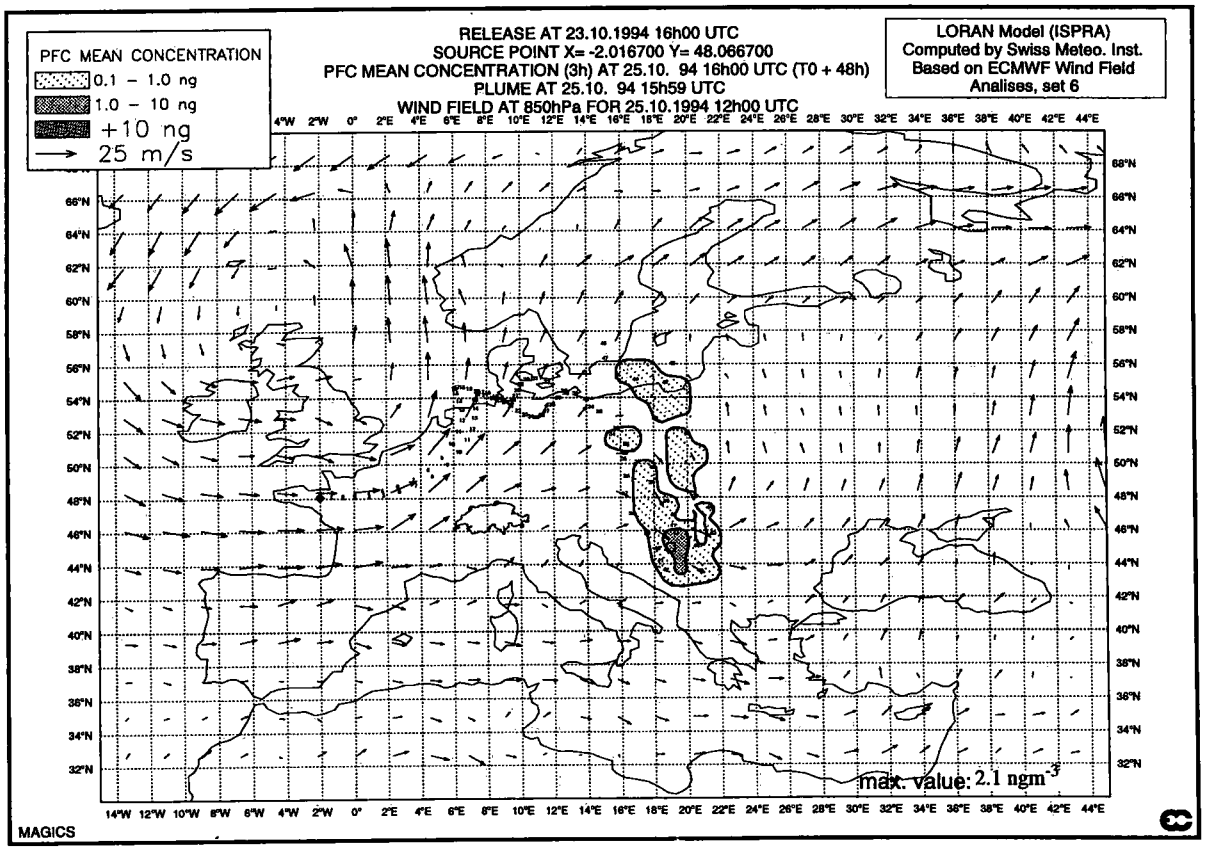


**Figure 19.** 1st experiment, concentrations at $T_o$ + 48 h, based on analyses (set 6)

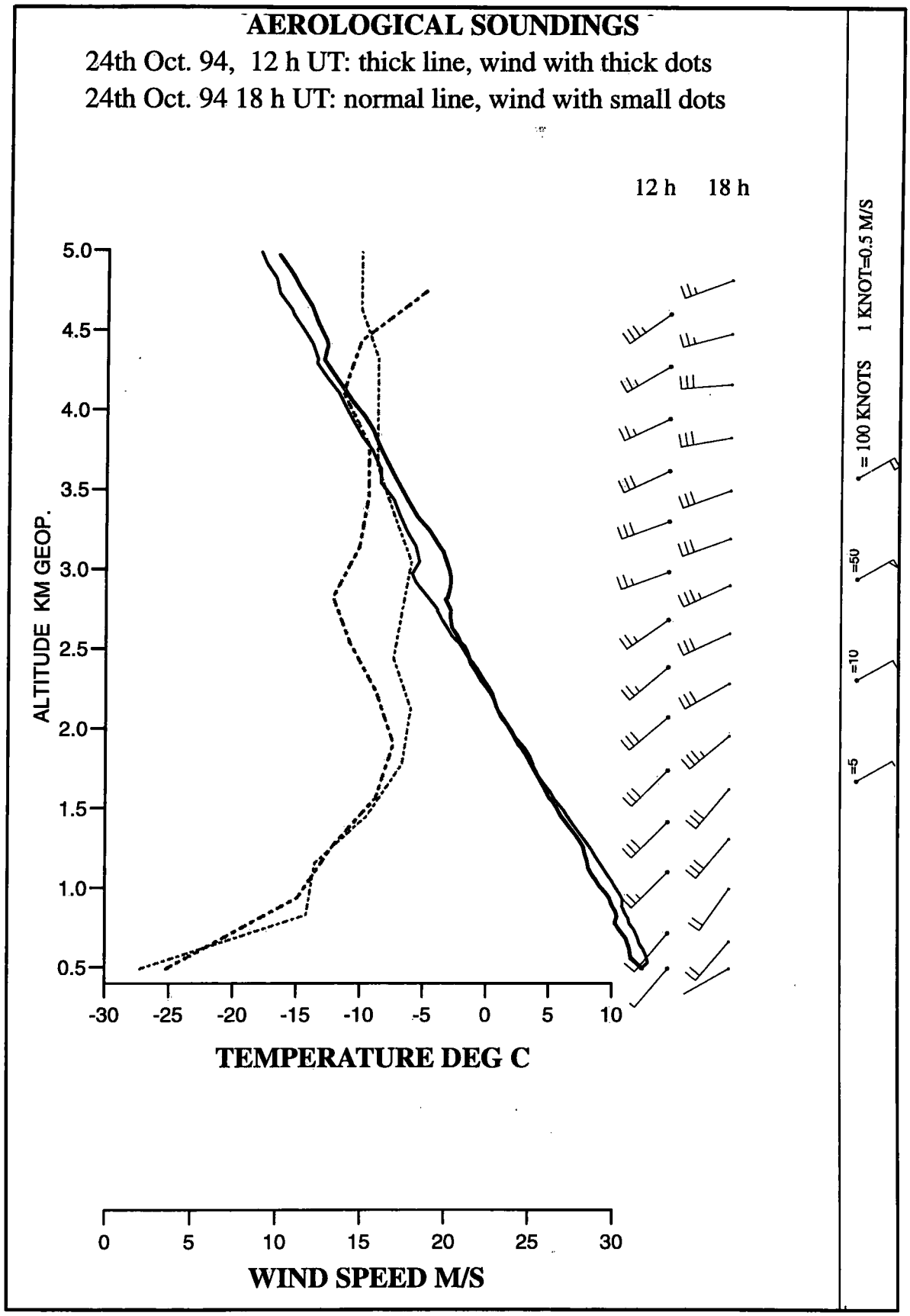


**Figure 20.** Aerological soundings, Payerne, 24 Oct. 94, 12 h and 18 h UT

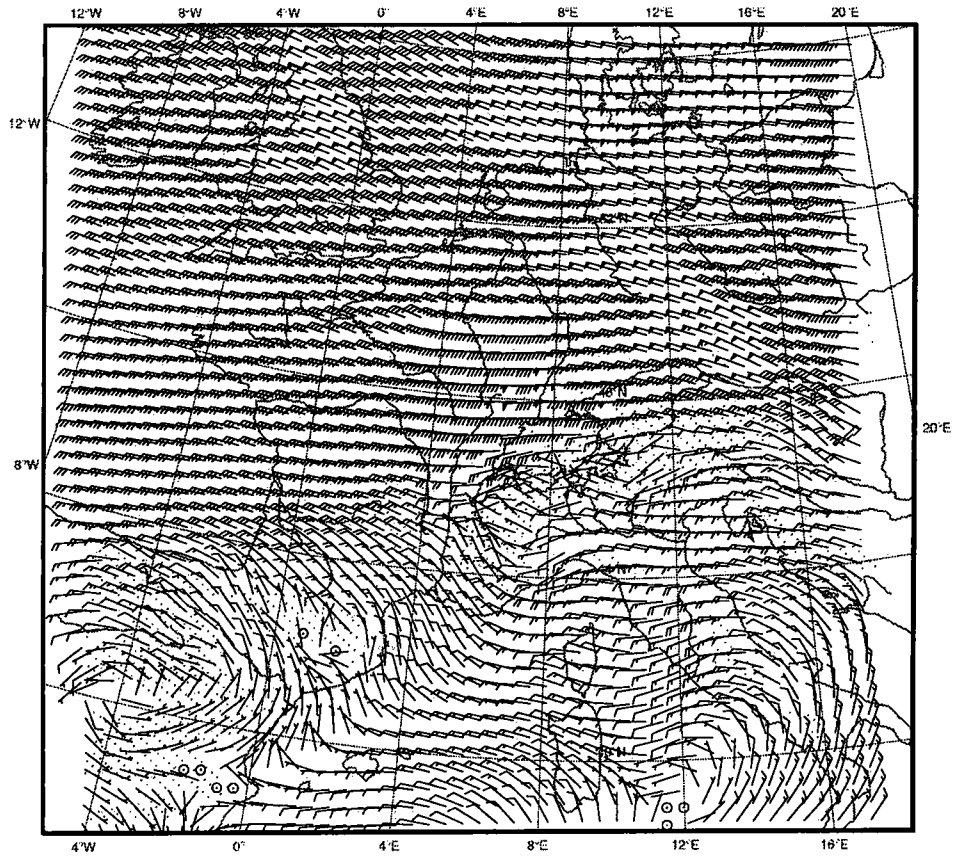


**Figure 21.** SM wind field at 850 hPa over Europe, 24 Oct. 94 at 06 h UT

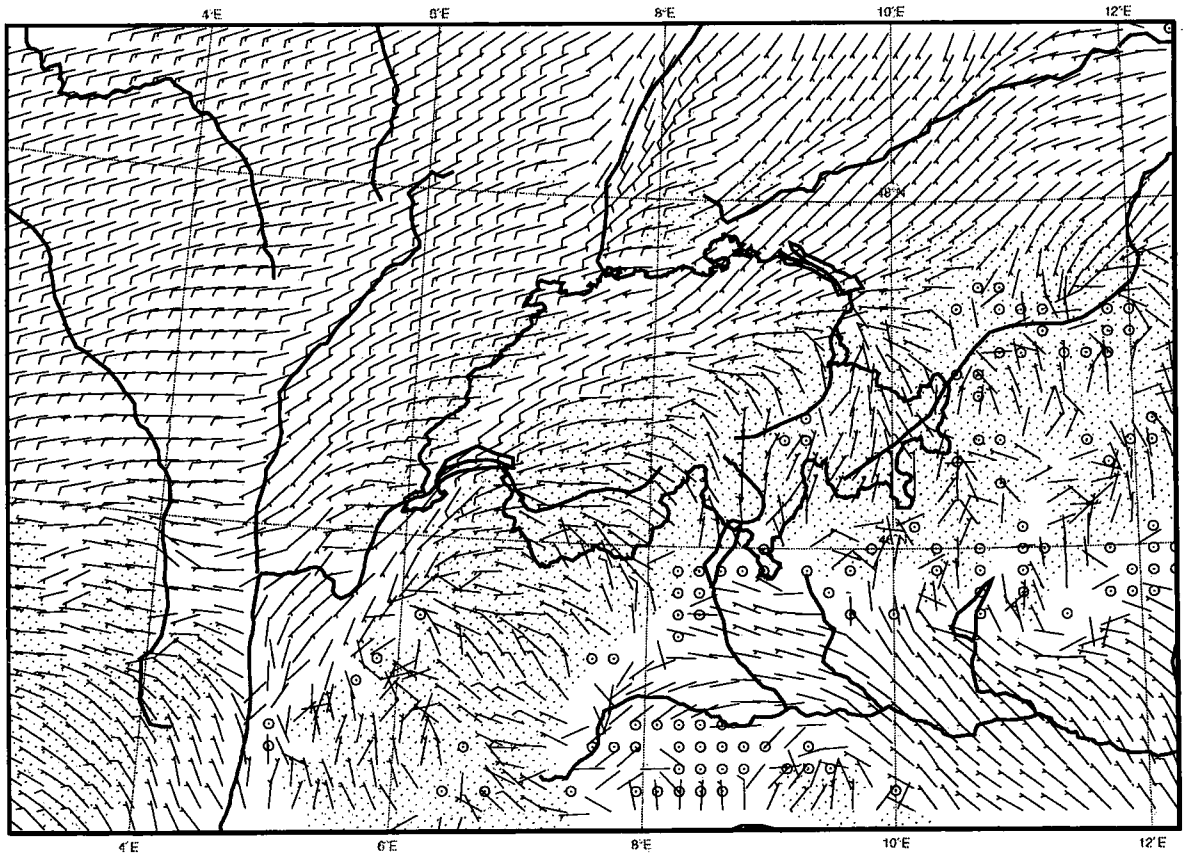


**Figure 22.** SM wind field at level 10 m, over Switzerland, 24 Oct. 94 at 06 h UT

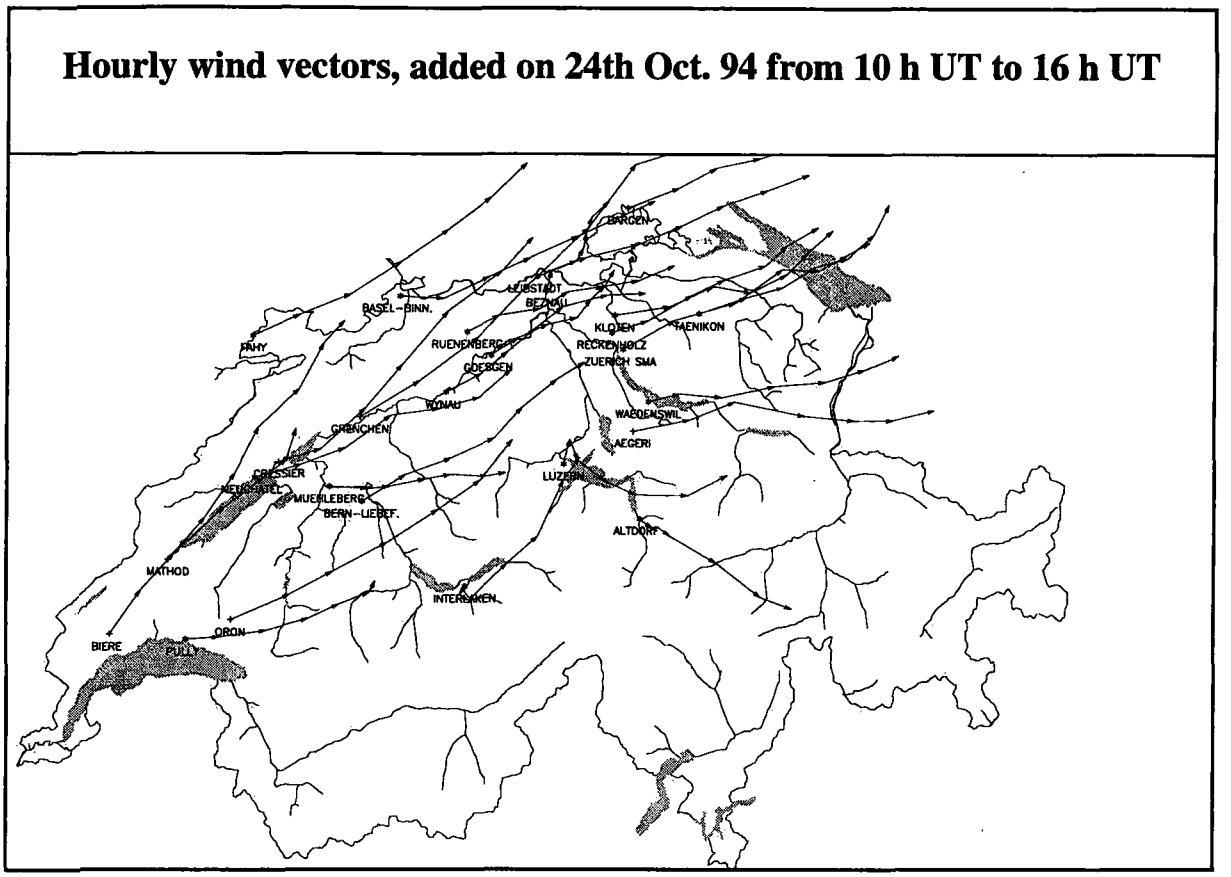


**Figure 23.** Virtual trajectories from plain stations 24 Oct. 94, 10 h - 16 h UT

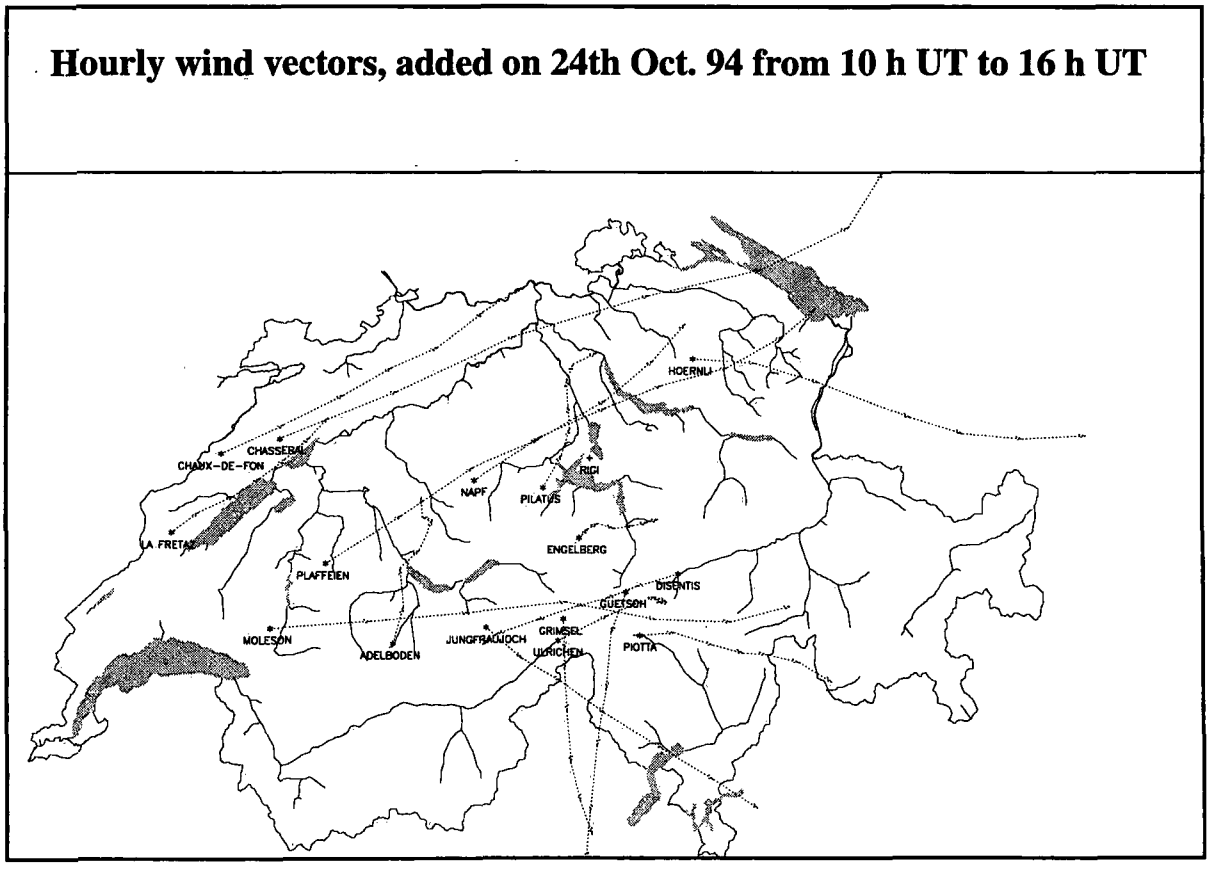


**Figure 24.** Virtual trajectories from mountain stations, 24 Oct. 94, 10 h - 16 h UT

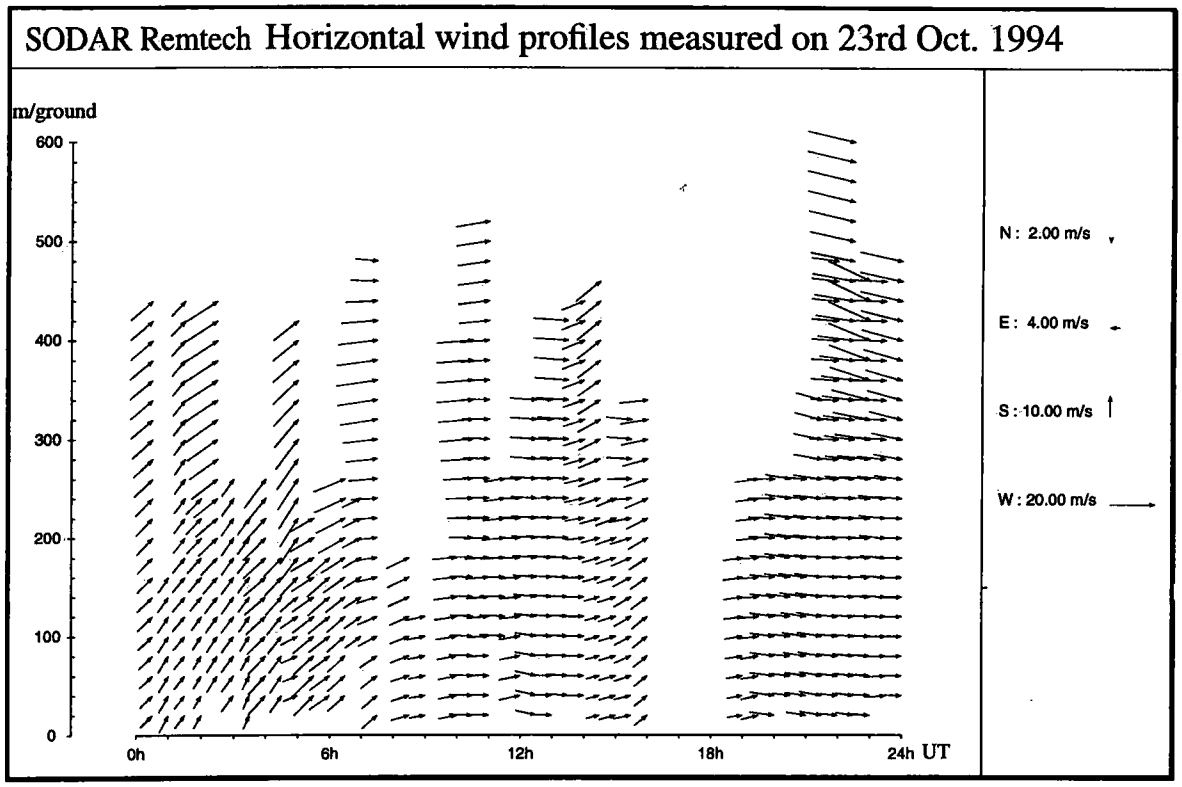


**Figure 25.** Profiles of horizontal wind over the release site, 23 Oct. 94

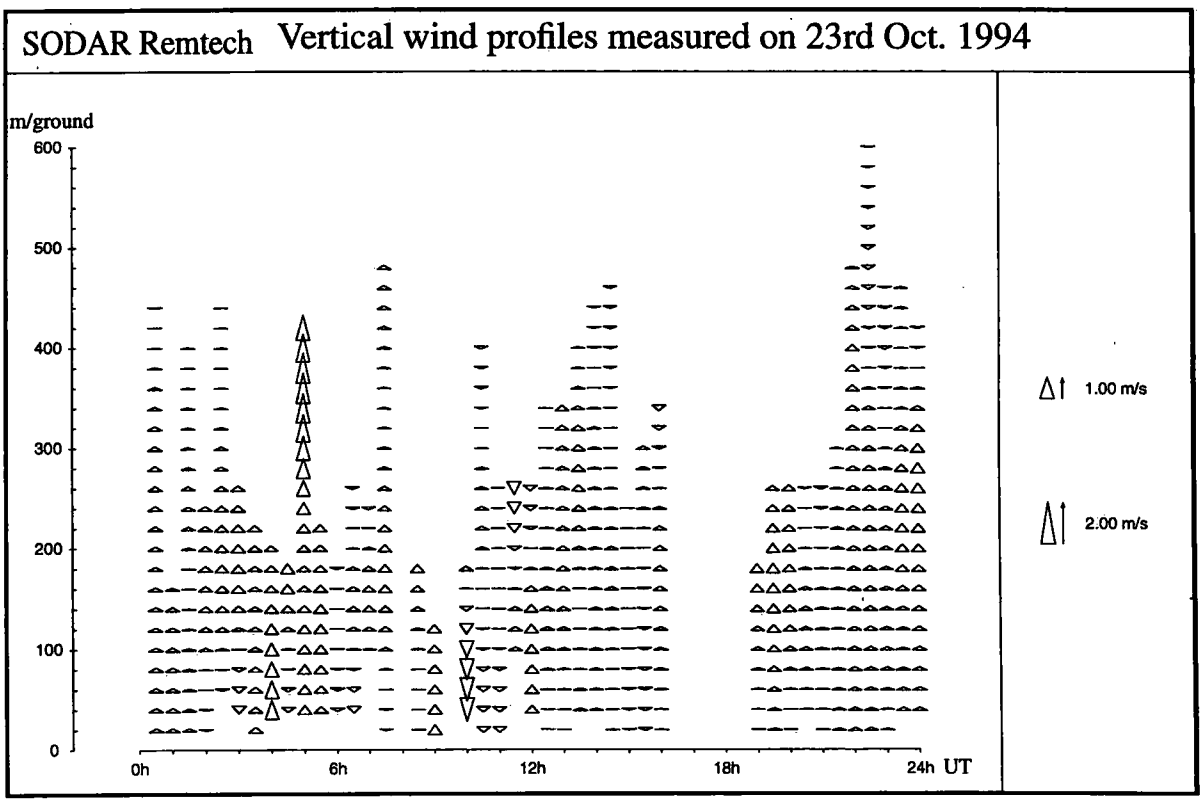


**Figure 26.** Profiles of vertical wind over the release site, 23 Oct. 94

## 3.5 Second tracer experiment on the 14th of November 1994

After the good result of the 1st tracer experiment, it was decided to undertake the second release. The next favourable situation occurred the third week of November, and the release was scheduled to start on 14th of November at 15 h UT, which corresponds to a synoptic time at which all meteorological measurements over the world are synchronized. The detailed specifications of the experiment are given in **Table 15,** and the set definitions in **Table 16.**

**Table 15.** Release specifications for the 2nd tracer experiment

| | |
|---|---|
| Release location | Rennes, France |
| Latitude $\phi$ | 48,04 deg. North |
| Longitude $\lambda$ | 2,01 deg. West |
| Release height | Surface |
| Release time | 14 November 94, 15h00 UT |
| Release period | 12 hours |
| Source strength | 11,3 $gs^{-1}$ |
| Material | Perfluoromethylcyclopentane |

**Table 16.** Sets definition for the 2nd tracer experiment

| Sets number | 1st available meteo field time | Forecasts initialization time | Number of 6-hour forecasts | Number of 6-hour analyses |
|---|---|---|---|---|
| Set 1 | 14 Nov. 94 12z | 14 Nov. 94 00z | 16 | 0 |
| Set 2 | 14 Nov. 94 12z | 14 Nov. 94 12z | 15 | 1 |
| Set 3 | 14 Nov. 94 12z | 15 Nov. 94 12z | 11 | 5 |
| Set 4 | 14 Nov. 94 12z | 16 Nov. 94 00z | 9 | 7 |
| Set 5 | 14 Nov. 94 12z | 16 Nov. 94 12z | 7 | 9 |
| Set 6 | 14 Nov. 94 12z | - | 0 | 16 |

After 24 hours, the predicted plume had already passed over the North of Switzerland (**Figure 27**). The analysis (**Figure 28**) showed weaker wind at 850 hPa, and the tail of the computed plume was still over our country. As the tracer measurement results for the 2nd experiment are not yet available, it is too early to comment these model results with confidence. One day later (**Figures 29 and 30**) the plume was located over the north of the Black Sea. The forecasted plume spread over a smaller region than the plume obtained later by analysed wind fields. The aerological soundings of Payerne (**Figure 31**) are characterized by a western synoptic wind above 2000 m AMSL. Within the lower layer, the wind direction turns to south-west under the channelling influence of the Jura Mountain and of the Alps. The prevailing

western wind at 850 hPa over West Europe appear also in the chart delivered by the SM model (**Figure 32**). The wind field computed at 10 m above ground (**Figure 33**) is strongly affected by the topography. The prevailing south-western wind near the ground had very probably prevented the tracer from reaching Switzerland during this second experiment. The virtual trajectories issued from plain stations (**Figure 34**) and from mountain stations (**Figure 35**) also have a general tendency to move toward the north-east. The vertical profiles of the horizontal wind component observed over the release site (**Figure 36**) indicate that the low level flow is coming from the south-west pushing the tracer plume north-easterly before it reaches the synoptic west current at higher level. The profiles of vertical wind component present apparent descending currents (**Figure 37**) probably due to precipitation.

The low level south-western wind at the release site and the south-western wind due to the effects of the Jura Mountain and of the Alps very probably drove the tracer more to the north of Switzerland than stated by the LORAN model.

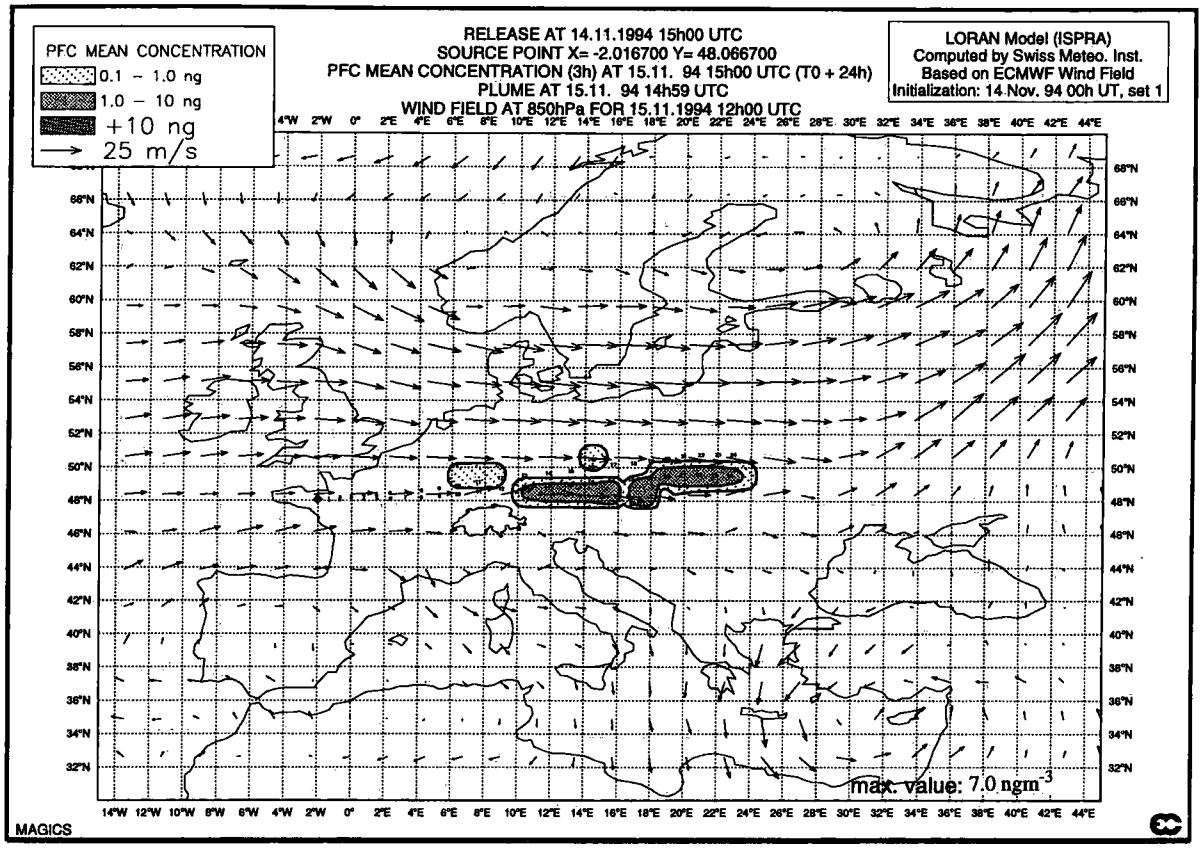


**Figure 27.** 2nd experiment, concentrations at $T_o$ + 24 h, based on forecasts (set 1)

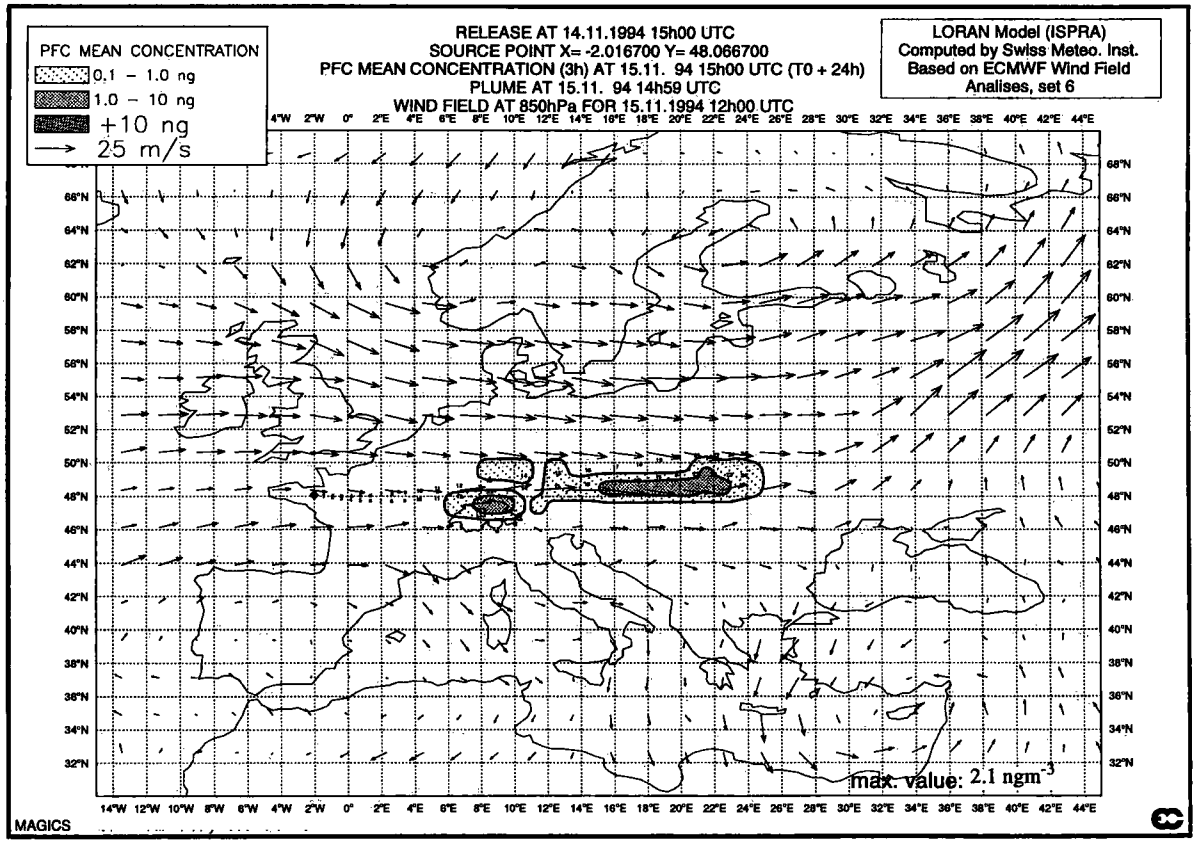


**Figure 28.** 2nd experiment, concentrations at $T_o$ + 24 h, based on analyses (set 6)

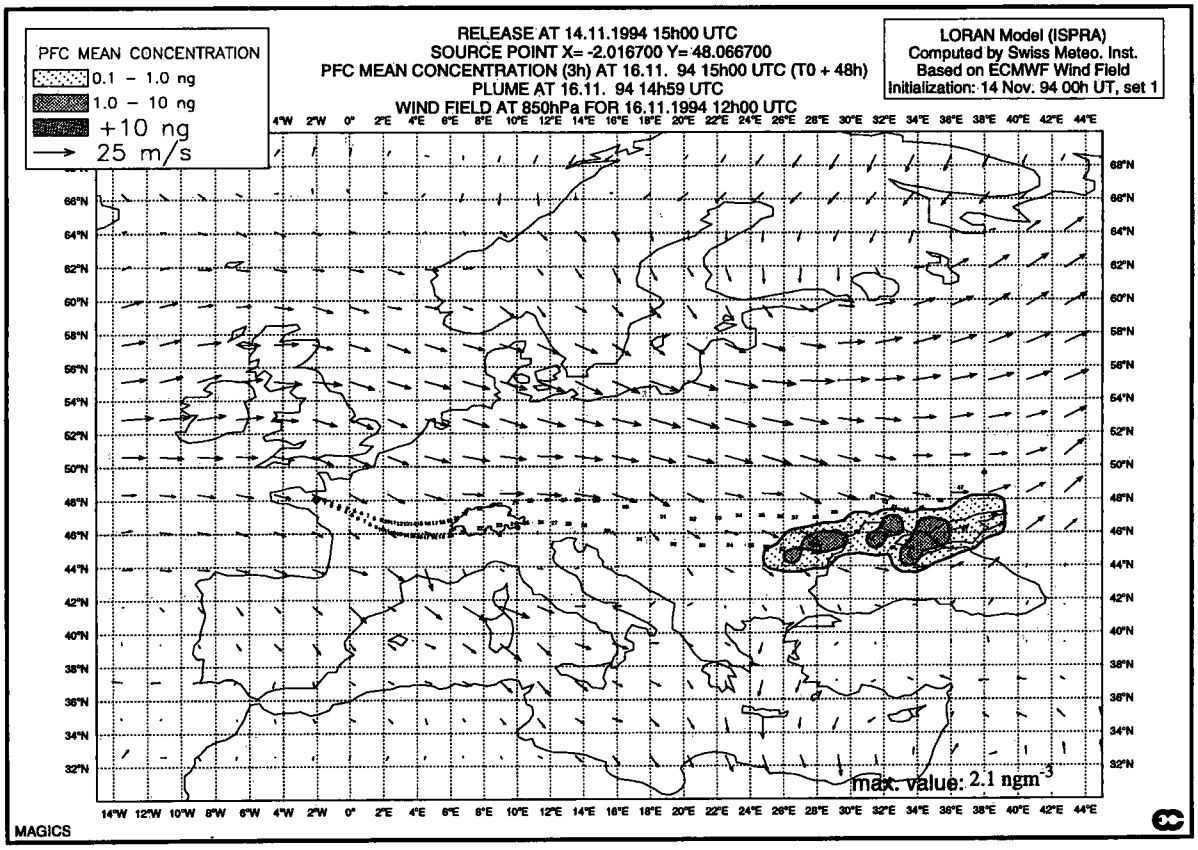


**Figure 29.** 2nd experiment, concentrations at $T_0$ + 48 h, based on forecasts (set 1)

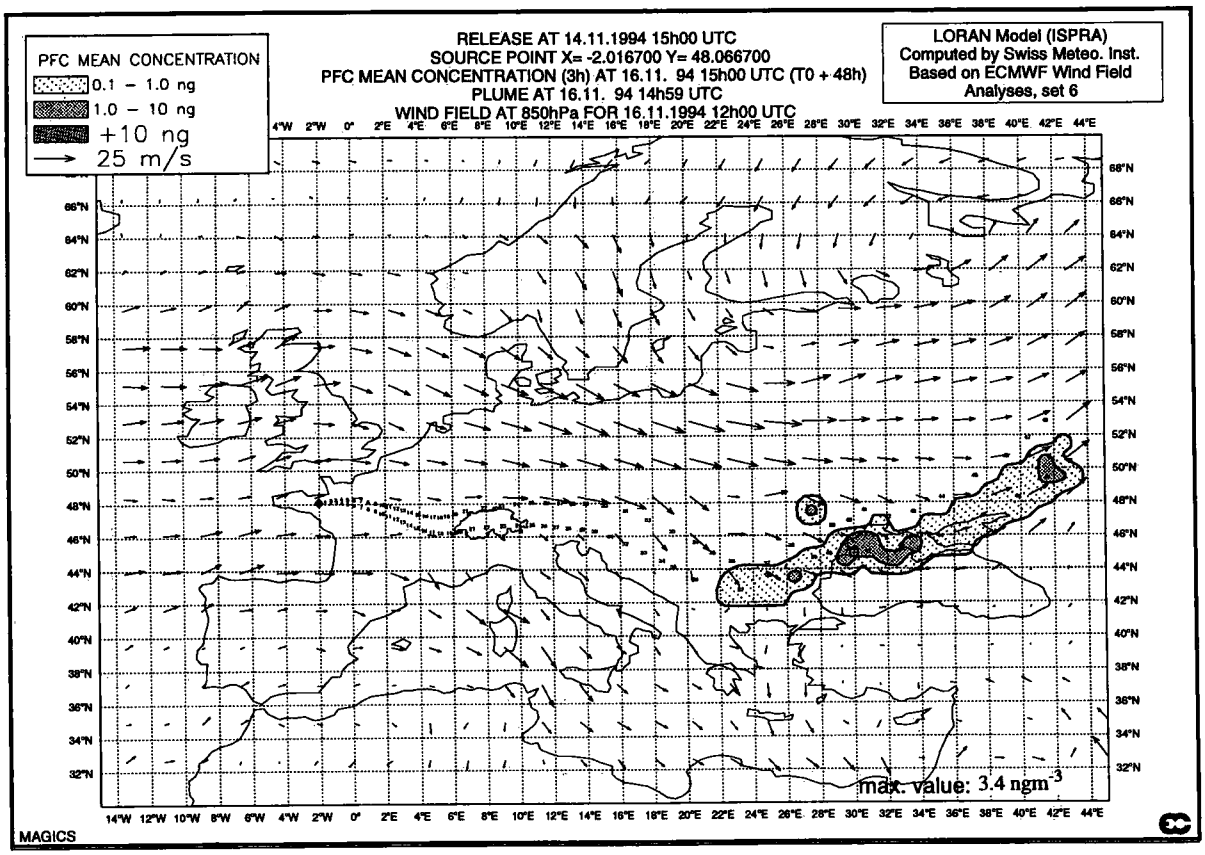


**Figure 30.** 2nd experiment, concentrations at $T_0$ + 48 h, based on analyses (set 6)

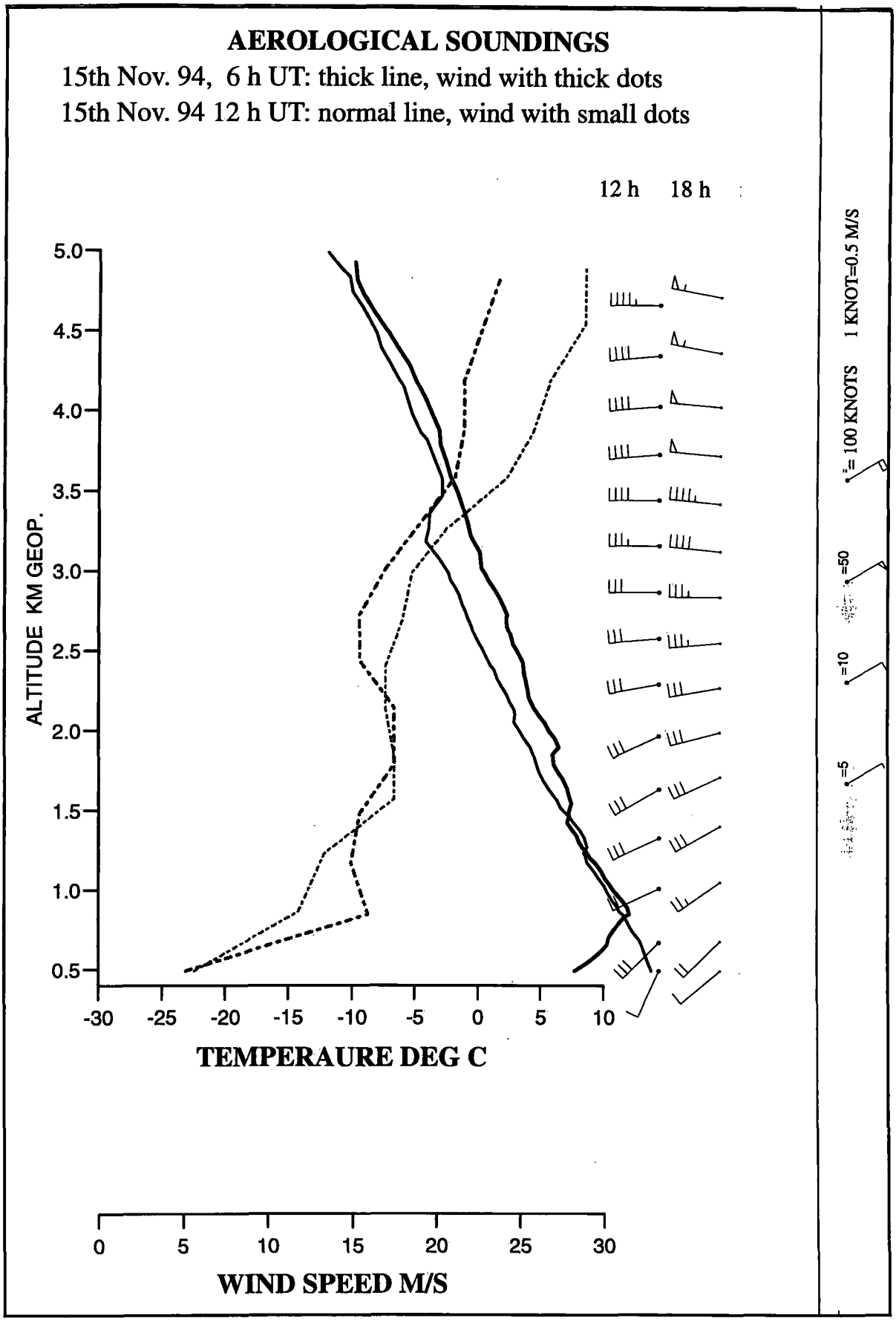


**Figure 31.** Aerological soundings, Payerne 15 Nov. 94, at 6 h and 12 h UT

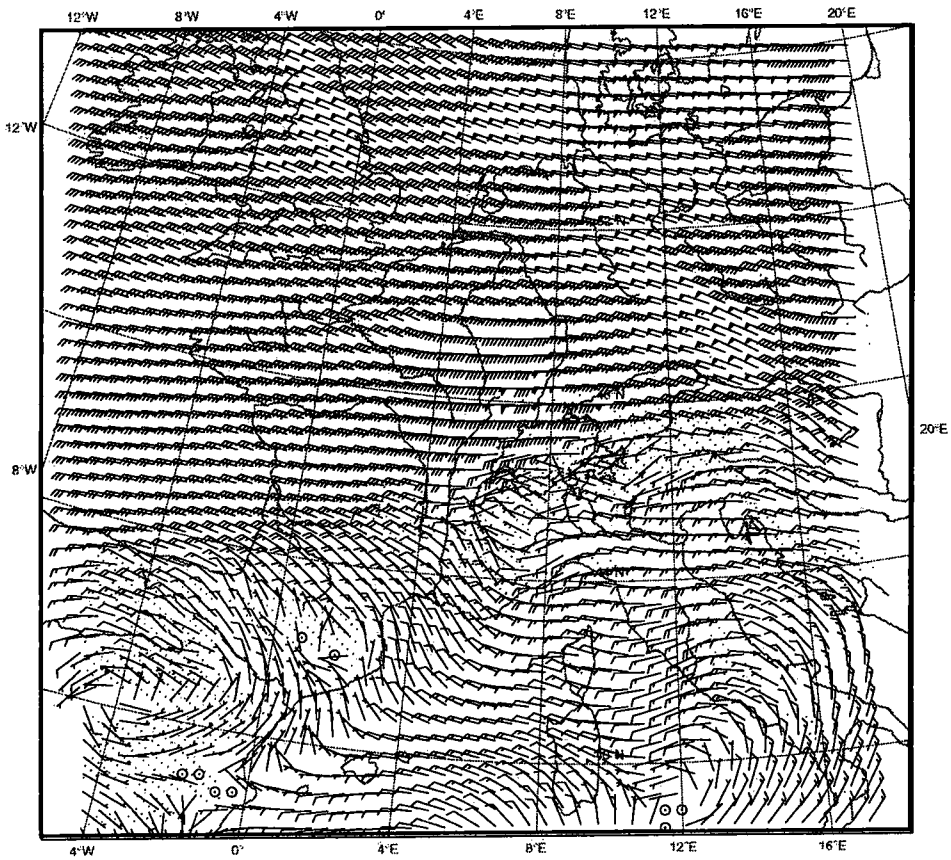


**Figure 32.** SM wind field at 850 hPa over Europe, 15 Nov. 94 at 06 h UT

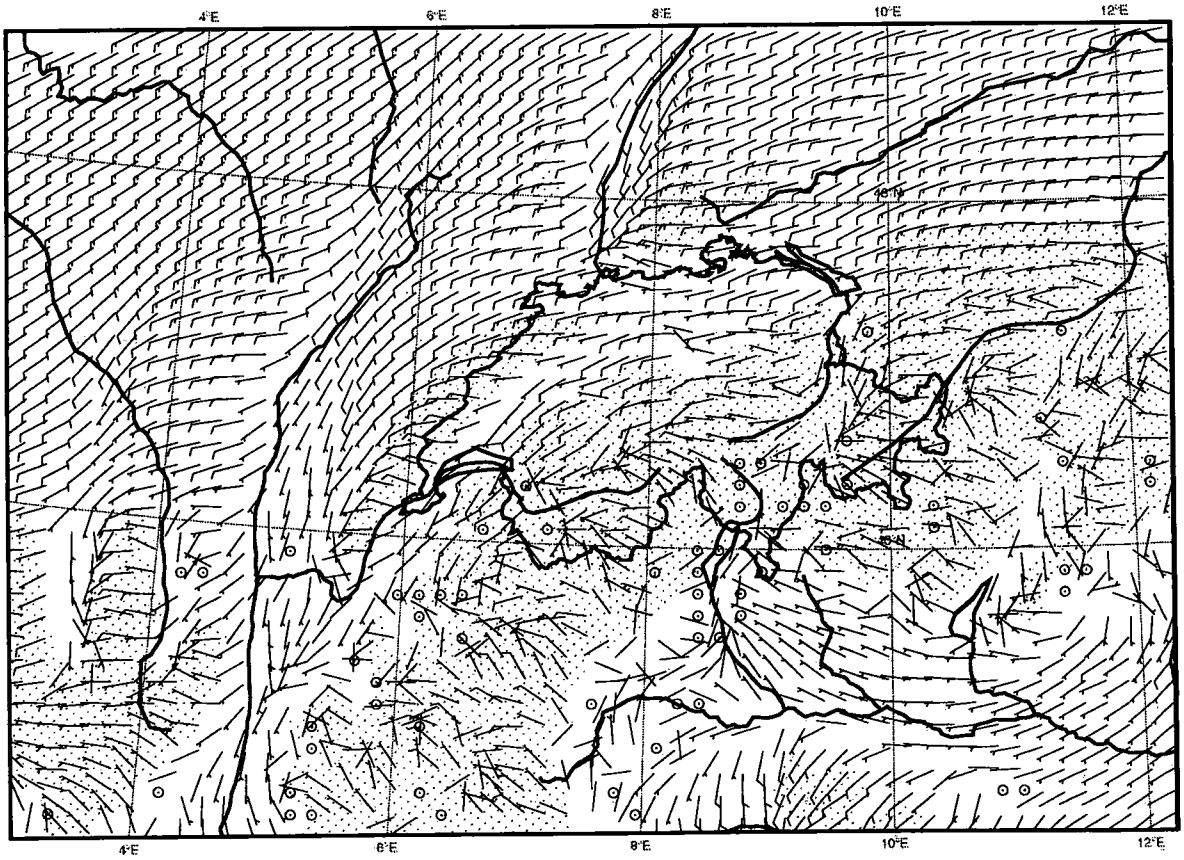


**Figure 33.** SM wind field at 10 m, over Switzerland, 15 Nov. 94 at 06 h UT

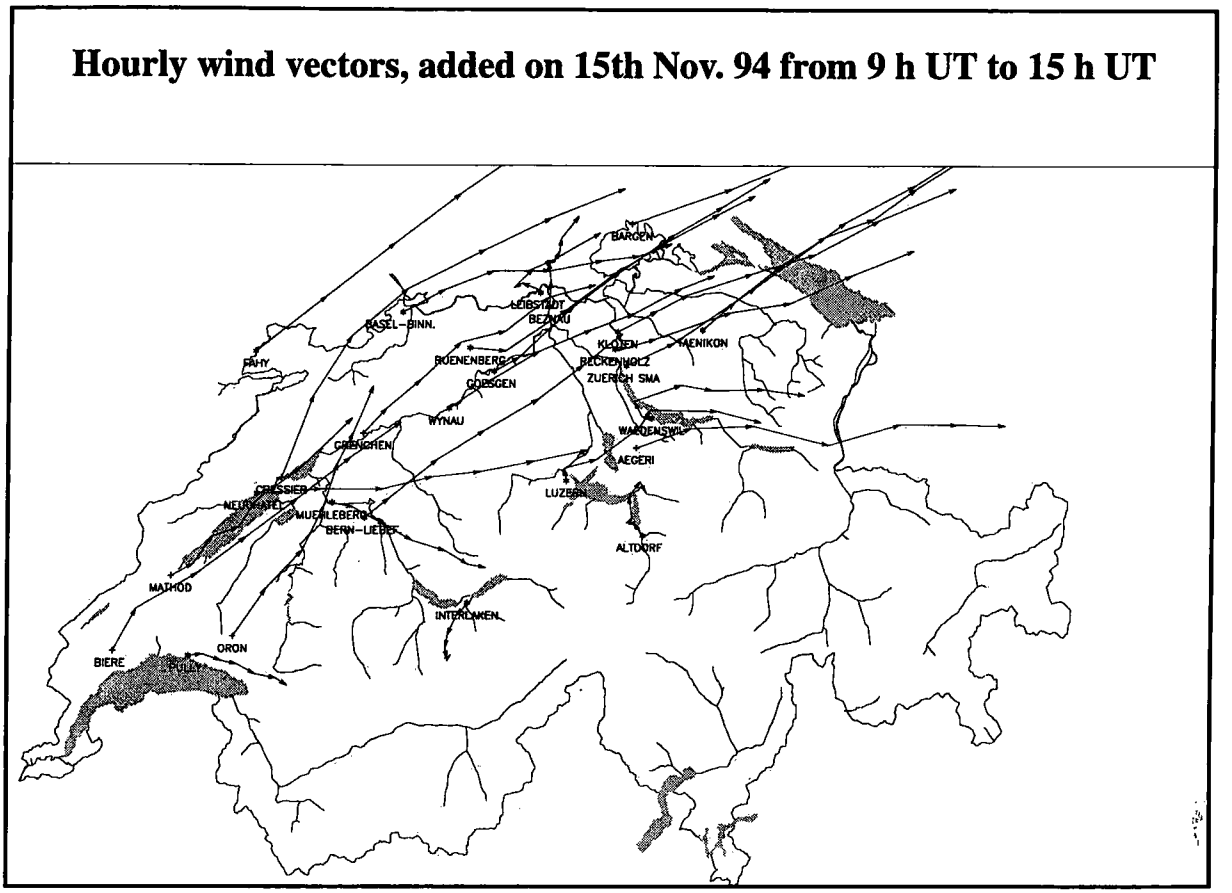


**Figure 34.** Virtual trajectories from plain stations, 15 Nov. 95, 9 h - 15 h UT

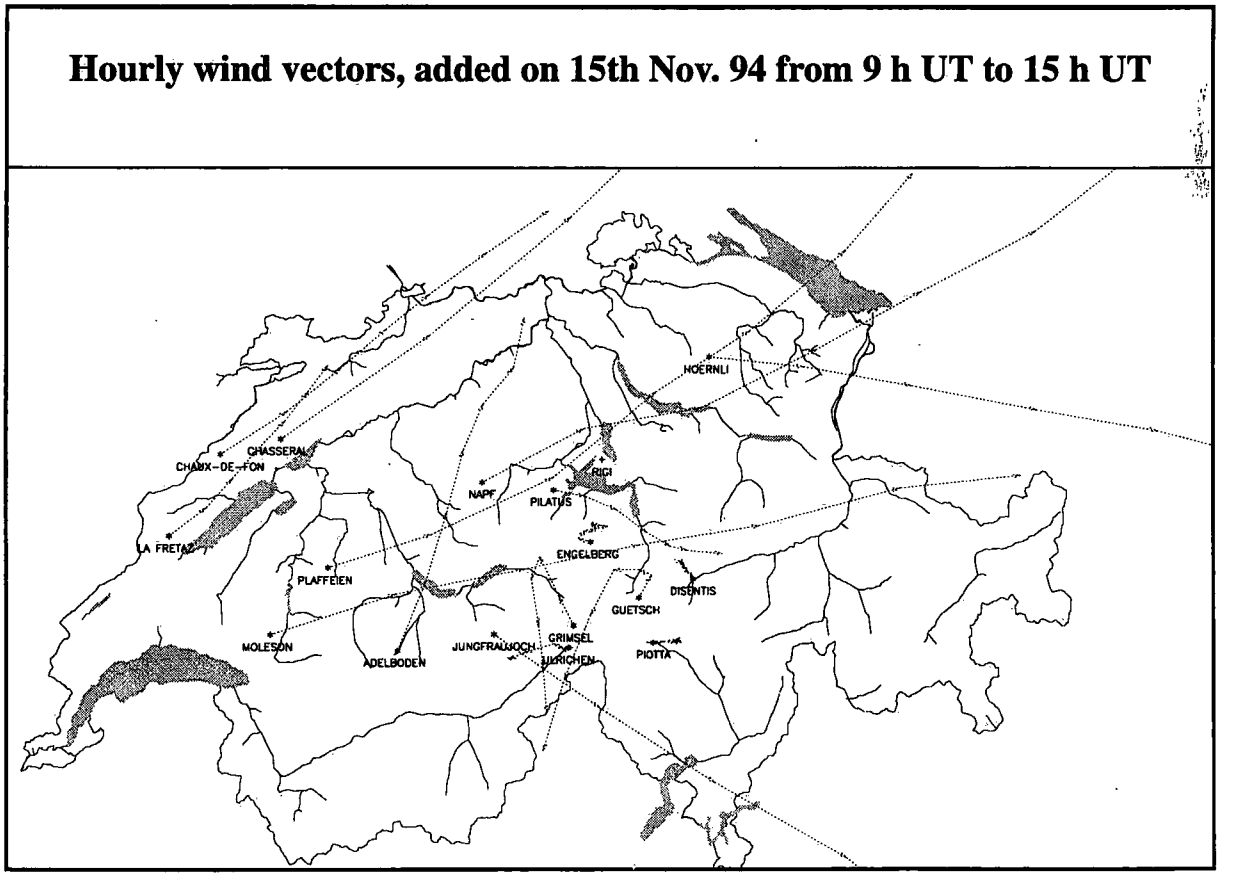


**Figure 35.** Virtual trajectories from mountain stations, 15 Nov. 95, 9 h - 15 h UT

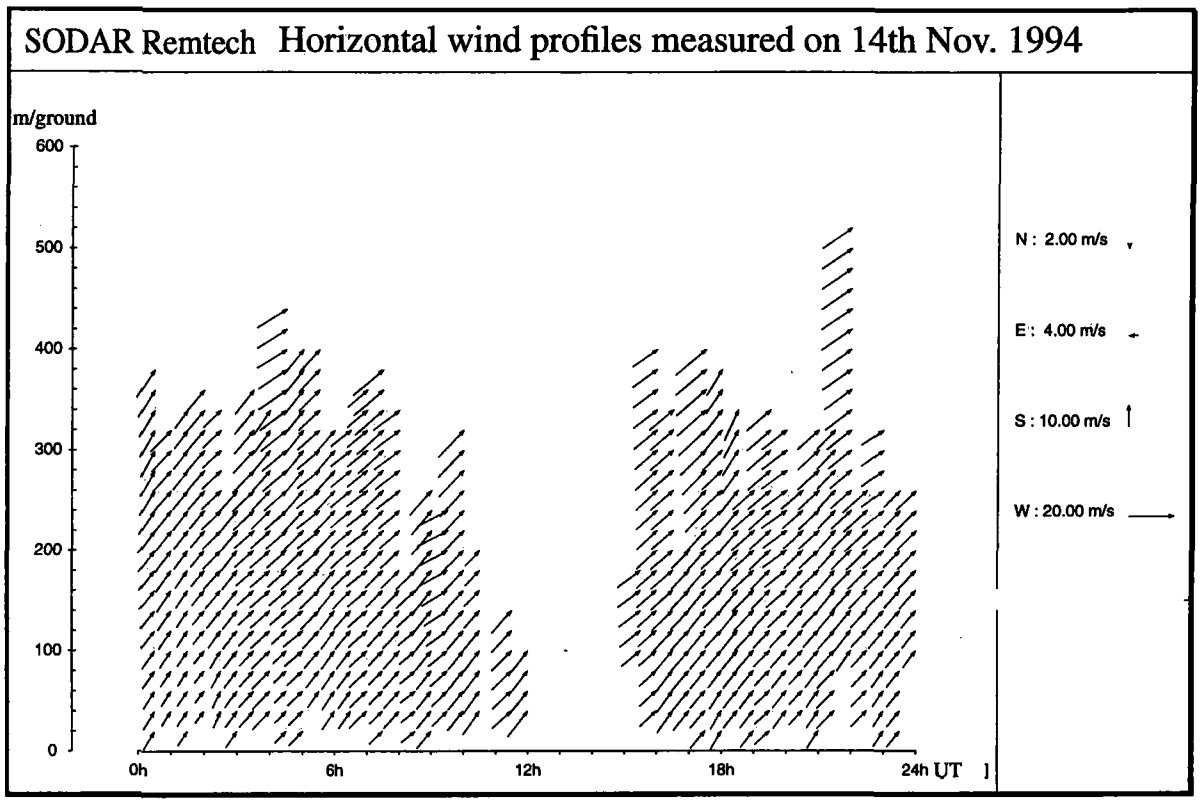


**Figure 36.** Profiles of Horizontal wind over the release site, 14 Nov. 94

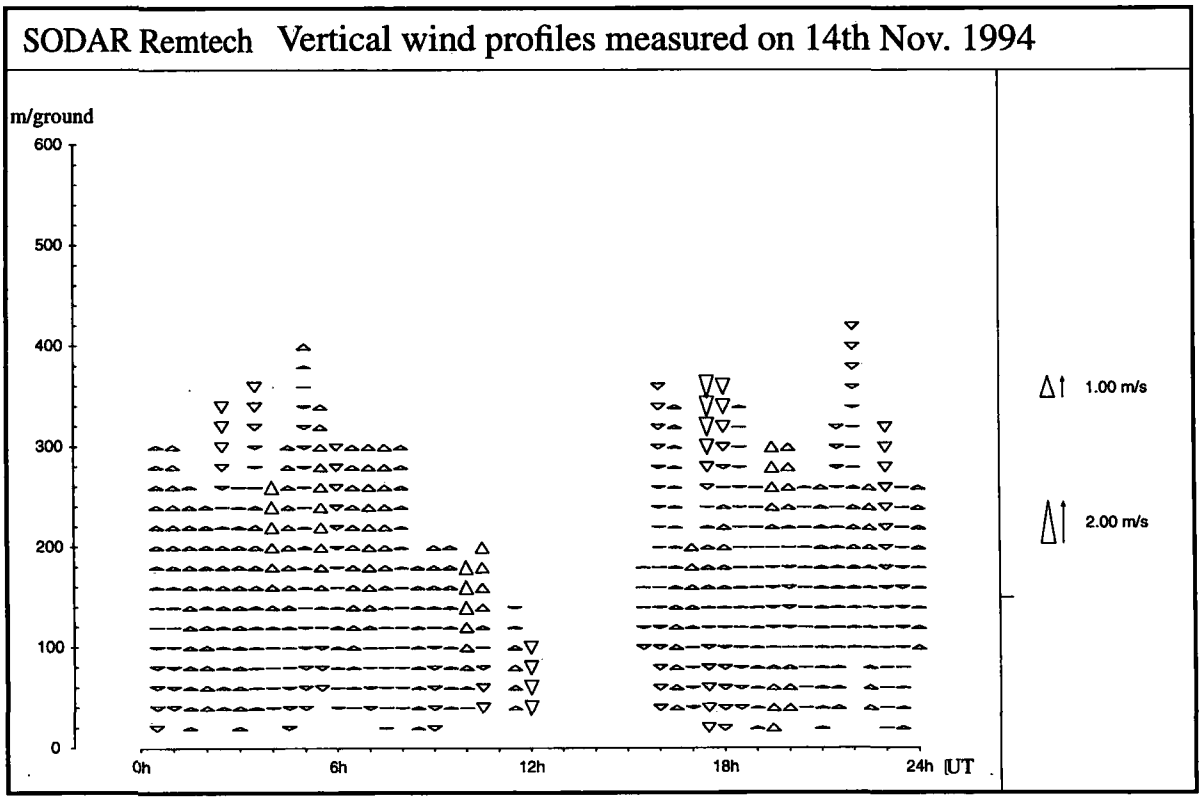


**Figure 37.** Profiles of vertical wind over the release site, 14 Nov. 94

# 4. Trajectory observations by constant volume balloons

## 4.1 Method of measurement

Constant volume balloons (CVB) manufactured by the Environment Meteorology Section of the SMI have a shape of tetrahedron and are made with a non-extensible material (a thin Hostaphan of 0.025 mm). With a volume of 1 $m^3$ filled with helium, they have a residual lift of 500 g., used to carry a radiosonde to measure pressure, temperature and humidy. The Vaisala Marwin MW-12 sounding system has the capability of using either the OMEGA and ALPHA, or the LORAN_C Navaid (navigation aid) system for wind measurement (ref. /2/). For ETEX, a local VLF receiving antenna was installed to receive Navaid signals and a 9-element UHF yagi antenna was mounted on a 30 m tower for the reception of the radiosonde emissions. The two types of radiosondes used for ETEX were RS80-15N using OMEGA and ALPHA Navaid, and Vaisala's RS80-15L, using LORAN_C Navaid. When used with constant volume balloons, the sensors are not ventilated and therefore the temperature measured under sunny conditions is too high (about 1°C for 700 $W/m^2$). Wind speed and wind direction are measured every ten seconds and the trajectory is computed by adding successive vectors from the launching point.

For the two tracer experiments, it was requested to fly simultaneously two constant volume balloons at the heights of 500 m and 1000 m AMSL before and during the tracer releases, with the aim of following the trajectory of the plume for the first 100 km to 200 km. The 1000 m AMSL balloons were launched by a crew from the CRA (Centre de Recherches Atmosphériques, Université Paul Sabatier, Lannemezan, France) (ref. /9/) and the other ones stabilized at 500 m AMSL were tracked by the crew of the SMI (ref. /3/) and are presented in this report. In reality, the balloon can fly at very different levels from the assigned one. On a convective situation, strong ascending flows can lift off the balloon well above its stabilization level (see trajectory number 2 of the first experiment). On other cases, depositions due to condensation or rain droplets on the surface of the tetrahedron increase its weight and can prevent it from ascending (see trajectory number 9 of the 2nd experiment).

The vectors represented every 1.125 degrees in **Figures 38 and 40** are the winds calculated at the 850 hPA pressure level by the ECMWF and used by the LORAN model to compute the trajectory and the dispersion of the tracer plume.The launching place was the tracer release site Monterfil, near Rennes (2° 0' 30" W, 48° 3' 30"N, 90 m AMSL).

## 4.2 Trajectories observed during the first tracer experiment

During the first tracer experiment (23rd and 24th October 1994) the meteorological situation on the release site was characterized by a humid but stable air mass, yielding some scattered showers. The westerly ground wind reached a speed ranging from 5 $ms^{-1}$ to 8 $ms^{-1}$. The pressure was increasing, the sky cleared during the night and the winds blew from east-north-east with decreasing speed. The five trajectories tracked during that time are given in **Table 17** and their horizontal projections are drawn in **Figure 42**. Wind measurements obtained

**Table 17.** CVB trajectories during the 1st tracer experiment

| No | Date | Start | Duration | Final distance | Mean altitude |
|---|---|---|---|---|---|
| A | 23 Oct. 94 | 13h19 UT | 0h39' | 21 km | 400 m to 100 m |
| B | 23 Oct. 94 | 16h36 UT | 2h20' | 122 km | 1500 m to 500 m |
| C | 23 Oct. 94 | 20h00 UT | 1h47' | 117 km | 900 m to 500 m |
| D | 24 Oct. 94 | 23h59 UT | 1h02' | 51 km | 550 m to 100 m |
| E | 24 Oct. 94 | 03h59 UT | 1h16' | 46 km | 550 m to 100 m |

by OMEGA and ALPHA Navaid gave good results and the reception of the radiosonde signals was strong enough to reach the maximum distance of 122 km for an end flight level of 500 m AMSL. The accuracy of the position can be estimated at about 1 km to 6 km at the end of the long trajectories (ref. /3/).

Plots of the second trajectory (B) are given in **Figures 38 and 39**. After 15 minutes, the tetroon transported by a moderate westerly wind (260 degrees, 13 $ms^{-1}$) reached its level of stabilization at about 500 m AMSL. An interesting feature of this trajectory is its great upward movement occurring after 50 minutes of flight. The balloon was carried by a convective motion and raised up to 1550 m AMSL. At this level the direction of the prevailing wind was 270 degrees, with a mean speed of 14 $ms^{-1}$. After a rapid descent down to 954 m AMSL the balloon was pushed up again to 1207 m AMSL. With periodical oscillations of about 20 minutes, it returned slowly to its level of stabilization at 500 m AMSL after 140 minutes, 190 km away from the release point. The wind direction reached 260 degrees again, but the speed became stronger (17 $ms^{-1}$to 19 $ms^{-1}$). These successive changes in wind direction are also apparent on the horizontal trajectory of **Figure 39.** This CVB trajectory attests that the tracer plume was certainly dispersed into the convective boundary layer up to an altitude of at least 1500 m AMSL during the first stage of its evolution.

## 4.3 Trajectories observed during the second tracer experiment

At the beginning of this period, the meteorological situation was typical of a warm air mass with a well established south-west wind of about 20 $ms^{-1}$ at 1000 m AMSL. The stratocumulus layer extended between 300 m and 2500 m AMSL and produced drizzle and showers. During the night, the rain became continuous because of the passage of a cold front. The next morning, the sky was mostly clear, except for some isolated cumuli. The winds near ground were westerly at 10 $ms^{-1}$. The four trajectories observed during this period are specified in **Table18** and their horizontal path is given in **Figure 43**.

**Table 18.** CVB trajectories during the 2nd tracer experiment

| No | Date | Start | Duration | Final distance | Mean altitude |
|---|---|---|---|---|---|
| A | 14 Nov. 94 | 13h03 UT | 0h48' | 62 km | no stabilisation |
| B | 14 Nov. 94 | 16h06 UT | 1h59' | 161 km | 1400 m |
| C | 14 Nov. 94 | 19h06 UT | 2h27' | 188 km | 2500 m |
| D | 14 Nov. 94 | 22h51 UT | 0h08' | 7 km | rain, no ascent |

The second trajectory (B), launched on the 14th of November 94 at 16h06 UT, is represented in detail in **Figures 40 and 41**. After a slow ascent of 27 minutes, the balloons reached their stabilization level at 1400 m AMSL. The well established western wind prevailing at this level was strong enough to transport the BVC over a distance of 161 km in 2 hours. In that case no vertical motion due to any convective process was noticeable.

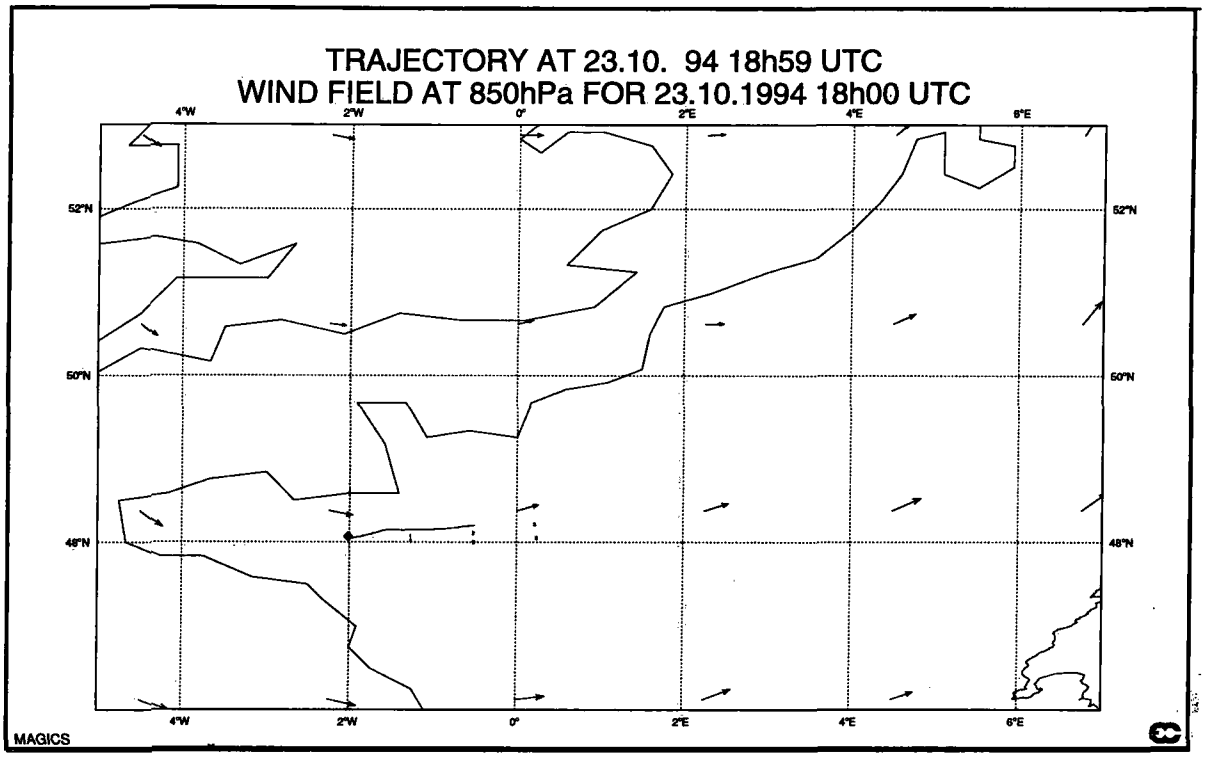


**Figure 38.** BVC trajectory, 23 Oct. 94, started at 16h36 UT, plan view

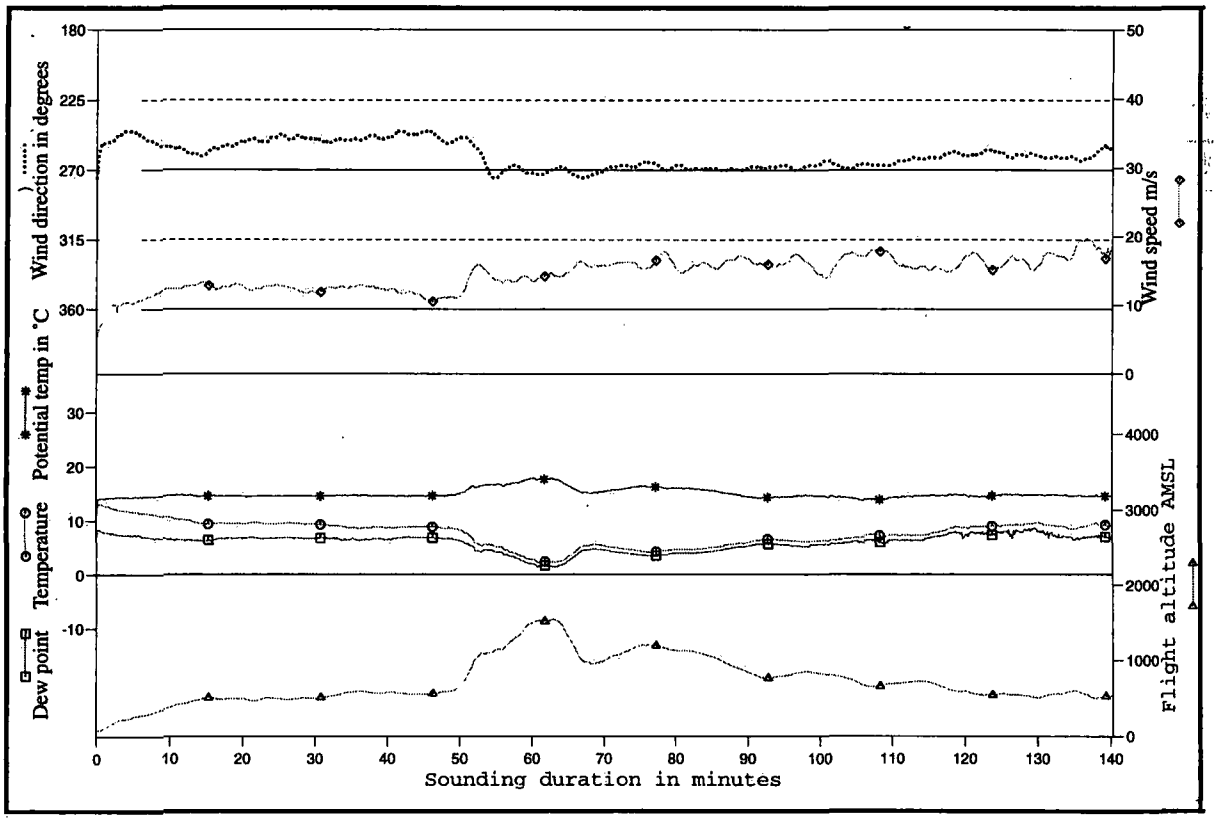


**Figure 39.** BVC trajectory, 23 Oct. 94, started at 16h36 UT, parameters

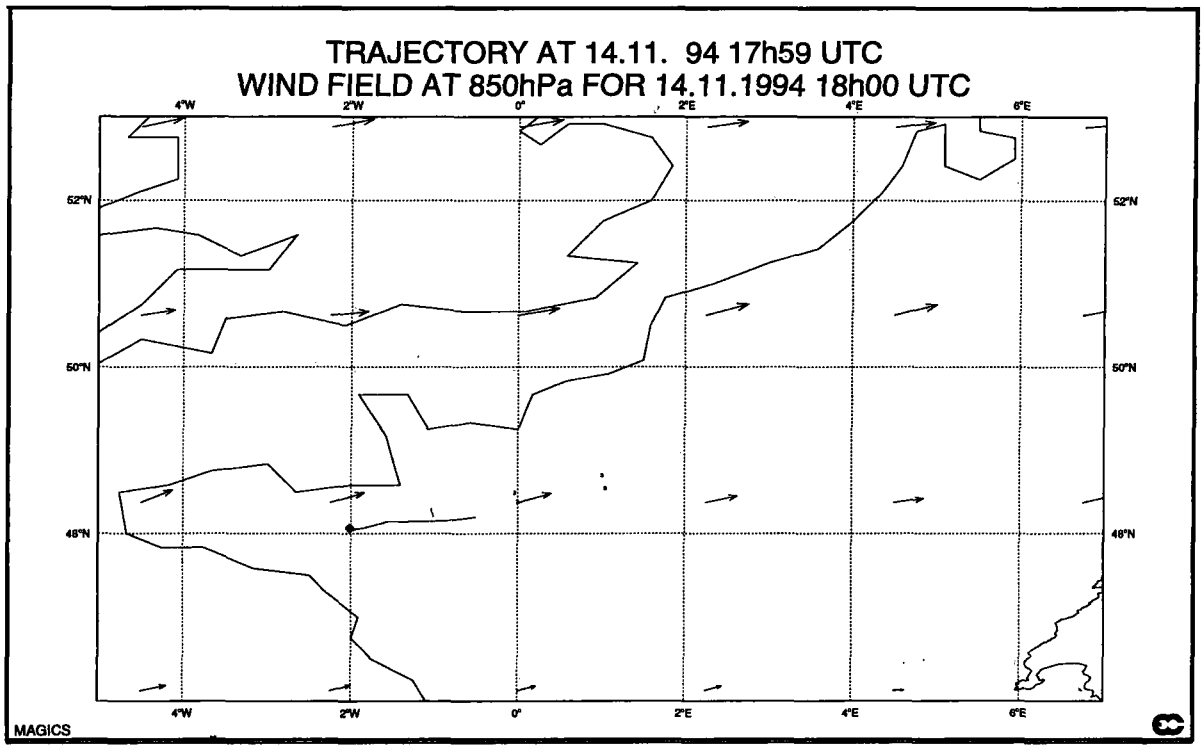


**Figure 40.** BVC trajectory 14 Nov. 94, started at 16h06 UT, plan view

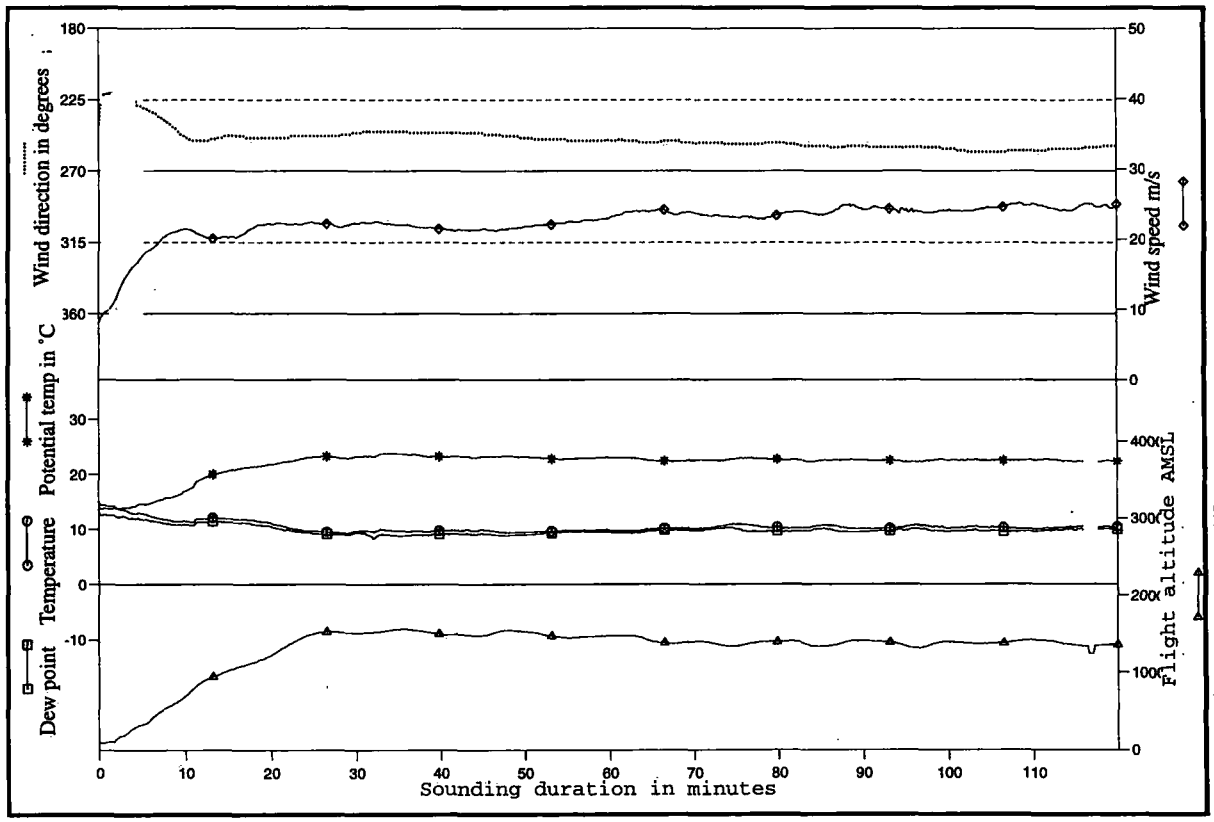


**Figure 41.** BVC trajectory, 14 Nov. 94, started at 16h06 UT, parameters

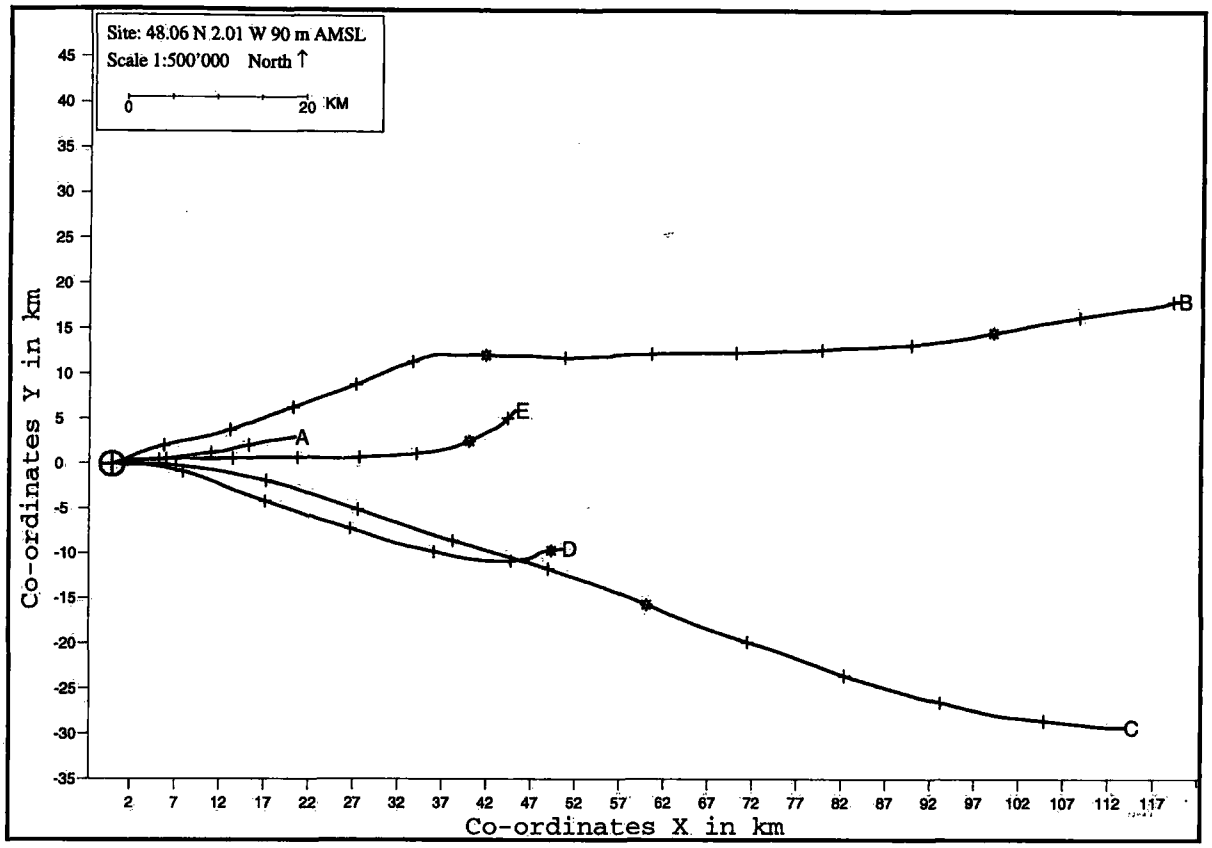


**Figure 42.** BVC trajectories observed during the 1st tracer experiment

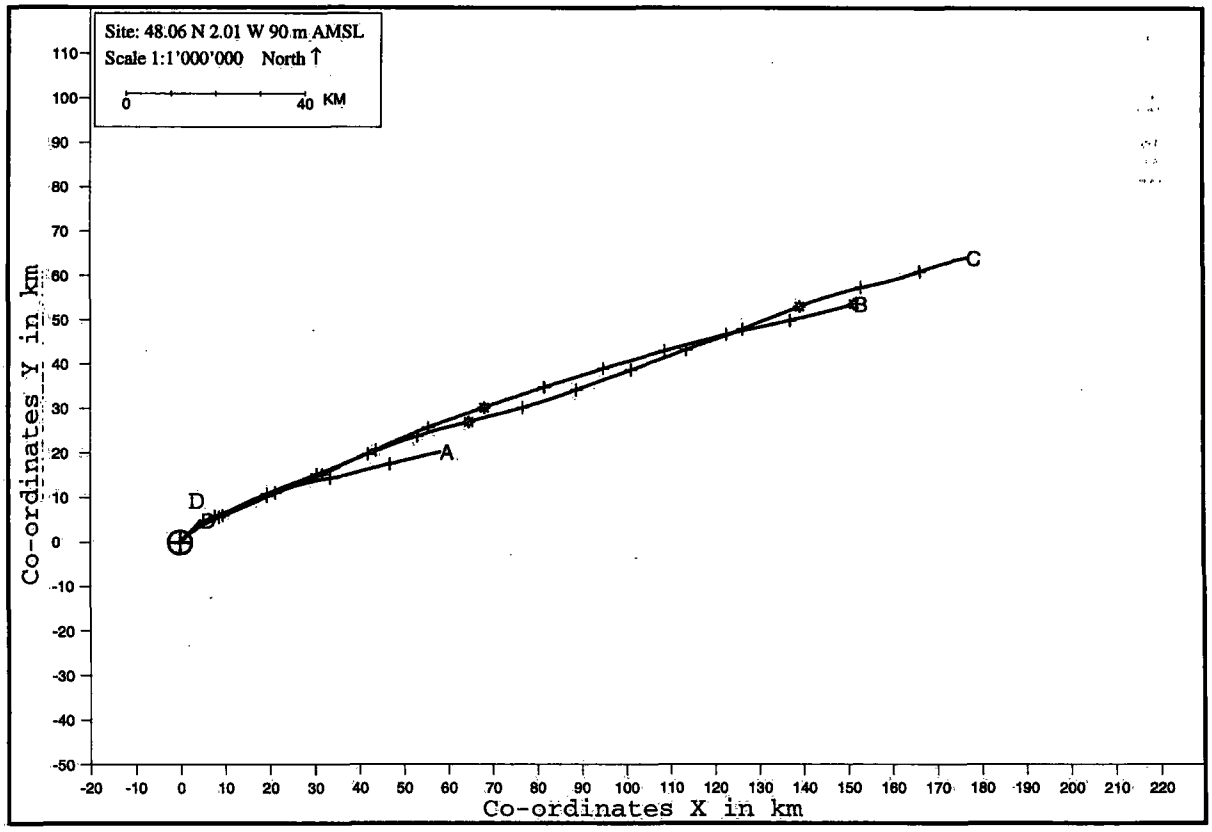


**Figure 43.** BVC trajectories observed during the 2nd tracer experiment

# 5. Concluding remarks

The purpose of this report is to recall the main objectives of the ETEX project and to present the specific contribution of the SMI to the three main topics of the project: meteorological measurement, tracer sampling and real time runs of dispersion model. This report should also be used as an introduction for users to the LORAN model which is briefly described and commented. The results obtained during the three dry runs serve as examples of model applications during various weather situations occurring over Europe. The preliminary comparisons of the measured evolution of the tracer plume with forecasts and analyses given by the model are very explanatory for what concerns the main characteristics of the LORAN model and the way to use it in emergency cases. It appears that, as a consequence of its very short computational times, the model can be used to deliver test preliminary answers about the dispersion evaluation. When the plume is obviously dispersing in regions far away from Central Europe this first guess might be sufficient. In case of doubt, we need to proceed with more sophisticated models to get more details on concentration fields, taking into account the wind stratification and considering the mesoscale flows, which can be rather different from the synoptic flow, especially in complex terrain like in the alpine regions. The first real experiment is a good example of such a situation. The calculation with LORAN indicated that the plume had a chance to reach the northern part of Switzerland, but in fact, no tracer was detected (as far as the last analysis of tracer measurements is concerned). The consideration of local wind presented on **Figures 23 and 24** gives some evidence that the south west wind prevailing on plain stations has effectively protected the Plateau from the tracer inflow.

## 5.1 Conclusions on experiments

The final interpretation of the model results for the concentrations to be expected in Switzerland must take into account the mesoscale characteristics of low level wind fields in the Plateau basin, over the Jura and the Alps. This analysis can be done by the virtual transportations calculated from plain and mountain stations, as shown in **Figures 23 and 24** or **figures 34 and 35.**

The comparison of concentrations fields calculated with forecasts and those obtained afterwards on the basis of analysed meteorological fields shows that divergences are generally small during the first 24 to 36 hours, but increase rapidly after 48 hours. It is too early to publish tracer concentration measurements, but the first available results show that Switzerland was probably not touched by the plume during both experiments.

## 5.2 Conclusions on LORAN model

We cannot imagine a better experiment than ETEX for the evaluation on long distance of the LORAN model. In its conception, the LORAN model takes into account the daily development of the mixing layer very carefully, and this is one of its major advantages. The fact that only one wind level (850 hPa) is considered is an important limitation, especially when the main meteorological situation is characterized by obvious wind shears, as it was the case for the first tracer experiment. Only the part of the plume travelling at this level is computed. The fact of ignoring other directions of transport prevailing at levels below and above 850 hPA prevents the plume from dispersing on other lateral sectors. For a better forecast, it is absolutely necessary to have a multilevel model. Another improvement would be to work at a smaller grid scale. The used mash of 1.125 degrees is too coarse to simulate real wind flow in the Alps region. Despite the weaknesses mentioned above, the LORAN model has the important advantages to deliver quick results over a large geographical extent and to provide forecasts over 72 hours at least. The predicted concentrations can be considered as a first guess, based on the main atmospherical flow at 850 hPA. In most of the accident cases far away from Switzerland, these results are good

enough to determine if our country has any chance of being touched or not by harmful plumes. This allows quick response to authorities' expectations and gives more time to compute, if required, detailed dispersion fields with other more sophisticated and more expensive models.

## 5.3 Main conclusions on ETEX

The ETEX project is one of the best tracer experiments conducted over Europe. This is due to the good organization and the participation of a large number of research institutes and meteorological organizations. The possibility given to modellers to compare their calculation with real data measured over great distances gives a very good base to evaluate existing models and also it indicates the way in which the models can be improved. In our opinion one of the main results of ETEX is the demonstration that a reliable dispersion forecast can only be supplied by a model which uses a sufficiently accurate description of the stratification of the wind field at mesoscale. It is also necessary to have a good simulation of the time evolution of the mixing layer height, particularly at the very beginning of the dispersion.

## Acknowledgements

The SMI participation to the ETEX project is due to the impulse of its director T. Gutermann and the head of the Weather division, M. Haug, official SMI representative for ETEX. The efficient collaboration with the JRC (Joint Research Centre) at Ispra (Italy) is indebted to F. Girardi, to G. Graziani and Mrs. K. Nodop, members of the ETEX steering committee. The Implementation of the LORAN dispersion model on the SMI informatic system has been realized with the support of one of its authors, S. Galmarini, who was a great help on many occasions, also during the elaboration of this report.

A. Rubli developed the preprocessing procedures used to acquire every day forecasted and analysed meteorological fields, needed as input data by the LORAN model from the ECMWF.

A. Lehmann wrote the interpolating programme to deliver the LORAN results under the format requested by the ETEX community. P. Overney worked on the graphical post-processing for a clear representation of the trajectories and concentrations of the computed tracer plume. Other graphical programmes for CVB trajectories, aerological soundings and virtual wind transport are due to B. Henchoz, A. Chassot and P.-A. Mettraux. We also thank P. Jeannet, head of the Environmental Meteorology Section for his constant support and encouragement. The technical crew, H. Berger, P. Wasserfallen and A. Vernez prepared and realized the CVB trajectories and SODAR measurements on the release site with great professionalism.

The Measurement Systems and Data Division, headed by G. Müller, took the responsibility of the tracer measurement at Zürich-Kloten, Payerne, Arosa and on the Jungfraujoch. The aerological section (P. Viatte) conducted additional PTU soundings during 5 days after both tracer releases. The numerical section delivered wind field forecasts computed by the SM (Swiss model) and we particularly thank J. Quiby, F. Schubiger and J. M. Bettems for their collaboration.

## References


/1/ Batchvarova E. and Gryning S.-E. (1991) Applied model for the growth of the daytime mixed layer. *Boundary-Layer Meteorol.* **56**, 261-274.

/2/ Berger H. (1994) Poursuite de ballons à volume constant au moyen du système de radio-sondage Vaisala Marwin-MW12. Description de l'équipement et procédure de filtrage des trajectoires. Swiss Meteorological Institute. Section for Environmental Meteorology CH-1530 Payerne, Switzerland. 17 p.

/3/ Berger, H. (1995) Constant volume balloons trajectories. ETEX 1994. Swiss Meteorological Institute. Section for Environmental Meteorology. CH-1530 Payerne, Switzerland. 17 p.

/4/ Galmarini S. Graziani G. and Tassone C. (1992) The atmospheric long range transport model LORAN and its application to Chernobyl release. *Environmental Software* **7**, 143-154.

/5/ Carras J. N. and Williams D. J. (1988) Measurements of relative $\sigma_y$ up to 1800 km from a single source. Atmospheric Environment **22**, 1061-1069.

/6/ Galmarini S. (1993) L.O.R.A.N. (Long Range Atmospheric Advection of Nuclides). Model User's Manual. (Multitrajectory Version). Appendix 2. CEC Joint Research Centre, Ispra Site, Ispra (VA), Italy. Personal communication 138 p.

/7/ Gifford F. A. (1984) The random force theory application to meso- and large-scale atmospheric diffusion. *Boundary-Layer Meteorology* **30**, 159-175.

/8/ Graziani G. Mosca S. (1994) The Second ETEX Dry-Run. CEC Joint Research Centre, Ispra Site, Ispra (VA), Italy.

/9/ Koffi E. Nodop K. Benech B. Schneiter D. and Berger H. (1996) Constant Volume Balloon capability to forecast tracer trajectories (ETEX experiment). European Geophysical Society (EGS) 21st general assembly, The Hague, 6-10 May.

/10/ Klug W. Graziani G. Grippa G. Pierce D. and Tassone C. (1992) Evaluation of long range atmospheric transport models using environmental radioactivity data from the Chernobyl accident. The ATMES Report. Elsvier Applied Science. London and New York. 366 p.

/11/ Klug W. Graziani G. Maineri M. Mosca S. (1993) Analysis of the first ETEX dry-run. CEC Joint Research Centre, Ispra Site, Ispra (VA), Italy. 276 p.

/12/ Klug W. Graziani G. Mosca S. Kroonenberger F. Archer G. Nodop K. and Stingele A. (1995) Real time long range dispersion model evaluation. ETEX first experiment. Draft Report prepared for ETEX Modellers' Meeting Prague, October.

/13/ Stull R. B. (1989) An Introduction to boundary layer meteorology. Atmospheric Sciences Library. Kluwer Academic Publishers, Dordrecht, The Niederlands. 666 p.

/14/ Tennekes H. and Driedonks A. (1981) Basic entrainment equations for the atmospheric boundary layer. *Boundary-Layer Meteorol.* **20/4,** 515-531.

/15/ Van Ulden A. P. and Holtslag A. (1985) Estimation of atmospheric boundary layer parameters for diffusion applications. *J. Appl Meteor.* **24,** 1196-1207.

## Abbreviations

| | |
|---|---|
| ABL | Atmospheric Boundary Layer |
| AMSL | Above Mean Sea Level |
| ATMES | Atmospheric Transport Model Evaluation Study |
| CVB | Constant Volume Balloon |
| EC | European Community |
| ECMWF | European Centre for Medium Range Weather Forecasts |
| ETEX | European Tracer Experiment |
| IAEA | International Atomic Energy Agency (Vienna) |
| JRC | Joint Research Centre, Ispra (Italy) |
| LORAN | Long Range Atmospheric Advection of Nuclides |
| MARS | Meteorological Archive and Retrieval System (of the ECMWF) |
| PTU | Pressure, Temperature, Humidity (type of aerological sounding) |
| SM | Swiss Model (version of the DWD model used by the SMI) |
| SMI | Swiss Meteorological Institute |
| SODAR | SOnic Detection and Ranging |
| UT | Universal Time |
| WMO | World Meteorological Organization (Geneva) |

Author's address:
Daniel SCHNEITER
Swiss Meteorological Institute
Aerological station
CH-1530 Payerne
E-mail dsc@sap.sma.ch
Tél. +41 37 62 62 64

# Appendix A. Mixing height calculation



## A. 1 Introduction

The LORAN (Long Range Atmospheric Advection of Nuclides) model computes the mixing height evolution for each segment of the plume according to the reached geographical location and to the weather situation prevailing at that time. The method used is based on works published by van Ulden and Holtslag (ref. /15/) and by Batchvarova and Gryning (ref. /1/). These authors propose a way of computing important parameters defining the main characteristics of the ABL (Atmospheric Boundary Layer), like the friction velocity $u_*$, the temperature scale $\theta_*$, and the Obukhov length L, by using only usual meteorological data produced by numerical models.

## A 1.1 Mixing height definition

The mixing height is considered here as the atmospheric boundary layer (ABL) that develops near the ground after sunrise in which the turbulence is strong enough to create and maintain a nearly uniform potential temperature profile. In this layer, turbulence is principally activated by convection and wind shear. It is capped by stable air aloft (ref. /13/). A residual ABL with a minimum height of 100 m is assumed to remain during the night.

## A 2. Physical process involved

During the night, when the outgoing infrared radiation is sufficient, the cooling of the ground by radiation divergence leads to a surface inversion roughly composed of two layers. The lower one is continuously turbulent, but the turbulence is not strong enough to destroy the temperature inversion. In the upper one, if the turbulence exists, it is only by intermittence and heat is mainly transferred through radiation. Above this inversion which has a minimum height of 100 m in the LORAN model, air is generally stable(ref. /14/).

Shortly after sunrise, in response to heating by shortwave radiation, the kinetic energy of the turbulence increases in the layer close to ground. The mixing of air is strong enough to give a nearly uniform distribution of the potential temperature. Over the mixing layer lies an entrainment zone in which the temperature increases with height to conform with the temperature of the warm stable air aloft. The top level of the entrainment layer is defined by the maximum height reached by the most vigorous eddies. As the mixing height grows, the more stable warm air above is embedded in the cooler mixed layer and the turbulent kinetic energy of the entrained air must increase to conform to the higher turbulence level within the mixed layer. The required energy is supplied by the turbulent kinetic energy within the mixed layer

where it is generated by convection and by wind shear (ref. /1/).

## A 3. Mixing height calculation by LORAN

The calculation of mixing height for a given point at a given time is a function of the following parameters:

- Geographical position: latitude $\varphi$ and longitude $\lambda$.
- Ground albedo r for a sky without clouds.
- Ground roughness $z_0$.
- Date and time.
- Reference temperature $T_r$ at 2 m above ground .
- Cloud cover N (from 0 for clear sky to 1 for overcast).
- Wind speed U at 10 m above ground.

The first step of the calculation scheme determines the Obukhov length L, which is a function of the temperature scale $\theta_*$ and the friction velocity $u_*$. The Obukhov length L defines four stability classes:

- Quasi neutral situation (L < -20 m).
- Instable situation (-20 m $\leq$ L < 0 m).
- Stable situation (0 m $\leq$ L < 40 m).
- Neutral situation (L $\geq$ 40 m).

The mixing height is then obtained by different equation sets within each of these classes.

## A 3.1 Obukhov length

The Obukhov length is obtained according to the method proposed by Van Ulden et al *(/15/)* which usually applies only to dry boundary layers in which no significant amount of clouds or fog is present.

The sun elevation $\phi$ calculation, a function of the latitude $\varphi$ of the site, of the date (season) and of the time h, determines the night situation ($\phi < 1{,}7°$), to which also belong situations without solar radiation in short wavelength ($Q_i^* = 0$) computed by the relation:

$$Q_i^* = K^* + L_i^* \qquad \textit{Eq. 8}$$

where

| | | |
|---|---|---|
| $Q_i^*$ | $Wm^{-2}$ | Isothermal net radiation |
| $K^*$ | $Wm^{-2}$ | Net shortwave radiation |
| $L_i^*$ | $Wm^{-2}$ | Isothermal net longwave radiation |

K* is a function of latitude $\varphi$ and of cloud cover N.

$$K^* = \underbrace{(a_1 \sin(\varphi) + a_2)}_{\text{I}} \underbrace{\left(1 - b_1 N^{b_2}\right)}_{\text{II}} \underbrace{(1 - r)}_{\text{III}} \qquad \textit{Eq. 9}$$

with:

| | |
|---|---|
| Part I | Incoming solar radiation. |
| $a_1$ | Empirical coefficient representing the maximal solar radiation in short waves, estimated as 900 $Wm^{-2}$. |
| $a_2$ | Empirical coefficient representing the maximal terrestrial radiation in infrared waves, estimated as -30 $Wm^{-2}$. |
| Part II | Reduction factor representing the interception of solar radiation by clouds. |
| $b_1$ | Empirical coefficient estimated to 0,75. |
| $b_2$ | Empirical exponent estimated to 3.4. |
| N | Cloud cover (0 = clear sky, 1 = overcast). |
| Part III | Reduction factor due to the reflection of incoming solar radiation at surface. |
| r | Reflection factor (albedo) (r = 0.08 on sea, r = 0.2 on land). |

and $L_i^*$ (*Eq. 8*) is given by

$$L_i^* = -\sigma\left(T_r^4\left(1 - c_1 T_r^2\right)\right) + c_2 N \qquad \textit{Eq. 10}$$

where

| | | |
|---|---|---|
| $c_1$ | $= 9.35\ 10^{-6}\ K^{-2}$ | Empirical coefficient. |
| $c_2$ | $= 60\ Wm^{-2}$ | Empirical coefficient. |
| N | (from 0 to 1) | Fraction of sky covered with clouds. |
| $T_r$ | [°K] | Air temperature at the reference height $z_r$ = 50 m/ground. |
| $\sigma$ | $= 5{,}67\ 10^{-8} Wm^2K^{-1}$ | Stefan-Boltzmann constant. |

A more practical form for equation 8 is obtained by assessing $T_r$=283 K (+8°C) in equation 10.

$$Q_i^* = K^* - (91 + 60N) \qquad \textit{Eq. 11}$$

### A.3.1.1 Obukhov length for night

By night the Obukhov length L is obtained from the friction velocity $u_*$ and from the temperature scale $\theta_*$.

$$u_* = kU(z) / [\ln((z_1/z_0) - \Psi_M(z_1/L) + \Psi_M(z_0/L))] \qquad \textit{Eq. 12}$$

where

| | |
|---|---|
| U(z) | Vertical profile of wind speed. |
| $z_0$ | Surface roughness length given in an external file for each grid element. $z_0$ = 0.001 m over sea, 0.2 m on terrain with an average altitude of more than 1000 m above sea level and 0.05 m elsewhere (ref. /4/). |
| $z_1$ | Height above ground of the wind measurements. $z_1$= 10 m |

Equation (12) is typically valuable for $z_0 << z < L$. It is to note that $u_*$ depends on L.

In stable atmospheric conditions the stability function $\psi_M$ is given by

$$\psi_M(z/L) = -17\,[1 - \exp(-0,29z/L)] \qquad \textit{Eq. 13}$$

$\theta_*$ is calculated by the following function valid for night:

$$\theta_* = T_r\{[(d_1 v_*^2 + d_2 v_*^3)^2 + d_3 v_*^2 + d_4 v_*^3]^{1/2} - d_1 v_*^2 - d_2 v_*^3\} \qquad \textit{Eq. 14}$$

where

$$v_* = u_*/(5gz_r)^{1/2} \qquad \textit{Eq. 15}$$

$$d_1 = \frac{1}{2k}\ln\frac{z_r}{z_h} = 15 \qquad \textit{Eq. 16}$$

$$d_2 = \left(\frac{1}{2}(1+S)\rho C_p (5gz_r)^{1/2}\right)/\left(4\sigma T_r^3 + A_G\right) \qquad \textit{Eq. 17}$$

$$d_3 = (-Q_i^*)/\left(4\sigma T_r^4 + A_G T_r\right) + \Gamma_d z_r/T_r \qquad \textit{Eq. 18}$$

$$d_4 = (1+S)\rho C_p (5gz_r)^{1/2}\theta_d/\left(4\sigma T_r^4 + A_G T_r\right) \qquad \textit{Eq. 19}$$

where

S Slope of saturation enthalpy curve for 270 K < $T_r$ <310 K.

$$S = \exp[0,055\,(T_r - 279)] \qquad \textit{Eq. 20}$$

and

| | | |
|---|---|---|
| $A_G$ | = 5 $Wm^{-2}K^{-1}$ | Empirical coefficient for the soil heat transfer. |
| $C_p$ | = 1005 J $Kg^{-1}$ $K^{-1}$ | Dry air specific heat, at constant pressure. |
| g | = 9.80 $ms^{-2}$ | Acceleration of gravitation. |
| k | ≈ 0.4 | Van Karman constant. |
| $T_r$ | [K] | Air temperature at a reference height $z_r$ (here at $z_r$= 2 m). |
| U(z) | [$ms^{-1}$] | Wind speed at level z. |
| $z_h$ | | Resistance for heat transfer near the surface, with ln ($z_r$ / $z_h$) = 30. |
| $z_r$ | = 50 m | Reference height. |

| | | |
|---|---|---|
| $\Gamma_d$ | $= 0{,}01$ K m$^{-1}$ | Dry adiabatic lapse rate. |
| $\theta_d$ | 0,033 K | Empirical temperature scale. |
| $\rho$ | 1,2 kg m$^{-3}$ | Air mass per unit volume. |
| $\sigma$ | $= 5{,}67\ 10^{-8}$Wm$^2$K$^{-1}$ | Stefan-Boltzmann constant. |

Then

$$L = u_*^2 / (kg\theta_*/T) \qquad \textit{Eq. 21}$$

T [K] Air temperature (here at 2m above ground).

This equation set is solved by iteration. A first guess of $u_{*g}$ is proposed by:

$$u_{*g} = kU(z) / \ln(z_1/z_0) \qquad \textit{Eq. 22}$$

Then $\theta_*$ is calculated by Eq. 14. If $\theta_* \leq 10^{-4}$ then $L=10^5$ which represents the neutral case. If $\theta_* > 10^{-4}$ the stability function $\psi_M(z/L)$ for z=10 m is obtained by Eq. 13 and $u_*$ is calculated again by Eq. 12 where the term $\psi_M(z_0/L)$ is neglected. If $|u_* - u_{*g}| < 0.001$ iteration is stopped. Otherwise a new estimation is taken as $u_{*g} = u_*$ and a new cycle is restarted. The number of iterations is limited to 20.

### A.3.1.2 Obukhov length for day

As for the night case the Obukhov length L is obtained from the friction velocity $u_*$ and temperature scale $\theta_*$. The following relations are considered:
Eq. (23) is typically valid for $z_0 << z < L$

$$u_* = kU(z) / [\ln((z_1/z_0) - \psi_M(z_1/L) + \psi_M(z_0/L))] \qquad \textit{Eq. 23}$$

If $L < 0$

$$\psi_M = 2\ln\left(\frac{1+x}{2}\right) + \ln\left(\frac{1+x^2}{2}\right) - 2\,\mathrm{atan}(x) + \pi/2 \qquad \textit{Eq. 24}$$

with x set to

$$x = (1 - 16z/L)^{1/4} \qquad \textit{Eq. 25}$$

If $L \geq 0$, then

$$\psi_M = -17\,[1 - \exp(-0{,}29z/L)] \qquad \textit{Eq. 26}$$

$$\theta^* = -\frac{[(1-\alpha)S+1]\,(1-C_G)\,Q_i^*}{(S+1)\,(1+C_H)\,\rho C_p u_*} + \alpha\theta_d \qquad \textit{Eq. 27}$$

$\alpha$ [1] = 1 Moisture parameter for normal wet grass in a moderate climate.

$C_H$ Empirical heating coefficient

$$C_H = 0,38\left[\frac{(1-\alpha)S+1}{S+1}\right] \qquad \textit{Eq. 28}$$

and for $C_G$

$$C_G = \left(A_G/\left(4\sigma T_r^3\right)\right)C_H \qquad \textit{Eq. 29}$$

$A_G$ = 5 $Wm^{-2}K^{-1}$ Empirical coefficient for the soil heat transfer

$$L = u_*^2 / (kg\theta_*/T) \qquad \textit{Eq. 30}$$

Resolution of this equations set is performed by iteration. A first estimation of $u_*$ is given by:

$$u_* = kU(z)/\ln(z_1/z_0) \qquad \textit{Eq. 31}$$

$\theta_*$ is then calculated (Eq.27). If $\theta_* \leq 10^{-4}$, then $L=10^5$ defines the neutral case. If $\theta_* > 10^{-4}$ the stability function $\psi_M(z/L)$ for z = 10 m is calculated by Eq. 26 and $u_*$ is recalculated with Eq. 23 neglecting the term $\psi_M(z_0/L)$. A new estimation is taken as $u_{*g} = u_*$ and a new cycle is restarted. Iteration stops when $|u_* - u_{*g}| < 0.001$ or after a maximum number of cycles fixed to 20.

## A 3.2 Determination of mixing layer height

Four stability classes are defined, according to the value of Obukhov length L: quasi neutral (L < -20 m), unstable situation (-20 m ≤ L < 0 m), stable (0 m ≤ L < 40 m) et neutral (L ≥ 40 m). The mixing layer height is then determined by different relations within each of these classes.

### A.3.2.1 Quasi neutral conditions

If L < -20 then the minimal value of h is limited to 100 m.

$$\left(\frac{h^2}{(1+2A)\,h_g - 2BkL}\right)\frac{dh}{dt} = \frac{(\overline{w'\theta'})}{\gamma} \qquad \textit{Eq. 32}$$

where

A Parameterized constant A = 0,2.

B Parameterized constant B = 2,5.
$h_g$ Guessed height of mixing layer.
k Von Karman constant. k = 0,4.
L Obukhov length.
γ Temperature gradient over inversion.

By integration, and with

$$L = -\frac{u_*^3 T}{kg(\overline{w'\theta'})} \qquad \textit{Eq. 33}$$

where
T Temperature.
g Gravitation.
the following relation is obtained:

$$h = \sqrt[3]{h_0^3 - 3\Delta t \frac{u_*^3 T}{g\gamma}\left(2B - \frac{1+2A}{kL}h_g\right)} \qquad \textit{Eq. 34}$$

$h_0$ Initial mixing height at time t = 0 and $h_0$ = 100m.
$h_g$ Guessed mixing height.
Δt Building duration. Δt = 6 hours = 21'600 seconds.

The calculation of h is done by iteration. The start value of h is given by $h_g$:

$$h_g = 0,33\left(\frac{u_*}{f}\right) \qquad \textit{Eq. 35}$$

f Coriolis parameter. f = $1.10^{-4}$.

Then h is calculated by Eq. 34. If h - $h_g$ < 10, h is accepted, otherwise $h_g$ = h and iteration continues, but with a maximum of 20 cycles.

### A.3.2.2 Unstable conditions

When -20 m ≤ L < 0 m, the mixing layer is unstable.
The model used by LORAN for the mixing layer height h evolution was proposed by Batchvarova et Gryning in 1991 (ref. /1/) and is defined by the differential equation:

$$\left\{\frac{h^2}{(1+2A)h - 2BkL} + \frac{Cu_*^2 T}{\gamma g\,[\,(1+A)h - BkL]}\right\}\frac{dh}{dt} = \frac{(\overline{w'\theta'})_s}{\gamma} \qquad \textit{Eq. 36}$$

A Constant. A = 0,2.

B Constant. B = 2,5.
C Constant. C= 8.
h Height of mixing layer.
k Von Karman constant. k = 0,4.
L Obukhov length.
$u_*$ Friction velocity.
$\gamma$ Potential temperature gradient above mixing layer.
$(\overline{w'\theta'})_s$ Vertical kinematic heat flux at the surface.

The first term stems from the combined effect of mechanical and convective turbulence. The second term is due to the spin-up effect which is important only near the ground or when the air is nearly neutrally stratified. In our case, this term can be ignored and the simplified equation becomes:

$$\left(\frac{h^2}{(1+2A)\,h-2BkL}\right)dh = \frac{(\overline{w'\theta'})_s}{\gamma}dt \qquad \textit{Eq. 37}$$

Integration of left-hand-side term gives a relation of the type:

$$\int \frac{h^2}{ah+b}dh = \frac{h^2}{2a} + \frac{-b}{a^2}h + \frac{b^2}{a^3}\ln(ah+b) + C \qquad \textit{Eq. 38}$$

C Integration constant.

If h = 0 at time t = 0, then h at time t is given by the equation:

$$\frac{h^2}{2(1+2A)} + \frac{2Bkl}{(1+2A)^2}h + \frac{(2Bkl)^2}{(1+2A)^3}\ln\left(\frac{(1+2A)\,h-2Bkl}{(1+2A)\,h_0-2Bkl}\right) = \frac{(\overline{w'\theta'})_s}{\gamma}\Bigg|_0^T - \frac{h_0^2}{2(1+2A)} - \frac{2Bkl}{(1+2A)^2}h_0 \qquad \textit{Eq. 39}$$

or

$$L = -\frac{u_*^3\,T}{kg\,(\overline{w'\theta'})} \qquad thus \qquad \frac{(\overline{w'\theta'})_s}{\gamma} = \frac{u_*^3\,T}{Lkg\gamma} \qquad \textit{Eq. 40}$$

which is a second degree equation of the type $ah^2 + bh + c = 0$, with the solution

$$h = \frac{-b \mp \sqrt[2]{b^2 - 4ac}}{2a} \qquad \textit{Eq. 41}$$

After multiplying Eq. 39 by (1+2A) we have:

*Eq. 42*

$$a = \frac{1}{2}$$

$$b = \frac{2Bkl}{(1+2A)}$$

$$c = \frac{u_*^3\, T(1+2A)}{Lkg\gamma} - \frac{h_0^2}{2} - \frac{2Bkl}{1+2A} h_0 - \frac{(2Bkl)^2}{(1+2A)^2} \ln\left(\frac{(1+2A)\,h_g - 2Bkl}{(1+2A)\,h_0 - 2Bkl}\right)$$

Taking the estimated starting value

$$h_g = 0,33\left(\frac{u_*}{f}\right) \qquad \textit{Eq. 43}$$

if $|h - h_g| < 10$, h is accepted, otherwise a new estimation is calculated by

$$\text{if } h > 0 \quad h_g = \frac{h_g + h}{2} \quad \text{or if } h < 0 \quad h_g = \frac{h_g}{2} \qquad \textit{Eq. 44}$$

### A.3.2.3 Stable conditions

When 0 m ≤ L < 40 m, the height of mixing layer in stable conditions is calculated by

$$h = (au_*f + b)\frac{u_*}{f} \qquad \textit{Eq. 45}$$

a Constant a= $1,4\ 10^3$

b Constant b= 0,06

f Coriolis Parameter f = $1.10^{-4}$

### A.3.2.4 Neutral conditions

When $|\theta_*| < 10^{-4}$ or $L \geq 40$ m the mixing layer height h is given (Van Ulden A.P., Holtslag 1985 ref. /15/) by:

$$h = 0,33\left(\frac{u_*}{f}\right) \qquad \textit{Eq. 46}$$

f Coriolis Parameter $f = 1.10^{-4}$

******